journal of the international meteor organization

# WGN

42:2
april 2014

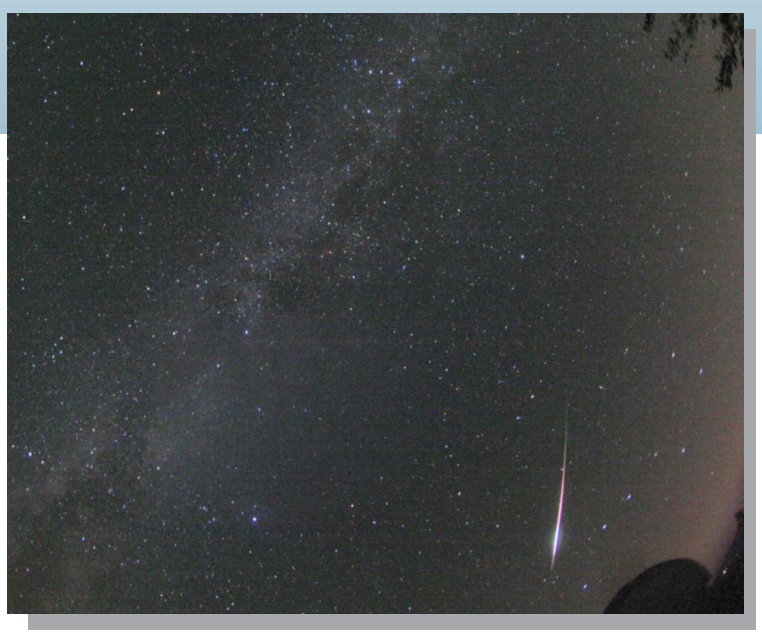

IMC 2014 announced
Activity of the September ε-Perseids in 2013
Fifteen new showers discovered
Collision risk of satellites with the Perseids assessed
Meteor shower search in the southern hemisphere
December–January video meteors

ISSN 1016-3115

WGN Vol. 42, No. 2, April 2014, pp. 35 – 86

## Conferences

International Meteor Conference 2014, 33rd edition, September 18–21, Giron, France *François Colas, Jean-Louis Rault, Jérémie Vaubaillon, Sylvain Bouley, Brigite Zanda, and Lucie Maquet* 35

## Meteor science

Peculiar activity of the September $\varepsilon$-Perseids on 2013 September 9 *Jürgen Rendtel, Esko Lyytinen, Sirko Molau, and Geert Barentsen* 40

The September epsilon Perseids in 2013 *Štefan Gajdoš, Juraj Tóth, Leonard Kornoš, Jakub Koukal, and Roman Piffl* 48

New showers from parent body search across several video meteor databases *Damir Šegon, Peter Gural, Željko Andreić, Ivica Skokić, Korado Korlević, Denis Vida, and Filip Novoselnik* 57

Bright Perseids 2007–2013 and artificial Earth satellites collision risk assessment *Andrey Murtazov* 65

Meteor showers of the southern hemisphere *Sirko Molau and Steve Kerr* 68

## Preliminary results

Results of the IMO Video Meteor Network — December 2013 *Sirko Molau, Javor Kac, Stefano Crivello, Enrico Stomeo, Geert Barentsen, Rui Goncalves, and Antal Igaz* 76

Results of the IMO Video Meteor Network — January 2014 *Sirko Molau, Javor Kac, Stefano Crivello, Enrico Stomeo, Geert Barentsen, Rui Goncalves, and Antal Igaz* 83

## Front cover photo

This fireball of the September $\varepsilon$-Perseids was captured on 2013 September 9 at $22^{\mathrm{h}}12^{\mathrm{m}}$ UT by all-sky camera located at the Gahberg observatory in Austria. Canon 350D equipped with Peleng fish eye lens, $f = 8$ mm was used for a 30 s exposure. Photo courtesy: Erwin Filimon.

## Writing for WGN

This Journal welcomes papers submitted for publication. All papers are reviewed for scientific content, and edited for English and style. Instructions for authors can be found in WGN **31:4**, 124–128, and at `http://www.imo.net/docs/writingforwgn.pdf` .

## Copyright



## Legal address

International Meteor Organization, Jozef Mattheessensstraat 60, 2540 Hove, Belgium.

# Conferences

## International Meteor Conference 2014, 33rd edition, September 18–21, Giron, France

*François Colas*[1], *Jean-Louis Rault*[2], *Jérémie Vaubaillon*[1], *Sylvain Bouley*[3], *Brigite Zanda*[4], *and Lucie Maquet*[1]

### Period and location

The 2014 International Meteor Conference, organized by IMCCE (Institut de Mécanique Céleste et de Calcul des Ephémérides) and IMO, will take place in Giron, France, from September 18 (Thursday evening) to September 21 (Sunday lunchtime).

Giron is a small village located in the Jura mountains close to Geneva.

The climate of GIRON is continental as the elevation is 1000 meters, winters are quite cold, allowing to ski, mainly cross country. Therefore, be aware that even in September temperatures could be as low as +10 or +5 degrees Celsius. The Jura mountains are known for their wildlife such as lynx and falcons and for cheese (Comté, Mont d'Or). Giron is located within the natural park: "Parc naturel régional du Haut Jura".


*Figure 1* – The IMC2014 logo.

### Accommodation

Most of the IMC2014 participants will be hosted in "Chalet de la Fauconière" which belongs to the "Fédération des Oeuvres Laïques", and additional rooms will be available at "Centre Montagnard" which is located at 1 km from the Chalet (see Figure 3, left and middle image).

The conference will take place in one single location, the "Chalet de la Fauconière". The lecture room (see Figure 3, right) and restaurant are in the same building. The "Centre Montagnard" is only 15 minutes by walk (1 km) from the Chalet.

There are 150 beds in the chalet with rooms with 3, 5 or 7 beds. The LOC decided to limit the number of persons to 100 in the Chalet to enhance comfort, and also to offer double accommodations. The lectures and the poster session will be held in the chalet conference room (150 places) as well as in the bar.


*Figure 2* – Location of Giron on the relief map of France.

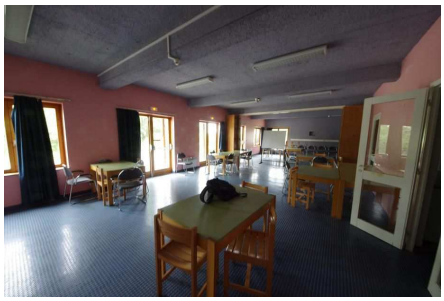

*Figure 3* – Chalet de la Fauconière from above (left), Centre d'accueil Montagnard (middle) and the lecture room (right).

[1]IMCCE – Institut de Mécanique Céleste et de Calcul des Ephémérides
[2]International Meteor Organization
[3]GEOPS – Université de Paris Sud
[4]LMCM – Muséum National d'Histoire Naturelle

## Programme and social events

**Lectures**

From 10 to 30 minutes, this duration must always include 2–3 minutes for questions or comments.

**Posters**

Some contributions are not suitable for a lecture and therefore the poster session offers a valuable alternative to present topics without the constraints of an oral presentation.

**Proceedings**

All presentations, both lectures and posters, will be included in the IMC Proceedings as a full paper or at least by an abstract. You are strongly recommended to prepare this article before the IMC while preparing your lecture or poster. Your Proceeding paper should be written in a similar way than a WGN article (see `http://www.imo.net/docs/writingforwgn.pdf` for details). The deadline for submission of your paper is in principle during the IMC in order to assure a timely production of the IMC Proceedings. All papers of the IMC Proceedings are registered on the Harvard-NASA Astrophysic Data System service.

**Workshops**

The presence of many specialists in the same domain makes it easy to have some dedicated sessions. The workshops can take place during the IMC, in the evening hours. It is possible to organise specialised workshops before or after the IMC as the chalet will be still available. This is preferable rather than to organise parallel sessions.

**The SOC**

The IMC is a conference focusing on all technical and scientific aspects of meteor astronomy. All presentations must be registered before the IMC in order to compile the conference program. A team of IMO members acts as SOC to supervise the quality of all presentations, to advice on the IMC program and the content of the IMC Proceedings.

**Socializing aspects**

All topics of a conference could be exchanged in principle by mail or as publication in some journal. A conference offers personal contacts and plenty of time for informal brainstorming. To stimulate these informal contacts the IMC reserves plenty of time for informal events, such as an opening reception, an excursion on Saturday afternoon and informal evenings in the bar and some musical sessions.

## Excursion to CERN

Founded in 1954, the CERN laboratory sits along the Franco-Swiss border, near Geneva. It was one of Europe's first joint ventures and now has 21 member states.

At CERN, the European Organization for Nuclear Research, physicists and engineers are probing the fundamental structure of the universe. They use the world's largest and most complex scientific instruments to study the basic constituents of matter – the fundamental particles. The particles are made to collide together close to the speed of light. The process gives the physicists clues about how the particles interact, and provides insights into the fundamental laws of nature.

The instruments used at CERN are purpose-built particle accelerators and detectors. Accelerators boost beams of particles to high energies before the beams are made to collide with each other or with stationary targets. Detectors observe and record the results of these collisions.

The visit to CERN will take place just after lunch at 1 pm on Saturday afternoon, to arrive at CERN and start the visit from 2 pm to 5 pm. CERN required to have 3 groups of 50 persons maximum with 3 different languages. So the excursion is definitively limited to 150 persons. 3 buses will be used, and English, German and French will be used for the languages during the visit. On your registration form, you must indicate the language of your choice with a second preference, just in case. Mark this in the comment field. We still hope to get two English groups but it will be a late information from CERN, in any case we cannot get 3 English groups.

## Travel information

As Giron is a small village, there is no bus connection, but a shuttle will be available from the closest railway station (Bellegarde sur Valserine) located 30 km from Giron.

**Travelling by plane**

From Geneva International Airport

Clearly the easiest airport to come to Giron is Geneva International Airport, the airport is connected world wide, for European destinations Easy Jet offers low cost tickets. At Geneva airport you have to take a train to go to the main railway station down town Genève-Cornavin, it is a 5 minutes trip. Genève-Cornavin has plenty of trains (SNCF) (every 30 minutes at rush hours, otherwise every hour) to Bellegarde sur Valserine. From Bellegarde it is a 30 minutes trip by car to Giron, we will organise an IMC shuttle from the Bellegarde station to Giron. Tell the IMC LOC about your arrival time at Bellegarde in the registration form.

From Lyon–Saint Exupéry

Lyon–Saint Exupéry is the French second biggest airport, it is connected world wide. To go to Giron you have first to take the Tramway Rhône-Express to Lyon down town railway station Lyon-Part-Dieu (30 minutes trip) and then to take a direct train (SNCF) to Bellegarde sur Valserine (about one hour trip). From Bellegarde it is a 30 minutes trip by car to Giron, we will organise an IMC shuttle from the Bellegarde station to Giron. Tell the IMC LOC about your arrival time at Bellegarde in your registration form.

**Travelling by train**

For the high speed train TGV tickets must be booked in advance as all seats require reservations and no free seats can be guaranteed without booking in advance.

From Geneva-Cornavin

Genève-Cornavin is the main Railway station, it is connected by intercity trains with all Swiss destinations by CFF and many French cities by SNCF (Lyon, Marseille, Paris...). Note that with the high speed TGV it is only 3 hours to go from Paris to Geneva, with many daily trains. Genève-Cornavin has plenty of trains (every 30 minutes at rush hours, every hour otherwise) to Bellegarde sur Valserine. From Bellegarde it is a 30 minutes trip by car to Giron, we will organise an IMC shuttle from the Bellegarde station to Giron. Inform the IMC LOC about your arrival time at Bellegarde when you complete the registration form.

From Bellegarde sur Valserine

Bellegarde is the closest railway station to Giron, there are direct trains from Lyon and Geneva, reservations can be made on the SNCF site. Note that with the high speed TGV it is only $2^{h}40^{m}$ to go from Paris to Bellegarde. From Bellegarde it takes 30 minutes by car to Giron, we will organise an IMC shuttle from the Bellegarde station to Giron. Inform the IMC LOC about your arrival time at Bellegarde when you complete the registration form.

**Travelling by bus**

Geneva is connected to many European cities, the "Gare Routière de Genève" (bus station) is close to Genève-Cornavin railway station. Genève-Cornavin has plenty of trains (every 30 minutes at rush hours, otherwise every hour) to Bellegarde sur Valserine. From Bellegarde it is a 30 minutes trip by car to Giron, we will organise an IMC shuttle from the Bellegarde station to Giron. Tell the IMC LOC about your arrival time at Bellegarde in the registration form.

**Travelling by car**

Giron is close to the Highway A40 between Geneva and Lyon.

**We encourage participants to consider carpooling. A list with sites of departure to Giron is maintained online on the IMC 2014 web site `http://www.imo.net/imc2014/`.**

1. If you come from the west (Paris or Lyon):
   You must leave the Highway A40 at exit 9 (Saint-Germain-de-Joux), take the direction Geneva until Saint Germain de Joux where you will find an indication for Giron.

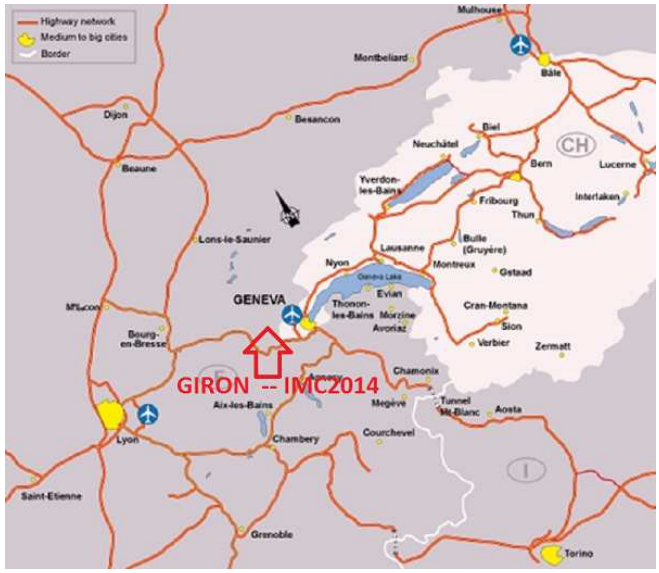


*Figure 4* – Location of Giron and the nearby airports.


*Figure 5* – Major roads in the general area of Giron.

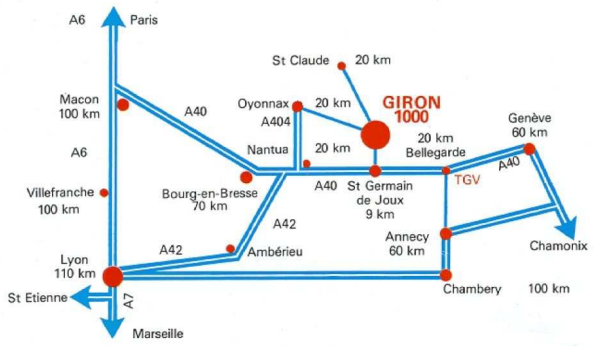


*Figure 6* – Distances between Giron and nearby towns.

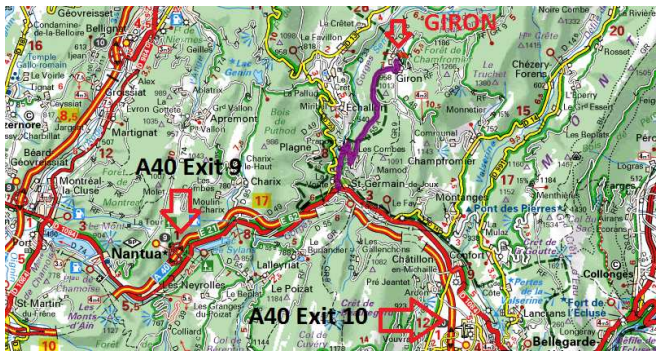


*Figure 7* – Detailed map showing highway exits to reach Giron.

2. If you come from the east (Geneva):
   You must leave the Highway A40 at exit 10 (Châtillon-en-Michaille), take the direction Châtillon-en-Michaille then Saint-Germain-de-Joux where you will find an indication for Giron.

**Carpooling**
Most people travel by car to IMCs often unaware about the travelling plans of others. By encouraging carpooling we want to reduce the number of cars, save you costs by sharing cars and meanwhile help the socializing aspects while travelling to the IMC. We display only limited information for privacy reasons of the participants. If you see a departure site with a ride to Giron that could be of interest to you, contact us (`imc2014@imo.net`) and we will bring you in contact with the right person.

GPS Position of Centre Accueil Montagnard : 46°13′33.95″ N, 5°46′27.54″ E.

## Registration

**Registration fee** The registration fee for the IMC2014 is 170 Euro early fee (before June 30, 185 Euro late fee after June 30 and no later than August 31) for basic accommodation (dormitory with 3 to 5 persons), for a double room you pay 25 Euro extra and 50 Euro for a single room, note that most of the single and double rooms will be available at "Centre Accueil Montagnard" with a limited number, so we cannot serve everybody with this kind of accommodation, our policy will be "first request, first served". The registration fee includes 3 nights accommodation (Thursday, September 18 to Sunday, September 21), full board (breakfast, lunch and dinner), IMC lectures, coffee breaks, excursion to CERN, t-shirt and IMC proceedings. Unless the "no accommodation" option is chosen, accompanying persons older than 12 years sharing a room with a participant must also register as a participant. Contact the organizers if you need an alternative accommodation. So early registration will be 170 Euro (shared room in a dormitory), 195 Euro (double) and 220 Euro (single) for early reservation (before June 30) and 185 Euro (shared room in a dormitory), 210 Euro (double), 235 Euro (single) for late reservation, note that the registration deadline will be 2014 August 31. Do not forget to tell the organisation with who you want to share your room.

You also have the option of the 100 Euro "no accommodation" fee (before June 30, 115 Euro after June 30). This option includes all conference benefits except accommodation and breakfast. In this case, you are responsible for arranging your own accommodation in Giron. We could recommend some alternative chalets if you wish.

**Extra nights**
People who need extra nights at "Chalet de la Fauconière" or at Centre Accueil Montagnard before or after the IMC can reserve these together with their IMC registration. You can choose between shared rooms in dormitory, double rooms or single rooms all with breakfast. For your lunch and dinners you are free to choose on site. Extra rooms can only be booked with the IMC until June 30. After this date you can only register directly with the hosts in Giron.

After 2014 June 30 a late booking fee of 15 Euro is added to the IMC fee.
Registration deadline for the IMC: 2014 August 31.
Deadline for extra nights: 2014 June 30.
Double rooms are only available for participants who register together.

**Cancellation policy**

- before 2014 July 1: full reimbursement, reduced with a cancellation fee of 15 EUR;
- from 2014 July 1 onward, but before 2014 August 31: partial reimbursement of 75 EUR.
- from 2014 September 1 onward: no reimbursement.

## Information and contact details

For further information, latest details, updates, registration and payment, please check the IMC 2014 web site: `http://www.imo.net/imc2014/`. You can also contact the organizers via e-mail: `imc2014@imo.net` or by telephone:
+(33) 14051 2266 (François COLAS)
+(33) 14051 2264 (Jérémie VAUBAILLON)
or by FAX:
+(33) 14633 2834 (IMCCE)

See you soon at IMC 2014!

IMO bibcode WGN-422-colas-imcann NASA-ADS bibcode 2014JIMO...42...35C

# International Meteor Conference
# 2014 September 18–21, Giron, France
# Registration form

**Do not use if you have internet access!** Please register electronically on `http://www.imo.net/imc2014` if you can. Only if you have **no** internet access, fill out one form for each individual participant and return it to Marc Gyssens, IMO Treasurer, Heerbaan 74, B-2530 Boechout, Belgium, as soon as possible. Registration will be guaranteed only after Marc Gyssens has received the full registration fee for the option chosen. We expect this payment to arrive within two weeks after the form.

Name: _____ Address: _____

_____

_____

Phone: _____ Fax: _____ E-mail: _____

- I wish to register for the IMC 2014 from September 18 to 21:
  - ○ I opt for the standard fee (170 EUR early/185 EUR late);
  - ○ I opt for arranging my own accommodation (100 EUR early/115 EUR late).
- I prefer to share a room with _____ (if applicable).
- I prefer a double room (add 25 EUR).
- I prefer a single room (add 50 EUR).
- T-shirt: Size (S–L–XL–XXL): _____ Gender: _____ (included in fee)
- Excursion guide language: English–French–German (please mark)
- Food requirements (e.g., vegetarian, nut allergy): _____
- I intend to travel by _____, together with _____
- I will arrive at _____ (e.g. Sep.18 15h), and my departure is _____ (e.g. Sep.21 14h).
- I need extra nights for the dates _____ (e.g. Sep.22–23) in a single or double room (mark choice).

For participants wishing to contribute to the program:

Lecture (title and author(s)): _____

Requirements: _____

Duration: _____ minutes (including a few minutes for questions and discussion)

Poster(s): _____ Space: _____ $m^2$

Comments:

○ I am paying the entire registration fee for the option selected.

○ I acknowledge having read and I agree with the cancellation policy.

The indicated amount should be sent to IMO Treasurer, Marc Gyssens. The following payment options are available:

- **International bank transfer** to the International Meteor Organization, Mattheessensstraat 60, B-2540, Hove, Belgium, IBAN account number: BE30 0014 7327 5911, BIC bank code: GEBABEBB (Fortis Bank, Belgium). This is recommended for people living in the European Union, as it is no more costly than a domestic bank transfer when done correctly.
- **PayPal payment** to `payment@imo.net`. In that case, we must ask you to add the costs involved in the transaction (3.4% of the total sum including costs, plus 0.35 EUR).
- **Other arrangements**. Please contact the IMO Treasurer for information.

# Meteor science

## Peculiar activity of the September $\varepsilon$-Perseids on 2013 September 9

*Jürgen Rendtel*[1], *Esko Lyytinen*[2], *Sirko Molau*[3], *and Geert Barentsen*[4]

The September $\varepsilon$-Perseids (224 SPE) showed increased activity on 2013 September 9. The outburst was not completely unexpected but was not announced earlier. At the peak position we find a peculiar low population index from video data ($r = 1.45 \pm 0.15$), applying a new technique. For calibration we used magnitude data of the shower off the peak ($r = 2.15 \pm 0.25$) and of sporadic meteors observed during the same period ($r = 2.95 \pm 0.20$). This is significantly lower than the long term average for the September $\varepsilon$-Perseids ($r = 2.50 \pm 0.25$) and indicates that the meteoroids causing the 2013 outburst deviate from the average particle size distribution of the stream. Due to the very low value of $r$, the ZHR and meteoroid flux $F$ reached rather moderate values: ZHR $= 32 \pm 8$, flux $F = 2.3 \pm 0.6 \times 10^{-3}\mathrm{km}^{-2}\mathrm{h}^{-1}$. The centre of the outburst (fit of the peak profile) was found at $\lambda_\odot = 167\,^\circ\!.200 \pm 0\,^\circ\!.005$ corresponding to 2013 September 9, $22^\mathrm{h}18^\mathrm{m}$ UT with a steeper ascending branch and possible sub-peaks. The duration (FWHM) was $0\,^\circ\!.034$, i.e. 50 minutes. Model calculations explain the 2013 outburst of the SPE based on the date and radiant of the 2008 outburst. The large number of minor to medium activity showers in September-October are interpreted as a group of meteoroid streams or trails which cause recognizeable rates only on a few occasions and remain below a detection limit over most of the time.

Received 2014 Mar 28

### 1 Introduction

First reliable visual observations have been obtained and analysed by Hoffmeister (1948). Despite the relatively small number of shower meteors, the shower named September Perseids passed all applied statistical tests and was included in his final list of permanent showers. The radiant and activity parameters match the currently known data quite well. Relations to the weaker $\delta$-Aurigids (current IAU Code: 228 DAU) go back to photographic data published by Drummond (1982) and visual data (Rendtel, 1990; 1993). However, the observational data obtained over more than a decade indicated, that the assumption of one source causing a permanent activity over more than four weeks cannot be proven. A later study of visual and orbital data (Dubietis & Arlt, 2002) indicated that the September $\varepsilon$-Perseids and the $\delta$-Aurigids are two separate showers. Moreover, a detailed analysis of video data revealed a larger number of weak showers with radiants in the Auriga-Lynx-Perseus region in September and October, i.e. on high inclination orbits.

Prior to the 2013 activity enhancement, the September $\varepsilon$-Perseid (IAU Code: 224 SPE) shower produced an unexpected outburst of bright meteors on 2008 September 9 (Rendtel & Molau, 2010). Next, we summarize and analyse the available data for the 2013 activity of the September $\varepsilon$-Perseids. Although the shower is traceable further into the past, there were obviously no further reported outbursts.

[1]Eschenweg 16, 14476 Potsdam, Germany.
Email: jrendtel@web.de
[2]Kehäkukantie 3 B, 00720 Helsinki, Finland.
Email: esko.lyytinen@jippii.fi
[3]Abenstalstr. 13b, 84072 Seysdorf, Germany.
Email: sirko@molau.de
[4]University of Herfordshire, Hatfield AL10 9AB, UK.
Email: geert@barentsen.be

IMO bibcode WGN-422-rendtel-spe2013
NASA-ADS bibcode 2014JIMO...42...40R

### 2 Observations in 2013

#### 2.1 Visual data

In the case of major showers, the main data sources for rates and fluxes are visual and video observations. In periods of usually low rates and no prominent showers—like in September—the coverage by visual observations is rather poor. This was the case in 2008 and also in 2013. So the closest reports listed in Table 1 cover intervals which are a few hours off the peak. Data were either submitted via the online form to the *IMO* webpage (Makarov, Morozov, Ross) or to the `meteorobs` webpage (Gliba, Martsching).

#### 2.2 Video data

The operation of numerous video cameras of the IMO Video Network in each cloudless night provided us with a substantial amount of data also for the period under study (Molau et al., 2013). So we are in the comfortable situation that we may select a consistent sample in terms of the conditions (limiting magnitude and location, i.e. the number of shower meteors) and the time coverage (duration of the observation). This was of particular interest for the determination of the population index. The complete list of contributing observers and camera systems is given in Molau et al. (2013).

#### 2.3 Other observations

Based on radio and video data, notes about enhanced activity of the September $\varepsilon$-Perseids were sent immediately after the event. One of the first reports was sent by Hirofumi Sugimoto of Japan. He kindly provided us with data from radio forward scatter observations he compiled and calculated. In Figure 1 we show the results from eleven Japanese observers, which are not calibrated to other data series.

Due to the large number of video camera stations, there were also numerous orbital data available for the outburst period of the September $\varepsilon$-Perseids. In this

*Table 1* – Compilation of the visual data close to the SPE outburst.

| Observer | Location | Time (UT) Sep 9 | LM | SPE | $h_{\mathrm{Rad}}$ |
|---|---|---|---|---|---|
| Paul Martsching | 93 °6W, 42 °0N | 0520–0620 | 5.60 | 2 | 36° |
| | | 0620–0720 | 5.50 | 8 | 46° |
| | | 0720–0820 | 5.50 | 6 | 56° |
| | | 0820–0920 | 5.40 | 5 | 66° |
| | | 0920–1005 | 5.20 | 1 | 75° |
| Terrence Ross | 103 °6W, 30 °3N | 0655–0800 | 6.34 | 9 | 39° |
| | | 0800–0900 | 6.29 | 6 | 50° |
| Alexei Makarov | 44 °3E, 39 °3N | 1700–1810 | 5.00 | 1 | 11° |
| Alexandr Morozov | 31 °9E, 52 °5N | 1918–2029 | 6.36 | 5 | 30° |
| | | Sep 10 | | | |
| Jürgen Rendtel | 16 °5W, 28 °3N | 0045–0200 | 6.46 | 5 | 54° |
| | | 0200–0315 | 6.46 | 6 | 65° |
| | | 0315–0430 | 6.45 | 8 | 71° |
| | | 0430–0554 | 6.41 | 8 | 67° |
| George Gliba | 78 °9W, 38 °9N | 0530–0630 | 5.80 | 4 | 46° |
| Paul Martsching | 93 °6W, 42 °0N | 0700–0800 | 5.50 | 3 | 72° |
| | | 0800–0900 | 5.70 | 4 | 81° |
| | | 0900–1000 | 5.60 | 1 | 84° |

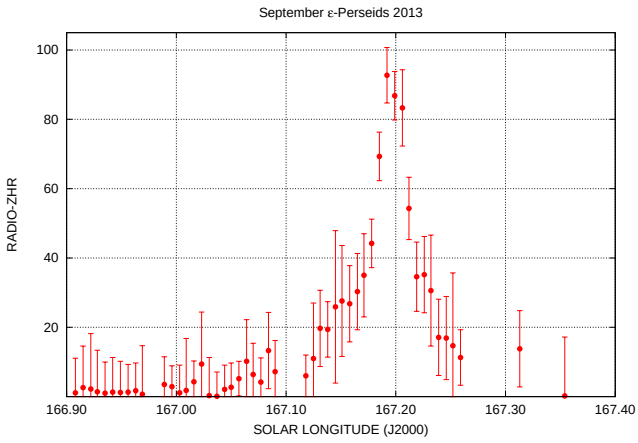


*Figure 1* – ZHR determined from eleven forward scatter radio recordings in Japan of the 2013 SPE outburst. Data and calculations provided by Hirofumi Sugimoto.

*Figure 2* – This fireball of the September $\varepsilon$-Perseids was captured on September 9, $22^{\mathrm{h}}12^{\mathrm{m}}$ UT by Erwin Filimon's all-sky-DSLR camera located at the Gahberg observatory in Austria. He used a Peleng fish eye lens, $f = 8$ mm and a Canon 350D. The image was exposed for 30 seconds. It was the brightest of four fireballs which were images by $22^{\mathrm{h}}16^{\mathrm{m}}$ UT and occurred close to the $r$-minimum/rate peak.

paper, we aim at the characteristics of the meteoroid stream, i.e. the population as well as the rate and the flux.

## 3 The population index

In order to correct appropriately for the true number of shower meteors, we first need to calculate the population index $r$ for the period of the increased rate and the surrounding intervals. The calculation of $r$ from visual data has been well established and is described in detail by Arlt (2003). Recently, analyses of magnitude data obtained from video observations have been processed to derive a population index (Molau et al., 2014). The method has been extended in a way, that the flux data calculated from cameras providing samples under similar conditions (range of limiting meteor magnitude) are compared, applying a range of the population index. The flux density value **and** population index $r$ which give the best coincidence for all camera magnitude groups defines the most probable value of $r$.

The first impression already indicated a peculiar magnitude distribution of the 2013 September $\varepsilon$-Perseids. Even video camera systems with relatively poor limiting magnitudes recorded a large number of

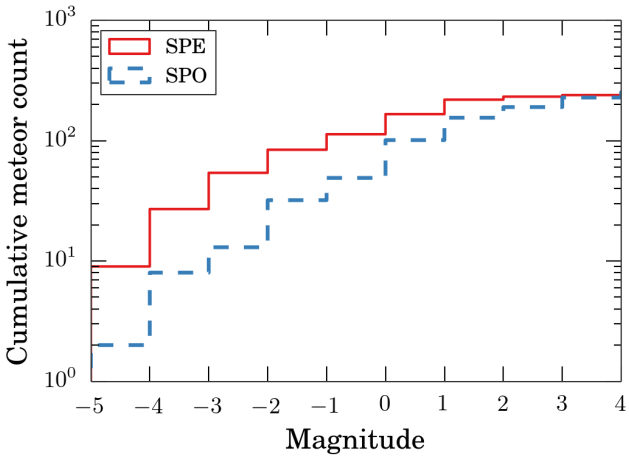


*Figure 3* – For a rough estimate of the population index $r$ the number of observed SPE meteors from video cameras was plotted. The slope of the number per magnitude class hints at a very low $r$.

shower meteors. Furthermore, there were several reports of fireballs as well as numerous fireball photos such as the one shown in Figure 2.

### 3.1 Visual data

The visual data close to the 2013 outburst are listed in Table 1. Despite the low number of shower meteors we calculated values of $r$ before and after the actual activity peak. Of course, the error margins are large, but the four obtained values give a consistent result. We find a value of $r = 2.15 \pm 0.25$ for the intervals listed in Table 1. This is considerably lower than the average $r = 2.50 \pm 0.23$ calculated from the period 1990–2007. This average shows only little variation over the the interval $\lambda_\odot = 160°$ to $175°$. We particularly checked the period corresponding to the position of the 2008 and 2013 outbursts but there is no indication that there is a recurrent longitude with a lower $r$.

### 3.2 Video data

A very first and elementary approach was made by just considering the observed number of bright shower meteors (omitting limitations occurring close to the limiting magnitude of the cameras). This yielded a rough estimate of $r = 1.4$ (Figure 3).

More detailed and reliable data can be calculated using a new approach of the $r$-calculation (Molau et al., 2014). The result for the peak period centered at $\lambda_\odot = 167\,^\circ\!.200 \pm 0\,^\circ\!.005$ corresponding to 2013 September 9, $22^\mathrm{h}18^\mathrm{m}$ UT is an extremely low $r = 1.45 \pm 0.15$ for the peak period.

For calibration reasons and to ensure that the result is not an artefact caused by an observational bias or a systematic effect of the method, we checked the result obtained from video camera data with two other values:

(i) we calculated the population index $r$ for sporadic meteors observed by visual observers and video cameras during the same period. The results are $r = 2.92 \pm 0.26$ (visual) and $r = 3.0 \pm 0.2$ (video).

(ii) we compared the population index $r$ for SPE meteors observed after the peak period and find $r = 2.02 \pm 0.33$ (visual). Considering only the video magnitude data beyond $\lambda_\odot = 167\,^\circ\!.260$ (fitting the interval covered by visual data) we find $r = 2.24 \pm 0.20$ based on only 70 meteors. Starting the reference interval earlier at $\lambda_\odot = 167\,^\circ\!.250$, the value is $r = 2.14 \pm 0.15$ (80 meteors).

Both pairs, the sporadic and post-peak SPE data, prove that the very low value of $r$ found for the activity peak period is not a result of an error in the method or another systematic effect. So we conclude that the particle composition is completely different from the average composition of the September $\varepsilon$-Perseid stream. The difference was still obvious later in the night 2013 September 9/10 after the peak when the activity level had returned to the average level (for example during the observation at Tenerife in the morning of September 10, see Table 1) with a considerable number of bright and even photographic meteors.

### 3.3 r-profile

So we conclude that we observe a distinguishable meteoroid population during the 2013 outburst which does not occur in the average stream. The results from the 2013 outburst and the average are shown in Figure 4. The minimum population index $r = 1.45 \pm 0.15$ occurred at 2013 September 9, $22^\mathrm{h}18^\mathrm{m}$ UT at the position of the activity peak.

A similar description of the outburst composition was given for the 2008 outburst of the September $\varepsilon$-Perseids, although no sufficient data is available to calculate a reliable population index. Nevertheless, the two events indicate that the central region of the stream consists of an peculiar particle size distribution. Values of $r$ in the range below 2.0 have been observed only on a few occasions. Most of these events have been found to consist of meteoroids trapped in resonances with Jupiter's orbital period (as an example, see Rendtel (2007) for the Orionids in 2006) and thus have seen a distinct selection process in their evolution. The lowest values have been calculated for the broad 1998 Leonid fireball maximum ($r = 1.19 \pm 0.02$ at $\lambda_\odot = 234\,^\circ\!.43$; Arlt, 1998) and the Orionid maximum in 2006 ($r = 1.58 \pm 0.08$ at $\lambda_\odot = 207\,^\circ\!.875$; Rendtel, 2007), both comprised of resonant meteoroids. Further events with low values of the population index are listed in Table 2.

## 4 The Zenithal Hourly Rate

Applying the calculated profile of $r$ with the low value valid for most of the actual peak period, we find the ZHR profile shown in Figure 5. It is a combination of the few visual data outside the peak and the peak period covered by video data. The peak is slightly asymmetric with a steeper ascending branch. A simple square fit of the peak profile is centered at $\lambda_\odot = 167\,^\circ\!.200 \pm 0\,^\circ\!.005$ (corresponding to $22^\mathrm{h}18^\mathrm{m}$ UT on 2013 September 9). The width (FWHM) is $0\,^\circ\!.034$ or 50 minutes. The video and visual data obtained close to the peak period.

*Table 2* – Lowest values of the population index $r$ observed in streams (sorted to lowest $r$). The June Bootids of 1998 are added for comparison with another resonant meteoroid population although values of $r \geq 2.0$ are common near the centre of major showers.

| Event | Population index $r$ | Remarks and reference |
|---|---|---|
| Leonids 1998 | $1.19 \pm 0.02$ | "Fireball storm", resonant meteors; Arlt, 1998 |
| Sept. $\varepsilon$-Perseids 2013 | $1.45 \pm 0.15$ | This work |
| Orionids 2006 | $1.58 \pm 0.08$ | Resonant meteors; Rendtel, 2007 |
| Leonids 2001 | $1.60 \pm 0.05$ | Background component; dust trails had $r \approx 2.2$ Arlt et al., 2001 |
| Geminids 2004 | $1.73 \pm 0.04$ | End of peak plateau; Arlt & Rendtel, 2006 |
| Perseids 1993 | $1.75 \pm 0.05$ | Dust trail; Rendtel, 1993 |
| Perseids 1994 | $1.76 \pm 0.02$ | Dust trail; Rendtel, 1994 |
| Perseids 1997 | $1.78 \pm 0.05$ | Dust trail; Arlt & Rendtel, 1997 |
| Orionids 2007 | $1.85 \pm 0.10$ | Resonant meteors; Arlt et al., 2008 |
| June Bootids 1998 | $2.22 \pm 0.07$ | Resonant meteors; Rendtel et al., 1998 |

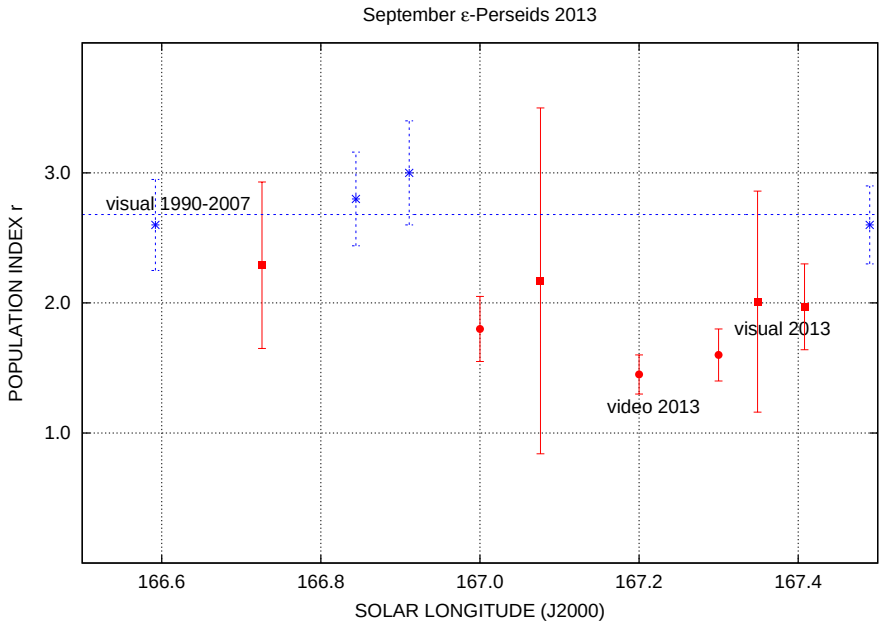


*Figure 4* – Population index $r$ of the 2013 SPE outburst calculated from visual (squares) and video (dots) data. For comparison, we add the average $r$ obtained from visual observations in the period 1990–2007 (asterisks).

## 5 Flux density

Seen the ZHR and very low value of the population index $r$, it is no surprise that the meteoroid flux is not exceptionally high. This holds even more for the spatial number density because of the high geocentric velocity.

The basics of the calculation from visual data have been derived by Koschack & Rendtel (1990). Peculiarly low (as well as high) figures of $r$ lead to unexpected differences in the appearance and the true numbers (examples shown in Rendtel, 2014).

Using the `meteorflux.io` webpage we can obtain a flux graph using the data of all video camera systems which were active in the selected interval. The current version does not yet allow to apply a $r$-profile but a fixed value. We adjusted the parameters to optimize between the number of data points and a sufficient sample per bin and used the population index profile as calculated before and allowed bins as short as possible to check for the precise start and end as well as for possible structures within the narrow peak. Although this probably is close to the limits, we see not only the asymmetric shape of the peak, but find that there is the highest flux peak immediately at the beginning at $\lambda_\odot = 167\,^\circ\!.191 \pm 0\,^\circ\!.003$ (corresponding to $22^\mathrm{h}05^\mathrm{m}$ UT on 2013 September 9). Another sub-peak occurs at $\lambda_\odot = 167\,^\circ\!.209 \pm 0\,^\circ\!.003$ ($22^\mathrm{h}32^\mathrm{m}$ UT). A late interval with a flux exceeding the neighbouring values is found at $\lambda_\odot = 167\,^\circ\!.223 \pm 0\,^\circ\!.003$ ($22^\mathrm{h}52^\mathrm{m}$ UT).

The SPE peak flux density of $F = 2.3 \pm 0.6 \times 10^{-3}\mathrm{km}^{-2}\mathrm{h}^{-1}$ is comparable with the value found for the $\alpha$-Capricornids with $F = 2.5 \pm 0.4 \times 10^{-3}\mathrm{km}^{-2}\mathrm{h}^{-1}$ but is much below the typical major stream fluxes such as the Perseids ($F = 42 \pm 4 \times 10^{-3}\mathrm{km}^{-2}\mathrm{h}^{-1}$) and the Geminids ($F = 75 \pm 5 \times 10^{-3}\mathrm{km}^{-2}\mathrm{h}^{-1}$).

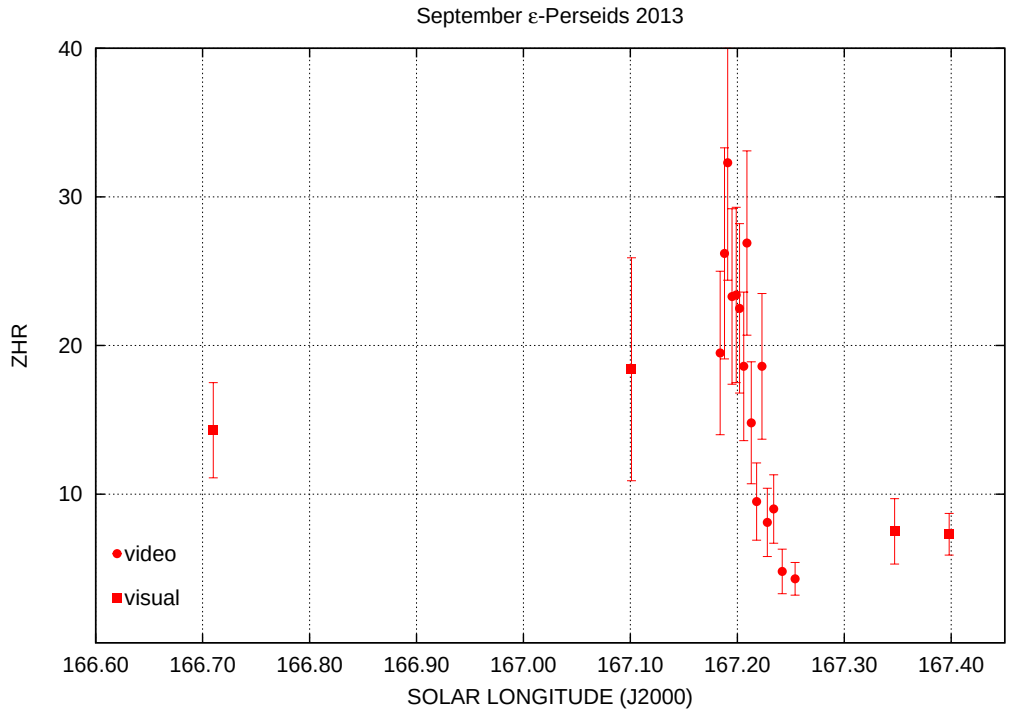


*Figure 5* – ZHR profile of the 2013 SPE outburst calculated from visual (squares) and video (dots) data, applying the $r$-profile derived from the video data (peak period) and the visual data (outside the peak).

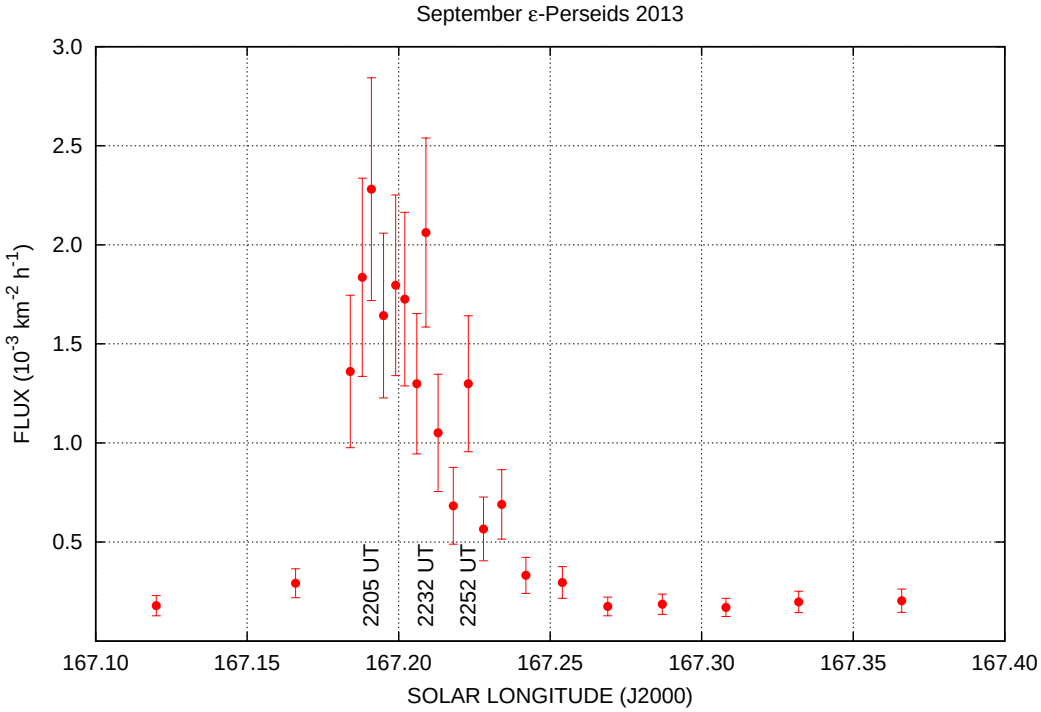


*Figure 6* – Flux calculated from data of all video camera systems of the IMO Video Meteor Network. The parameters set for this plot are: 12 meteors per bin, min. collecting area 15000 km$^2$×h, bin length 5 min–120 min, $r$-profile, $\gamma = 1.4$, $h_{\mathrm{Rad}} \geq 10°$.

## 6 Modelling the outbursts

Generally, outbursts of long period comets are caused by meteoroid dust trails that pass in the vicinity of the Earth orbit within a few million kilometers and the same trail persists for several tens or even hundreds of years. Planetary perturbations shift the trail with periods of each planet's orbital period. Occasionally an encounter with the Earth's orbit at the time when the Earth also is in the same crossing node is possible.

A model considering the motion of the planetary system barycenter was first suggested by Jenniskens (1997) to explain the outburst of the $\alpha$-Monocerotids (246 AMO). A more complete theory suitable for general trail calculations with exact timing was published

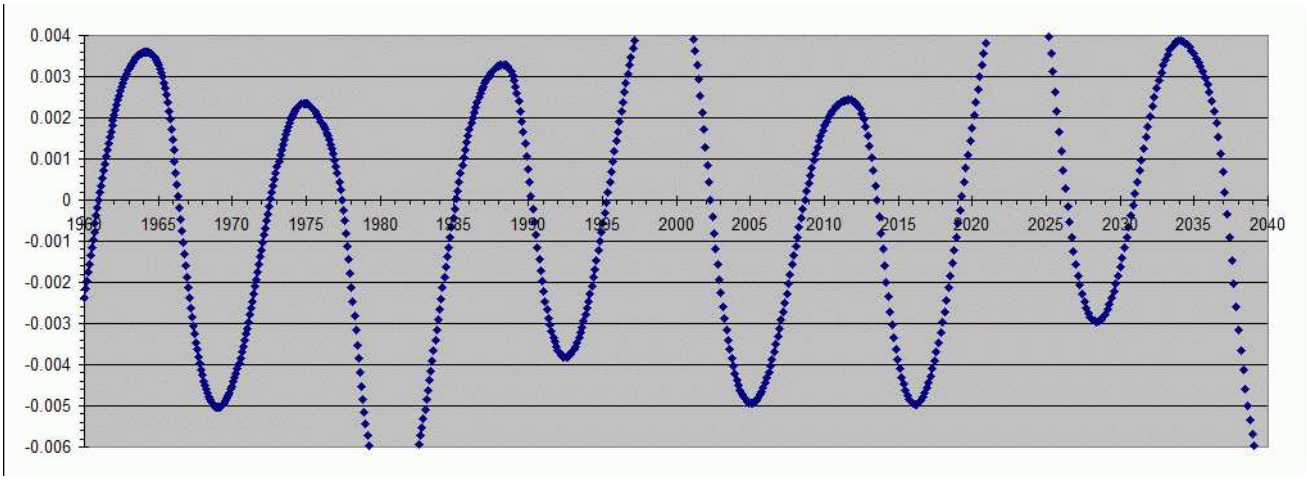


*Figure 7* – Results of the model of the SPE stream which included the prediction of the 2013 outburst for the period until 2040. Each year mark on the abscissa points at the beginning of the given year and the vertical axis shows the $r_D - r_E$ value.

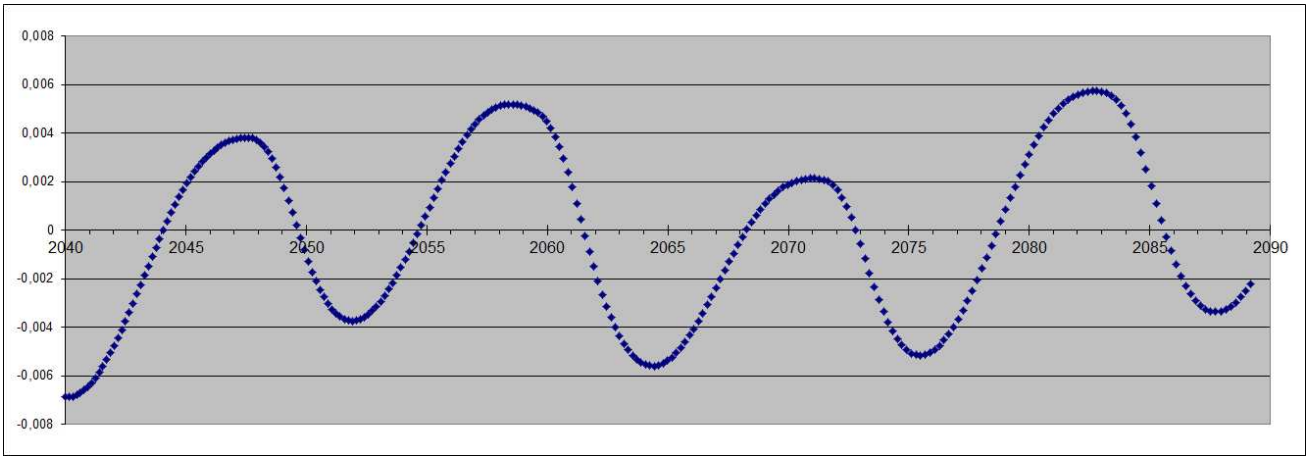


*Figure 8* – Model calculation of the further SPE stream evolution continuing the model shown in Figure 7. Each year mark on the abscissa points at the beginning of the year and the vertical axis gives the $r_D - r_E$ value.

by Lyytinen & Jenniskens (2003). It became evident that such outbursts can only occur from one revolution trails. Parent comets closer to the applicable smaller orbital period range (about 300 years, like the Lyrids) can also produce weaker outbursts from trails which are older than one revolution. The method may be applicable for orbital periods up to about 2000 years. The theory would also hold for longer orbital periods but the trails will quickly become much too long and stretched to create a noticeable outburst. A particularly big comet could in principle push that limit further. Jenniskens & Docters van Leeuwen (1995) published predictions for several outburst cases that have been observed only once. The 2013 SPE may be one of this type as suspected in CBET 3652. If the presumptions are correct, we can derive predictions of further outbursts knowing only the shower's peak time and radiant coordinates. The accuracy of the radiant position is the limiting factor for the prediction.

Known examples of medium-long period meteor showers and outbursts are the Lyrids (006 LYR) and Aurigids (206 AUR) with known parent comets and the already mentioned $\alpha$-Monocerotids with no known parent comet. Perhaps the (annual) October Camelopardalids (281 OCT) is another example, although their nature as a Halley-type or long period type requires further investigation.

In the case of outbursts with no known parent comet we have no information how central the encounter with the trail has been. From all known cases we can estimate a typical distance which is of the order of a few times of 0.0001 au or possibly smaller. For larger minimum distances the expected rates decrease quickly.

After the 2008 September $\varepsilon$-Perseid outburst there were thoughts that it was one of a long period type. This outburst was not visible from Europe, but via Jeff Brower observations of three reliable multi-station meteors became available. Based on this data an orbit was calculated. Because the velocity difference of meteors from long period comet orbits and from Halley-type orbits is very small it was not possible to distinguish between these two alternatives. The average $1/z$ corresponded to the Halley-type, but it was not accurate enough to judge for. While some of the other events with extremely low $r$-values listed in Table 2 are caused by resonant meteoroids, this is not the case for both the 2008 and 2013 SPE outbursts. This is also supported by the very well defined edges of the narrow peak and

the accuracy of the two fitted encounters. Both indicate that the Earth was close to the stream's centre. Further, a tendency to see an increased portion of larger meteoroids is expected if an encounter happens prior to the comet approach.

A medium long-period comet computer model clearly predicted an SPE outburst for September 2013. Unfortunately, this result was somehow "forgotten". It seems that there was a read error of the year from the graph, and the 2013 outburst was neither anticipated nor announced. Further, the uncertainty about the nature of the 2008 outburst—long period or not—was a reason for low expectations.

The calculated trail is shown in Figure 7. The marks refer to the beginning of the given year. The vertical axis gives the $r_D - r_E$ value, that is the difference of the calculated descending node distance between the trail and the Earth's orbit in au. In the computer model the nodal shifts caused by planetary perturbations are included. The model gives a peak for 2013 September 9, $22^{\mathrm{h}}15^{\mathrm{m}}$ UT (Solar longitude $167\overset{\circ}{.}200$) based on the data from the 2008 outburst.

The calculations yielded an ecliptic crossing of the trail in 2013 which is 0.00036 au closer to the Sun than in 2008. However, it remains uncertain how central each of the two encounters were. So it could be possible that both encounters had a distance of about 0.002 au, for example. Future encounters are indicated from Figure 7 in 2026 and 2030 but the minimum distance may be not close enough to cause outbursts.

## 7 Conclusions

Video observations show a short lived peak of the September $\varepsilon$-Perseids centered at $\lambda_\odot = 167\overset{\circ}{.}200 \pm 0\overset{\circ}{.}005$ (corresponding to $22^{\mathrm{h}}18^{\mathrm{m}}$ UT on 2013 September 9). The width (FWHM) of the fitted peak profile is $0\overset{\circ}{.}034$ or 50 minutes. The activity profile is slightly asymmetric with a steeper ascending branch. The highest flux peak occurs at the beginning at $\lambda_\odot = 167\overset{\circ}{.}191 \pm 0\overset{\circ}{.}003$ ($22^{\mathrm{h}}05^{\mathrm{m}}$ UT). Further peaks are found at $\lambda_\odot = 167\overset{\circ}{.}209 \pm 0\overset{\circ}{.}003$ ($22^{\mathrm{h}}32^{\mathrm{m}}$ UT) and at $\lambda_\odot = 167\overset{\circ}{.}223 \pm 0\overset{\circ}{.}003$ ($22^{\mathrm{h}}52^{\mathrm{m}}$ UT).

The most peculiar feature of the 2013 SPE outburst is their low population index $r = 1.45 \pm 0.15$ in the central region. Even at the "wings" of the outburst we find a low $r = 2.15 \pm 0.25$ from both visual and video observations in 2013. This is significantly below the long-term average $r = 2.50 \pm 0.25$ found for the September $\varepsilon$-Perseids in the period 1990–2007 and belongs to the lowest values of $r$ on record. Due to the low value of $r$, the large number of observable meteors and in particular of bright meteors translates into rather low figures of ZHR and flux.

The 2013 SPE outburst is another event related to one of the showers occurring in September–October from high-inclination orbits in the Auriga-Perseus-Lynx region. It was already speculated earlier that this may be a complex of streams related to a group of comets on medium to long orbital periods. Another example with significantly more excentric orbits is the Kreutz comet group.

The difficulty to isolate the individual radiants from video data in previous studies (see, for example, Rendtel & Molau, 2010) can be interpreted such, that the activity of the showers varies from one return to another and we recognize the activity only if it exceeds a certain threshold. In this context, the enhanced activities of the September $\varepsilon$-Perseids may just be significant "peaks" exceeding over the background. This may also be an explanation why the $\delta$-Aurigids are currently at the detection limit and are observable in October only, while the shower obviously produced a substantial number of photographic fireballs in the 1960-s which led to Drummond's (1982) analysis.

We assume that the 2008 and 2013 enhancements are related to an approach of an yet unknown parent to the inner Solar system. However, as we know from showers related to other medium or long-period comets, activity outbursts are not related to the vicinity of the parent (Lyytinen & Jenniskens, 2003). The Lyrid outburst in 1982 (Rendtel & Arlt, 2007) caused by C/1861 G1 (Thatcher) with an orbital period of 415 years, the 1995 $\alpha$-Monoceroitid outburst with no known parent yet (Rendtel, Brown, & Molau, 1995) and the 2007 Aurigid outburst (Jenniskens & Vaubaillon, 2007; Rendtel, 2007) of C/1911 N1 (Kiess) are two prominent examples. If the suspected stream pattern is true, we may expect future sudden activity signs at various positions from high inclination showers of the "Perseus-Auriga complex". A literature and database search yielded no hint at increased SPE rates in the past. Considering the model shown in Figure 7, the returns in 1972 and 1975 (less likely) may have provided earlier activity.

## Acknowledgements

We are grateful to Hirofumi Sugimoto of Japan for providing us with data of Japanese radio observers. Erwin Filimon of Austria kindly permitted to reproduce his impressive SPE fireball image. The analysis was only possible thanks to the regular effort of the video camera operators in the IMO Video Meteor Network.

## References

Arlt R. (1998). "Bulletin 13 of the International Leonid Watch: the 1998 Leonid meteor shower". *WGN, Journal of the IMO, Journal of the IMO*, **26**, 239–248.

Arlt R. (2003). "Bulletin 19 of the International Leonid Watch: population index study of the 2002 Leonid meteors". *WGN, Journal of the IMO*, **31**, 77–87.

Arlt R., Kac J., Krumov V., Buchmann A., and Verbert J. (2001). "Bulletin 17 of the International Leonid Watch: first global analysis of the 2001 Leonid storms". *WGN, Journal of the IMO*, **29**, 187–194.

Arlt R. and Rendtel J. (1997). "First analysis of the 1997 Perseids". *WGN, Journal of the IMO*, **25**, 207–209.

Arlt R. and Rendtel J. (2006). "The activity of the 2004 Geminid meteor shower from global visual observations". *MNRAS*, **367**, 1721–1726.

Arlt R., Rendtel J., and Bader P. (2008). "The 2007 Orionids from visual observations". *WGN, Journal of the IMO*, **36**, 55–60.

Drummond J. (1982). "A note on the $\delta$-Aurigid meteor stream". *Icarus*, **51**, 655–659.

Dubietis A. and Arlt R. (2002). "The current delta Aurigid meteor shower". *WGN, Journal of the IMO*, **30**, 168–174.

Hoffmeister C. (1948). *Die Meteorströme*. Barth, Leipzig.

Jenniskens P. (1997). "The $\alpha$-Monocerotids meteor outburst: the cross section of a comet dust trail". *Planet. Space Sci.*, **45**, 1649–1652.

Jenniskens P. and Docters van Leeuwen G. (1995). "Meteor stream activity. II. meteor outbursts". *Astron. Astrophys.*, **295**, 206–235.

Jenniskens P. and Vaubaillon J. (2007). "Aurigid predictions for 2007 September 1". *WGN, Journal of the IMO*, **35**, 30–34.

Koschack R. and Rendtel J. (1990a). "Determination of spatial number density and mass index from visual meteor observations (I)". *WGN, Journal of the IMO*, **18**, 44–58.

Koschack R. and Rendtel J. (1990b). "Determination of spatial number density and mass index from visual meteor observations (II)". *WGN, Journal of the IMO*, **18**, 119–140.

Lyytinen E. and Jenniskens P. (2003). "Meteor outbursts from long-period comet dust trails". *Icarus*, **162**, 443–452.

Molau S., Kac J., Crivello S., Stomeo E., Barentsen G., and Goncalves R. (2013). "Results of the IMO Video Meteor Network – September 2013". *WGN, Journal of the IMO*, **41**, 207–211.

Molau S., Kac J., Crivello S., Stomeo E., Barentsen G., and Goncalves R. (2014). "Results of the IMO Video Meteor Network – November 2013". *WGN, Journal of the IMO*, **42**, 25–30.

Rendtel J. (1990). "Radiants in the Per-Aur region between August and October". In Heinlein D. and Koschny D., editors, *Proc. IMC 1989*. pages 37–41.

Rendtel J. (1993a). "Delta Aurigids and September Perseids". In Štohl J. and Williams I., editors, *Meteoroids and their parent bodies. Proc. Int. Astron. Symp., Smolenice*. pages 185–188.

Rendtel J. (1993b). "Perseids 1993: a first analysis of global data". *WGN, Journal of the IMO*, **21**, 235–239.

Rendtel J. (1994). "A first global analysis of the 1994 Perseids". *WGN, Journal of the IMO*, **22**, 205–209.

Rendtel J. (2004). "Almost 50 years of visual Geminid observations". *WGN, Journal of the IMO*, **32**, 57–59.

Rendtel J. (2007a). "Three days of enhanced Orionid activity in 2006 - meteoroids from a resonance region?". *WGN, Journal of the IMO*, **35**, 41–45.

Rendtel J. (2007b). "Visual observations of the Aurigid peak on 2007 Sep 1". *WGN, Journal of the IMO*, **35**, 108–112.

Rendtel J. (2014). "From rates to fluxes of meteoroid streams". In Gyssens M., Roggemans P., and Żołądek P., editors, *Proc. IMC 2013*. page (submitted).

Rendtel J. and Arlt R. (2007). "The Lyrid meteor shower in 2006 and 2007". *WGN, Journal of the IMO*, **35**, 74–78.

Rendtel J., Arlt R., and Velkov V. (1998). "Surprising activity of the 1998 June Bootids". *WGN, Journal of the IMO*, **26**, 165–172.

Rendtel J., Brown P., and Molau S. (1995). "The 1995 outburst and possible origin of the alpha-Monocerotid meteoroid stream". *MNRAS*, **279**, L31–L36.

Rendtel J. and Molau S. (2010). "Meteor activity from the Perseus-Auriga region in September and October". *WGN, Journal of the IMO*, **38**, 161–166.

*Handling Editor:* Javor Kac

This paper has been typeset from a LaTeX file prepared by the authors.

# The September epsilon Perseids in 2013

*Štefan Gajdoš[1], Juraj Tóth[1], Leonard Kornoš[1], Jakub Koukal[2], and Roman Piffl[2]*

An unexpected high activity (outburst) of the meteor shower September epsilon Perseids (SPE) was observed on 2013 September 9/10. The similar event occurred in 2008. We analysed SPE meteors observed in a frame of the European stations network (EDMONd) and collected in the video meteor orbits database EDMOND. Also, we compared two AMOS all-sky video observations of SPE meteors, performed at the Astronomical and Geophysical Observatory in Modra (AGO) and Arborétum in Tesárske Mlyňany (ARBO) stations of the Slovak Video Meteor Network (SVMN). We obtained activity profiles of the 2013 SPE outburst during four hours around its maximum. Along with SPE activity profiles binned at 10 minutes for single-station meteors, we gained orbital characteristics of SPE meteors observed during the outburst, as well as a mean orbits of the SPE meteor stream in interval 2001–2012. The SPE outburst was confirmed by radio forward-scatter observations as well. The obtained observational results might be the starting point for modeling and explanation of SPE outbursts.

Received 2014 March 7

## 1 Introduction – SPE overview

The September epsilon Perseids meteor shower (SPE, IAU MDC code 208) has a quite long and interesting history. The name was applied for the first time by Denning (1882) who noticed displays of SPE in observations performed on 1869–1880. Hoffmeister (1948) described the SPE by radiant position with coordinates at RA = 53°, DEC = +41°. Drummond (1982) established a new meteor shower – the Delta Aurigids (DAU) active mainly in October – one century after Denning. For a long time, discrepancies were present due to misleading timing of the DAU activity. Recently, Rendtel (1993) searched the IMO database of visual meteors for radiants in area of Perseus and Auriga constellations. He found two separate sources of meteors active in September and October. Rendtel's analyses clarified the correct periods of activity of the two subsequent meteor showers, also. In the meantime, the SPE were misleadingly attributed as an early appearance of the DAU. The September Perseids are thought active from September 7 to 23 with the maximum on September 12, whilst the DAU are active in the period September 29 – October 18 (Jenniskens, 2006). No source gives ZHR of SPE meteor shower, and no outbursts are mentioned in previous history of September Perseids (Jenniskens, 2006). Besides, SonotaCo (2009) identified September-Perseids meteor shower distinctly through 109 SPE meteors (Table 3 therein), with radiant coordinates as presented in the summary Table 5. Designations as Xi Perseids, September Perseids, September (beta) Perseids and September (epsilon) Perseids are to be found throughout literature.

The SPE were found in the IAU MDC database of precise photographic meteor orbits. Terentjeva (1989) used the name Xi Perseids in her list of 78 bolide meteor showers, for the SPE shower. By using the D-criterion (Southworth & Hawkins, 1963) Porubčan & Gavajdová (1994) found SPE bolides in the IAU MDC database of 3518 meteor orbits. Ten years later, Gajdoš & Porubčan (2005) found September Perseids meteors in the extended and homogenized database of 4581 orbits.

An outburst of mostly bright September Perseid meteors (SPE) occurred on 2008 September 9. Jenniskens et al. (2008) and other observers (Cooke, 2008; Hergenrother, 2008) reported the outburst with the peak at $8^{\rm h}20^{\rm m} \pm 20^{\rm m}$ UT (solar longitude $\lambda_\odot = 166\,\overset{\circ}{.}9$). At the Astronomical and Geophysical Observatory (AGO) in Modra, we covered three full nights in the period of 2008 September 6 – 9. We concentrated on detection, as well as confirmation of a rising activity of the shower. We confirmed that neither outburst nor higher activity of SPE meteors started before $3^{\rm h}20^{\rm m}$ UT, on 2008 September 9, hence we constrained a start of the four-hour-long SPE outburst (Gajdoš et al., 2008). A summary of all above mentioned data along with our new results, presented in this work, are shown in Table 5.

## 2 Observation of the 2013 outburst of the SPE

In this work, we present an analysis of meteor observations performed by TV/video stations of the European network EDMONd - European viDeo Meteor Observation Network (Kornoš et al., 2013) on 2013 September 9/10. Technical details and operation rules of individual local networks or stations can be found on web-pages of local operators. The EDMONd is a continuously growing network in spread, with coverage from the East to the West Europe. The densest net of TV meteor stations range across the Central-to-South European region. "Extremes" span from UK in the West to the Eastern Ukraine (Figure 1). The EDMONd is operated with various video systems, indeed with individual technical (PC/OS, lenses, detector, intensifier, detection and analysing software, sensitivity, field of view) and observational characteristics. Nontheless, the observations are comparable and complementary at the same time.

EDMONd network observations with cooperation and data sharing resulted to a creation of the database of meteor orbits EDMOND – European viDeo MeteOr

[1]Faculty of Mathematics, Physics and Informatics, Comenius University, Mlynská dolina, 842 48 Bratislava, Slovak Republic
[2]CEMeNt – Central European Meteor Network

IMO bibcode WGN-422-gajdos-spe2013
NASA-ADS bibcode 2014JIMO...42...48G

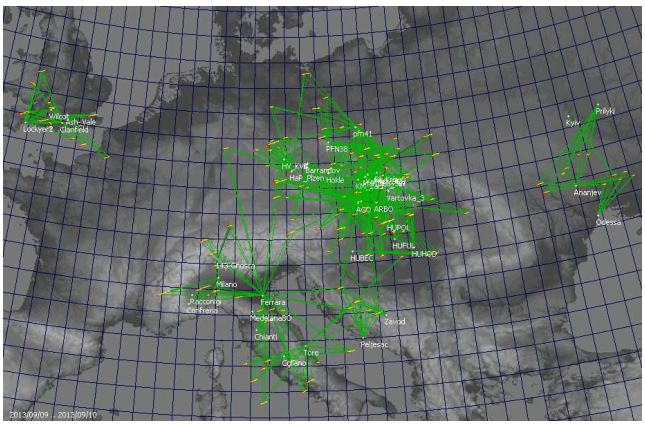


*Figure 1* – EDMONd observing sites distribution and multi-station SPE meteors recorded during the night of 2013 September 9/10.

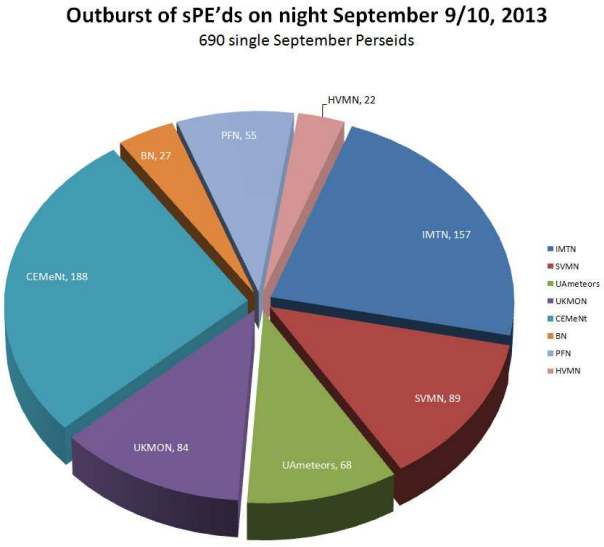


*Figure 2* – Total counts of SPE meteors observed by EDMONd stations during the whole night of 2013 September 9/10 – a diagram showing the contribution of local nets.

Database (Kornoš et al., 2014). The database contains more than 1.6 million single-station meteors and 83 369 reliable multi-station meteor orbits. Altogether eight local nets with acceptable weather conditions took part in observations the night 2013 September 9/10. An overview of the EDMONd operation, and counts of observed SPE meteors during the 2013 SPE outburst, is shown in the pie-chart (Figure 2).

## 2.1 SPE activity profile from all-sky observations

The all-sky observations of the SPE outburst were performed by video systems AMOS at the AGO in Modra and Arborétum in Tesárske Mlyňany (ARBO) on 2013 September 9/10. The system AMOS is described by Zigo at al. (2013) and is able to capture meteors down to visual magnitude $+3.5^{\mathrm{m}}$. Two stations performed observation over the whole night and we captured the whole display of the SPE outburst.

At the AGO we captured 60 SPE meteors between $21^{\mathrm{h}}$ UT (on September 9) and $01^{\mathrm{h}}$ UT (on September 10). In the same time span, 42 SPE meteors were recorded at the ARBO station. At both stations, 33 SPE meteors were simultaneously detected (Table 1). Considering negligible interference by clouds, the different counts of detected SPE meteors by one third (the same ratio is valid for overall detected meteors, including non-SPE meteors, for the whole night) can be accounted for instrumental difference and local sky conditions of the two stations. Nevertheless, we tried to find out profiles of SPE activity over four hours around its maximum, for both stations separately, and to compare them.

*Table 1* – Counts and ratios of SPE meteors recorded at the AGO and ARBO stations, also number of double-station SPE meteors.

| Interval of 4-hours on 2013 Sep 9/10 | Station AGO | Station ARBO | Double-station SPE meteors |
|---|---|---|---|
| Number of SPEs | 60 | 42 | 33 |
| Common SPEs ratio | 55% | 79% | – |

The numbers of SPE meteors binned in 10 minutes intervals were corrected for radiant elevation for both stations. Other corrections were not applied. Histograms (Figure 3) depict the SPE activity behaviour. The diagrams are apparently the same in profile at both stations, with only small deviations caused by different SPE meteor counts. We tried a binning in shifted intervals (5 or 10 minutes) but no significant differences occur and the resulting histograms are almost identical.

The SPE outburst began suddenly with a steep increase in meteor frequency, with the first display at about $21^{\mathrm{h}}30^{\mathrm{m}}$ UT. It continued with a broader maximum phase with a first peak at about $22^{\mathrm{h}}05^{\mathrm{m}}$ UT $\pm 10$ minutes, followed by some decrease (gap) of SPE activity, before its next peak at about $22^{\mathrm{h}}40^{\mathrm{m}}$ UT $\pm 10$ minutes. Afterwards, the SPE activity fell to a smooth level, with a frequency similar to the usual SPE maxima in recent years (ZHR 1 to 3 meteors). The broader maximum (with two separated peaks) began and ended with strict "edges". The main phase ended at the last little peak at about $23^{\mathrm{h}}05^{\mathrm{m}}$ UT $\pm 10$ minutes. According to our records, the maximum (the outburst) lasted no more than two hours.

Single-station SPE radiants for both stations were determined by Gajdoš & Tóth (2013). Here, we only report the mean SPE radiant with coordinates at RA $= 47\overset{\circ}{.}4 \pm 0\overset{\circ}{.}1$, DEC $= +39\overset{\circ}{.}5 \pm 0\overset{\circ}{.}1$ for solar longitude $\lambda_{\odot} = 167\overset{\circ}{.}2$. Individual values are in Table 5. However, radiants derived from multi-station meteor orbits are more reliable and correct. Thus we calculated radiants of SPE orbits based on EDMOND data. The results are presented in Chapter 2.3.

## 2.2 SPE 2013 activity profile from EDMOND

All single-station SPE meteors detected by EDMONd from the evening at Ukrainian stations on 2013 September 9 to the morning at UK stations on 2013 September

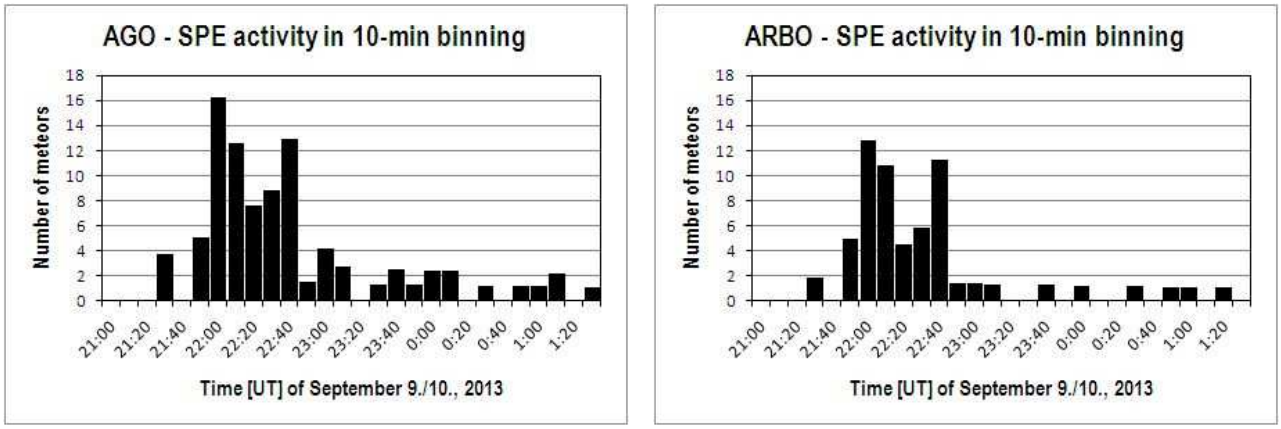


*Figure 3* – Number of SPE meteors detected at AGO (left) and ARBO (right) stations binned in 10-min intervals.

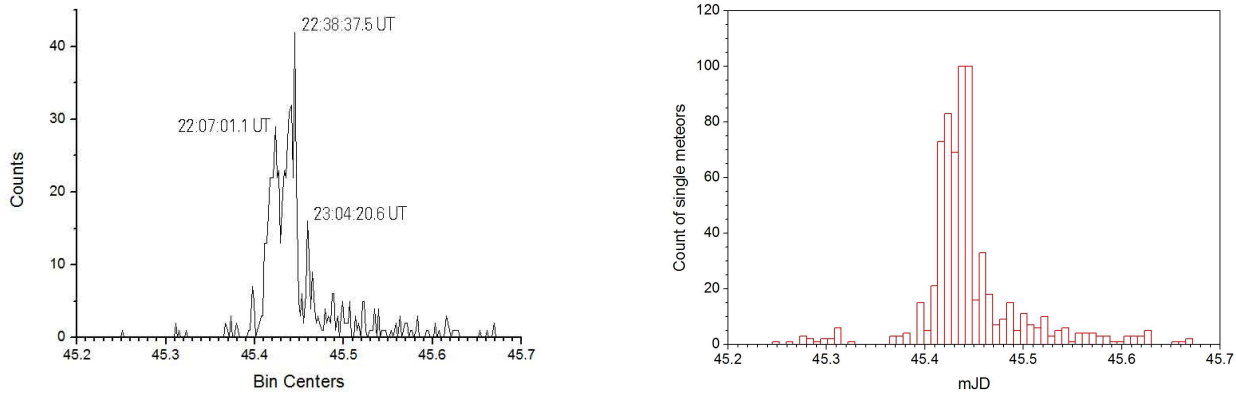


*Figure 4* – Counts of EDMOND single-station SPE meteors in smoothed 2-min bins, with three SPE maximum peaks (left), and 10-min bins histogram (right).

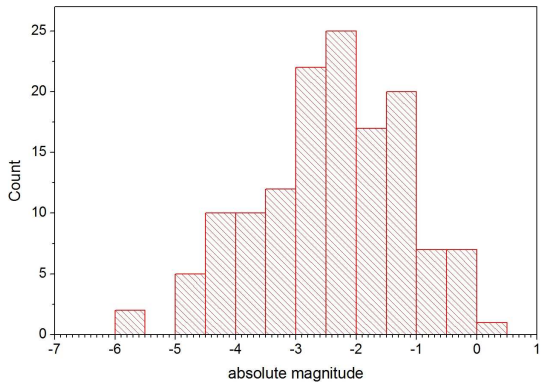


*Figure 5* – Absolute magnitude distribution of SPE meteors during outburst 2013.

10, are included in Figure 4, with binning 2 and 10 minutes, respectively. The diagrams reveal a detailed SPE activity over half a day and are consistent with all-sky data.

The only feature which should be resolved in comparison with all-sky data (Figure 3) is a more populated second peak of a broader "plateau" of the maximum. We assume that it simply reflects the number of video stations in operation across Europe at this time. This could multiply counts of meteors, as one meteor trail can be captured by more stations simultaneously, and so, multiple single-station records of one meteor are present in the EDMOND database (e.g. mid 2012 version contained 11% of multiple records). The situation can be emphasized by presence of brighter meteors which are also detectable (even though at small elevation) at distant stations. This could happen with a prevalence of bigger dust particles (= brighter meteors) in the SPE stream. Such a behaviour with mostly bright meteors was noticed Jenniskens (2008; 2013) in the SPE outburst in 2008, and also after the 2013 outburst. In the EDMOND data we can recognize an occurrence of meteors with visual magnitude mostly in range from $+2^{\mathrm{m}}$ to $-4^{\mathrm{m}}$ during the 2013 SPE outburst, but no dimmer. But the lower visual magnitude value ($+2^{\mathrm{m}}$) is also an instrumental limit for most video stations of the EDMONd network. The absolute magnitude distribution of SPE meteors during the 2013 outburst is shown in Figure 5.

## 2.3 SPE activity profile from radio forward scatter observations

The single-station (including all-sky) video observations described above gave an activity profile of SPE mete-

*Table 2* – Technical parameters and maintenance data of contributing forward-scatter stations.

| Name/station | City | State | Location | Antenna | Az | El | Freq. | Receiver | Software |
|---|---|---|---|---|---|---|---|---|---|
| SMRST | Vsetín | CZE | 17 °996 E 49 °204 N | X-Beam | 80 | 10 | 49.75 | AOR 8000 | HROFFT |
| E. Stomeo, AAV | Venezia | ITA | 12 °374 E 45 °417 N | Yagi 6 el | 294 | 30 | 143.05 | Yaesu FT817 | HROFFT |
| G. de Wilde | Dessel | BEL | 5 °100 E 51 °233 N | RHCP | 95 | 45 | 49.99 | SDR | php script |
| K.-H. Gansel | Dingden | GER | 6 °617 E 51 °767 N | T2FD | 170 | 0 | 143.05 | ICOM PCR 1000 | php script |
| I. Sergey | Molodechno | BLR | 26 °733 E 54 °267 N | Yagi 5 el | 270 | 0 | — | Car radio | MetAn |
| J. Welkenhuyzen | Lanaken | BEL | 5 °627 E 50 °893 N | DIY HB9CV | 75 | 30 | 49.99 | SDR | Speclab |

ors during the outburst on 2013 September 9/10 with quite a fine time resolution. We also tend to confirm SPE behaviour detected that night by other kinds of observations. As to visual observation, our (JK from Kroměříž) attempt failed due to local fog at the observing site, thus we have no own information on SPE activity in a visual magnitude range down to $+6^{\mathrm{m}}$.

Another relevant source of usable data arises from radio forward-scatter observations. We present a diagram of overall meteor activity during 2013 September 9/10, as observed by six stations across the Europe (summary in Table 5). Due to differing instrumental configurations, each of the stations has an individual level of meteor echo counts. We normalized these counts and averaged them to uncover the daily profile of meteor frequency in hourly steps. Figure 6 depicts the averaged meteor hourly rates (solid black line) over one day centered at 2013 September 9.90 UT. The data starting to rise before September 9.85 ($20^{\mathrm{h}}24^{\mathrm{m}}$) UT and then peaked at about September 9.93 ($22^{\mathrm{h}}19^{\mathrm{m}}$) UT, which matches video results. Unfortunately, an averaged trend after September 9.95 UT is rather uncertain due to loss of the SMRST station echoes (line with deepest decline; transmitter failure). As the rates presented are not corrected for an observability function, we can only refer to common timing of distinguishable peaks in individual curves. The peak on September 9.95 UT in forward-scatter meteor echoes we account for contribution by enhanced SPE activity.

Coincidence of radio echoes detected by the SMRST station with video counts of SPE video meteors (dark line with a narrow peak) is not evident directly in Figure 7. Corrected hourly rates of meteors detected by SMRST station are depicted by solid line. Vertical lines denote number of meteor echoes (Y-axis, right) lasting over 10 s and are only indication of incoming SPE outburst. They are in agreement with video observations. The gap in meteor counts after September 9.95 UT is due to transmitter failure and loss of radio signal.

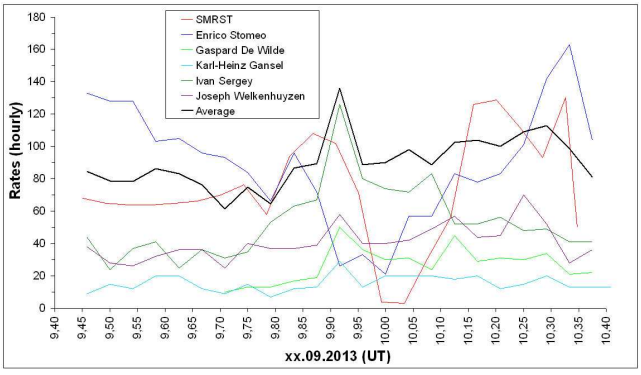


*Figure 6* – Forward-scatter observations: averaged hourly rates of echoes on 2013 September 9/10, recorded from six stations across the Europe. Line with deepest decline outlines SMRST station.

## 2.4 SPE 2013: meteor orbits and radiants from EDMOND

Based on precise SPE meteor orbits collected in EDMOND, we tried to find out parameters, scale (range) and scattering of SPE stream within a Solar system space. A preview of SPE stream structure is shown in Figure 11.

The video observations within CEMENt and SVMN provided 241 orbits with sufficient quality according to the Kornoš et al. (2014) quality criteria. After the application of radiant ($\pm 5°$) and geocentric velocity ($\pm 10\%$) selection method, 138 SPEs had been identified. As it is clear from Figure 10 (left), the distribution of geocentric velocity $Vg$ is not symmetric as one can expect for very narrow meteor stream. A detailed inspection of video records showed that the spread is caused by uncertainty in velocity determination, mostly due to a small number of measured points along the meteor trail (short angular length and duration of meteor appearance).

To find the core of the stream, the first part of the Welch method (Welch, 2001) with the Southworth-Hawkins $D$ criterion (Southworth & Hawkins, 1963) was applied to the set of 138 SPEs. Using the Welch equa-

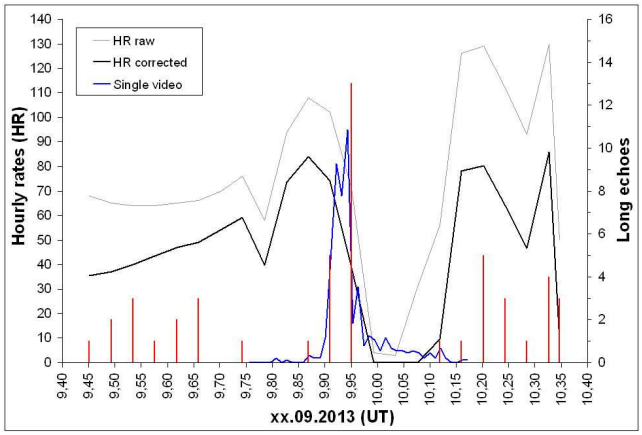


*Figure 7* – Radio forward-scatter observation from SMRST station: raw and corrected hourly rates of meteor echoes on 2013 September 9/10. Included are counts of single-station video SPE meteors (dark line with a narrow peak), for comparison. Vertical lines denote number of meteor echoes (Y-axis, right) lasting over 10 s.

tion, the procedure creates a group of meteors around each meteor orbit from the examined shower.

$$\rho_j = \sum_{i=1}^{N} \left(1 - \frac{D_{ij}^2}{D_c^2}\right) \; ; \qquad D_{ij} \leq D_c \; . \qquad (1)$$

In the Equation (1), $\rho_j$ is a $j$-th group density at a point in orbital elements space, $N = 138$ is the number of all SPE meteors, $D_{ij}$ is the value obtained for the $i$-th meteor in the SPE list by comparing its orbit with the orbit which initiates the $j$-group, and $D_c$ is the threshold value that determines the dynamical similarity among meteor orbits. On the basis of the Equation (1), the value of the density ($\rho$) is determined for each group and its highest value defines the core of the stream. Satisfying the limiting value $D_c = 0.1$, we have found the core of SPE consisting of 74 meteors. They are presented in Table 3 together with the weighted mean orbit of SPE and standard deviations of all parameters. The comparison of all 138 SPEs (empty columns) with those selected by Welch method (filled columns) is shown in the histograms of the perihelion distance and eccentricity (Figure 8), inclination and argument of perihelion (Figure 9), and geocentric velocity (Figure 10, left), respectively. In the diagram of the radiant position of SPE meteors (Figure 10, right), the core of the stream with higher precision in radiant position is highlighted by black circles, among others (plus signs).

## 3 Results and discussion

All-sky, single-station video observations, along with radio forward scatter observations gave an activity profile of the SPE during outburst on 2013 September 9/10 with high temporal resolution, and raw overall meteor activity during the night, respectively. We detected distinct peaks, gap and sharp edges in the SPE frequency. We can simply describe the SPE outburst in 2013 as a double-peaked maximum, with three dominant fluctuations (central gap and two edges) during observed interval. Moreover these features are clearly confirmed by both all-sky (Figure 3) and single-station video observations (Figure 4) with very close timing, one notable difference is present. A central gap (in fact a decline of meteor counts) is surrounded by two peaks. But the tops of these peaks differ in level, perhaps depending on the manner of data retrieval. The first peak at $22^{\rm h}05^{\rm m}/22^{\rm h}07^{\rm m}$ UT (before the gap) is higher in all-sky systems, while the second peak at $22^{\rm h}40^{\rm m}/22^{\rm h}38^{\rm m}$ UT (after the gap) is dominant in histograms based on single-station meteors gathered in EDMOND database. We also identified the third smaller peak at $23^{\rm h}05^{\rm m}/23^{\rm h}04^{\rm m}$ UT.

The detected gap as well as the sharp edges in SPE meteor frequency during its outburst are real manifestations of a fine structure of the SPE stream. They could be assigned to two possible reasons: an impossibility of detection of fainter meteors by the video systems used due to their limited instrumental sensitivity, and/or a real absence of smaller particles and thus fluctuations in the mass exponent within a core of the SPE meteor stream. This could imply the filamentary structure of the stream caused by variation in the flux of dust particles, or variations in population index within the stream. An alternative to the existence of filaments with various size of dust particles is a variable volume density of particles inside the narrow core of the meteoroid stream. Data from visual observation could complete our understanding of the fine structure of the SPE meteor stream.

Mostly brighter meteors were recorded during the SPE outburst in 2013. This could indicate a depletion of smaller dust particles inside the SPE stream. So the Earth crossed a rather older filament mostly occupied by larger particles in the 2013 display. The filament could originate long ago from a parent body, not yet discovered, that would most probably be of the Halley/Thatcher comet type. As to the recurence of the SPE outbursts, a question arose of the possibility of connecting the events from 2008 and 2013 and making predictions for future.

## Acknowledgements

This work was supported by grant APVV-0517-12. We are very grateful to all the forward-scatter observers who provided us with radio data.

## References

Astapovič I. S. and Terentjeva A. K. (1968). "Fireball radiants of the 1st-15th centuries". In L. Kresák and Millman P. M., editors, *IAU Symp. 33, Tatranská Lomnica, Czechoslovakia, 1967*, Physics and Dynamics of Meteors, Dordrecht. Reidel, pages 308–319.

Cooke B. (2008). "Fireball outburst". `http://www.spaceweather.com/archive.php?view=1&day=10&month=09&year=2008` . (10. 9. 2008).

Denning W. F. (1882). "The September Perseids". *The Observatory*, **5**, 262–265.

Drummond J. D. (1982). "A note on the Delta Aurigid meteor stream". *Icarus*, **51**, 655–659.

Gajdoš Š. (2005). *Bolide meteor streams*. PhD thesis, Comenius University, Bratislava. (in Slovak).

Gajdoš Š. and Porubčan V. (2005). "Bolide meteor streams". In Kneževič Z. and Milani A., editors, *Dynamics of Populations of Planetary Systems, IAU Coll. 197, Belgrade 2004*, Cambridge. Cambridge University Press, pages 393–398.

Gajdoš Š. and Tóth J. (2013). "Septembrové Perzeidy v roku 2013". *Meteor reports*, **34**, 85–93. (comprehensive abstract in English).

Gajdoš Š., Tóth J., and Kornoš L. (2008). "Septembrové Perzeidy v roku 2008". *Meteor reports*, **29**, 44–50. (comprehensive abstract in English).

*Table 3* – The core of the September Perseids during outburst on 2013 September 9/10 consisting of 74 orbits. The weighted mean orbit with standard deviations is also presented ($\lambda_\odot$ – solar longitude, $RA$, $DEC$ – radiant position, $V_g$ – geocentric velocity, $q$ – perihelion distance, $e$ – eccentricity, $\omega$ – argument of perihelia, $\Omega$ – ascending node, $i$ – inclination, $D_{SH}$ – orbital similarity criterion of meteor orbit). The last two lines are a weighted average, and weighted SD.

| $\lambda_\odot$ [°] | $RA$ [°] | $DEC$ [°] | $V_g$ [km/s] | $q$ [AU] | $e$ | $\omega$ [°] | $\Omega$ [°] | $i$ [°] | $D_{SH}$ |
|---|---|---|---|---|---|---|---|---|---|
| 167.202 | 47.6 | +39.8 | 64.43 | 0.721 | 0.972 | 244.9 | 167.2 | 138.7 | 0.03 |
| 167.202 | 47.8 | +39.5 | 63.13 | 0.701 | 0.889 | 249.3 | 167.2 | 138.6 | 0.09 |
| 167.203 | 47.1 | +39.4 | 63.24 | 0.692 | 0.906 | 250.0 | 167.2 | 138.4 | 0.09 |
| 167.204 | 47.4 | +39.4 | 65.22 | 0.724 | 1.022 | 243.6 | 167.2 | 139.5 | 0.08 |
| 167.206 | 47.4 | +39.9 | 62.87 | 0.699 | 0.884 | 249.6 | 167.2 | 137.6 | 0.10 |
| 167.206 | 47.0 | +39.1 | 64.17 | 0.701 | 0.960 | 247.7 | 167.2 | 139.2 | 0.03 |
| 167.206 | 48.7 | +38.8 | 64.03 | 0.716 | 0.916 | 246.8 | 167.2 | 140.8 | 0.05 |
| 167.208 | 47.0 | +39.6 | 64.09 | 0.707 | 0.962 | 246.9 | 167.2 | 138.3 | 0.03 |
| 167.208 | 48.0 | +39.3 | 64.09 | 0.716 | 0.938 | 246.3 | 167.2 | 139.5 | 0.02 |
| 167.208 | 48.4 | +39.2 | 65.05 | 0.731 | 0.989 | 243.3 | 167.2 | 140.5 | 0.06 |
| 167.208 | 48.2 | +39.2 | 64.01 | 0.715 | 0.928 | 246.6 | 167.2 | 139.9 | 0.03 |
| 167.210 | 47.8 | +39.4 | 63.39 | 0.704 | 0.901 | 248.6 | 167.2 | 138.9 | 0.07 |
| 167.210 | 47.7 | +39.4 | 64.26 | 0.716 | 0.955 | 245.9 | 167.2 | 139.3 | 0.00 |
| 167.211 | 47.2 | +38.7 | 65.51 | 0.715 | 1.036 | 244.5 | 167.2 | 140.6 | 0.09 |
| 167.211 | 47.3 | +39.7 | 64.48 | 0.717 | 0.979 | 245.3 | 167.2 | 138.7 | 0.03 |
| 167.211 | 47.6 | +38.3 | 64.94 | 0.707 | 0.988 | 246.4 | 167.2 | 141.2 | 0.05 |
| 167.212 | 47.5 | +39.3 | 63.52 | 0.701 | 0.914 | 248.7 | 167.2 | 138.9 | 0.06 |
| 167.214 | 47.0 | +39.3 | 63.83 | 0.697 | 0.943 | 248.5 | 167.2 | 138.8 | 0.05 |
| 167.214 | 45.9 | +40.1 | 64.12 | 0.702 | 0.990 | 247.0 | 167.2 | 136.8 | 0.06 |
| 167.216 | 47.8 | +39.6 | 65.23 | 0.731 | 1.018 | 242.8 | 167.2 | 139.5 | 0.08 |
| 167.216 | 48.3 | +39.4 | 64.88 | 0.731 | 0.984 | 247.9 | 167.2 | 138.5 | 0.04 |
| 167.217 | 47.8 | +39.3 | 64.29 | 0.715 | 0.956 | 246.0 | 167.2 | 139.4 | 0.00 |
| 167.218 | 47.3 | +40.3 | 64.63 | 0.728 | 0.997 | 243.6 | 167.2 | 137.8 | 0.06 |
| 167.218 | 48.1 | +40.1 | 64.06 | 0.728 | 0.943 | 244.6 | 167.2 | 138.4 | 0.03 |
| 167.224 | 47.4 | +37.5 | 64.73 | 0.688 | 0.972 | 249.1 | 167.2 | 142.2 | 0.08 |
| 167.228 | 46.8 | +38.9 | 64.99 | 0.706 | 1.013 | 246.1 | 167.2 | 139.8 | 0.06 |
| 167.229 | 47.9 | +39.5 | 63.71 | 0.710 | 0.919 | 247.4 | 167.2 | 139.0 | 0.04 |
| 167.230 | 48.1 | +38.7 | 65.09 | 0.721 | 0.993 | 244.6 | 167.2 | 141.0 | 0.05 |
| 167.231 | 47.3 | +39.1 | 63.44 | 0.693 | 0.912 | 249.7 | 167.2 | 139.0 | 0.08 |
| 167.233 | 47.4 | +40.2 | 64.27 | 0.723 | 0.972 | 244.7 | 167.2 | 137.9 | 0.04 |
| 167.235 | 50.5 | +39.8 | 63.93 | 0.752 | 0.884 | 242.6 | 167.2 | 140.4 | 0.10 |
| 167.236 | 48.2 | +39.0 | 65.13 | 0.727 | 0.998 | 243.7 | 167.2 | 140.5 | 0.06 |
| 167.238 | 46.2 | +40.7 | 63.35 | 0.703 | 0.944 | 247.8 | 167.2 | 135.8 | 0.07 |
| 167.244 | 46.0 | +39.4 | 64.65 | 0.699 | 1.014 | 246.9 | 167.2 | 138.2 | 0.07 |
| 167.267 | 47.2 | +39.3 | 64.02 | 0.703 | 0.952 | 247.6 | 167.3 | 138.8 | 0.03 |
| 167.271 | 48.8 | +39.4 | 65.20 | 0.740 | 0.995 | 242.0 | 167.3 | 140.4 | 0.08 |
| 167.284 | 47.0 | +39.4 | 63.79 | 0.699 | 0.943 | 248.3 | 167.3 | 138.4 | 0.05 |
| 167.206 | 47.6 | +39.4 | 64.27 | 0.714 | 0.959 | 246.1 | 167.2 | 139.1 | 0.04 |
| 0.02 | 0.7 | 0.5 | 0.52 | 0.012 | 0.032 | 1.8 | 0.0 | 1.1 | 0.02 |

| $\lambda_\odot$ [°] | $RA$ [°] | $DEC$ [°] | $V_g$ [km/s] | $q$ [AU] | $e$ | $\omega$ [°] | $\Omega$ [°] | $i$ [°] | $D_{SH}$ |
|---|---|---|---|---|---|---|---|---|---|
| 167.169 | 47.7 | +39.5 | 63.26 | 0.703 | 0.897 | 248.9 | 167.2 | 138.6 | 0.08 |
| 167.171 | 47.9 | +39.0 | 64.13 | 0.710 | 0.939 | 246.9 | 167.2 | 139.9 | 0.03 |
| 167.172 | 47.5 | +39.0 | 64.21 | 0.705 | 0.952 | 247.4 | 167.2 | 139.8 | 0.03 |
| 167.182 | 48.9 | +39.4 | 64.25 | 0.730 | 0.931 | 244.5 | 167.2 | 140.1 | 0.04 |
| 167.183 | 46.6 | +39.8 | 64.64 | 0.713 | 1.003 | 245.4 | 167.2 | 138.2 | 0.05 |
| 167.185 | 47.1 | +39.0 | 64.02 | 0.699 | 0.948 | 248.2 | 167.2 | 139.3 | 0.04 |
| 167.187 | 46.6 | +38.9 | 64.64 | 0.699 | 0.994 | 247.3 | 167.2 | 139.5 | 0.05 |
| 167.188 | 47.5 | +39.5 | 65.30 | 0.728 | 1.027 | 243.0 | 167.2 | 139.4 | 0.09 |
| 167.188 | 47.5 | +39.4 | 63.89 | 0.707 | 0.938 | 247.4 | 167.2 | 138.9 | 0.03 |
| 167.189 | 47.2 | +39.2 | 64.13 | 0.703 | 0.955 | 247.6 | 167.2 | 139.2 | 0.03 |
| 167.189 | 47.5 | +40.7 | 63.99 | 0.730 | 0.956 | 244.1 | 167.2 | 137.1 | 0.05 |
| 167.190 | 47.6 | +39.3 | 63.88 | 0.707 | 0.933 | 247.6 | 167.2 | 139.2 | 0.04 |
| 167.191 | 47.4 | +39.6 | 63.76 | 0.708 | 0.933 | 247.4 | 167.2 | 138.5 | 0.04 |
| 167.192 | 49.5 | +40.1 | 63.74 | 0.741 | 0.895 | 243.8 | 167.2 | 139.2 | 0.07 |
| 167.192 | 47.6 | +40.4 | 63.47 | 0.719 | 0.920 | 246.3 | 167.2 | 137.3 | 0.05 |
| 167.192 | 47.3 | +39.4 | 65.34 | 0.725 | 1.030 | 243.4 | 167.2 | 139.6 | 0.09 |
| 167.193 | 46.5 | +39.0 | 63.52 | 0.683 | 0.930 | 250.6 | 167.2 | 138.7 | 0.09 |
| 167.194 | 47.9 | +39.6 | 64.93 | 0.730 | 0.997 | 243.3 | 167.2 | 139.4 | 0.06 |
| 167.195 | 46.3 | +39.4 | 64.39 | 0.698 | 0.990 | 247.4 | 167.2 | 138.4 | 0.05 |
| 167.195 | 47.4 | +39.3 | 64.60 | 0.713 | 0.981 | 245.7 | 167.2 | 139.4 | 0.03 |
| 167.195 | 46.5 | +41.0 | 62.89 | 0.706 | 0.912 | 248.0 | 167.2 | 135.4 | 0.09 |
| 167.195 | 48.7 | +39.3 | 64.31 | 0.728 | 0.937 | 244.8 | 167.2 | 140.2 | 0.03 |
| 167.195 | 47.2 | +39.4 | 65.18 | 0.722 | 1.023 | 243.9 | 167.2 | 139.4 | 0.08 |
| 167.195 | 47.6 | +39.5 | 63.01 | 0.698 | 0.884 | 249.8 | 167.2 | 138.4 | 0.10 |
| 167.195 | 47.2 | +40.9 | 64.36 | 0.734 | 0.988 | 242.9 | 167.2 | 136.7 | 0.08 |
| 167.196 | 48.2 | +39.5 | 65.30 | 0.737 | 1.014 | 242.2 | 167.2 | 139.9 | 0.09 |
| 167.196 | 47.9 | +39.0 | 64.79 | 0.720 | 0.980 | 244.9 | 167.2 | 140.2 | 0.04 |
| 167.196 | 48.0 | +39.0 | 64.59 | 0.717 | 0.966 | 245.6 | 167.2 | 140.3 | 0.02 |
| 167.197 | 49.5 | +38.9 | 64.59 | 0.737 | 0.935 | 243.6 | 167.2 | 141.4 | 0.06 |
| 167.198 | 47.7 | +40.6 | 64.86 | 0.742 | 1.009 | 241.6 | 167.2 | 137.7 | 0.10 |
| 167.198 | 47.7 | +39.6 | 65.15 | 0.730 | 1.014 | 243.1 | 167.2 | 139.4 | 0.08 |
| 167.198 | 46.9 | +39.4 | 63.97 | 0.702 | 0.954 | 247.7 | 167.2 | 138.5 | 0.04 |
| 167.199 | 47.6 | +39.3 | 64.09 | 0.710 | 0.945 | 246.9 | 167.2 | 139.3 | 0.02 |
| 167.201 | 46.9 | +39.7 | 64.49 | 0.713 | 0.988 | 245.6 | 167.2 | 138.4 | 0.04 |
| 167.201 | 48.8 | +39.4 | 64.92 | 0.739 | 0.975 | 242.5 | 167.2 | 140.3 | 0.07 |
| 167.201 | 48.1 | +39.2 | 63.25 | 0.702 | 0.886 | 249.2 | 167.2 | 139.3 | 0.09 |

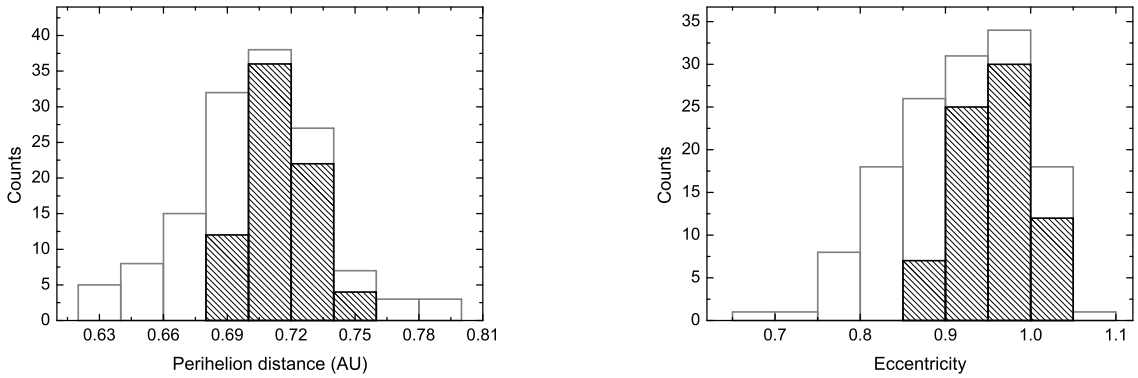


*Figure 8* – Histogram of SPE meteors perihelion distances (left) and eccentricities (right). Empty columns depict all SPE orbits, whereas filled ones depict the SPE core.

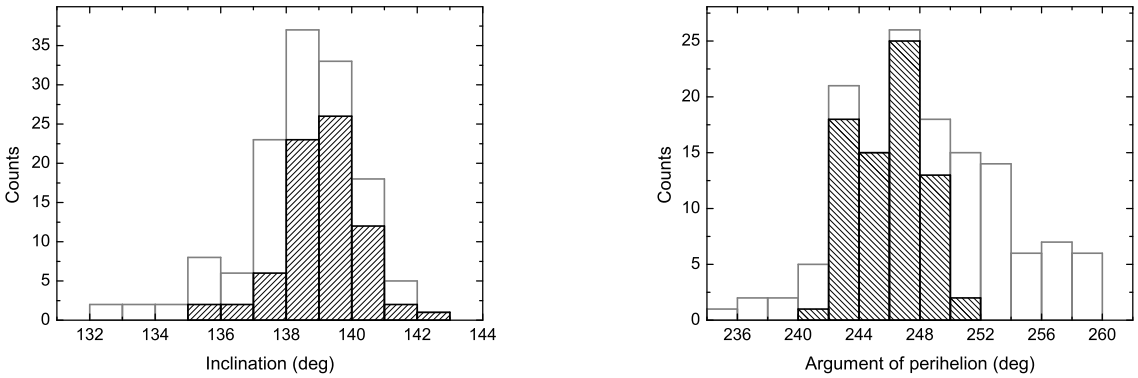


*Figure 9* – Histogram of SPE meteors inclination (left) and argument of perihelion (right). Empty columns depict all SPE orbits, whereas filled ones depict the SPE core.

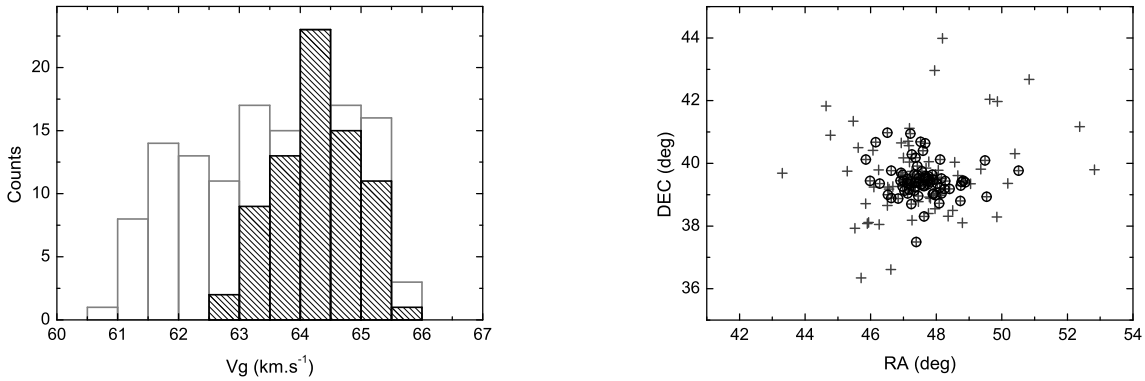


*Figure 10* – Histogram of SPE meteors geocentric velocities (left) and diagram of SPE radiants (right). Empty columns depict all SPEs, whereas filled ones depict the SPE core. The core of the stream with higher precision in radiant position is highlighted by black circles, among others (plus signs).

Gavajdová M. (1994). "On the population of very bright meteors in meteor streams". *Contrib. Astron. Obs. Skalnaté Pleso*, **24**, 101–110.

Hergenrother C. (2008). "Sept 8/9 meteors". `http://transientsky.wordpress.com/2009/09/09/sept-89-meteors/` . (9. 9. 2008).

Hoffmeister C. (1948). *Meteorströme*. J. A. Barth, Leipzig, 79-93 pages.

Jenniskens P. (2006). *Meteor Showers and Their Parent Comets*. Cambridge Univ. Press, Cambridge, U.S.A.

Jenniskens P. (2013). "September epsilon Perseids 2013". *CBET*, **3652**.

Jenniskens P., Brower J., Martsching P., Lyytinen E., Entwistle D., and Cooke W. J. (2008). "September Perseid Meteors 2008". *CBET*, **1501**.

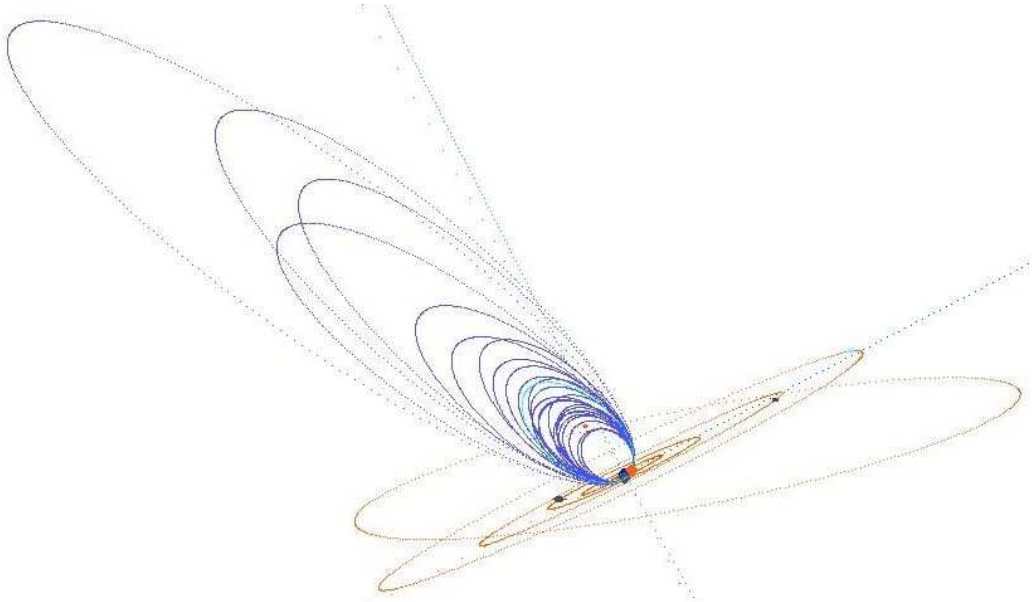

*Figure 11* – Orientation and form of the SPE meteor stream – orbits in 2013.

*Table 4* – A comparison of the SPE orbits: from IAU MDC, orbit from EDMOND for 2001–2012, averaged orbit from EDMOND for 2007–2012, and mean orbit for outburst 2013 (Year/Source, $RA$, $DEC$ – radiant position, $V_g$ – geocentric velocity, $q$ – perihelion distance, $e$ – eccentricity, $\omega$ – argument of perihelia, $\Omega$ – ascending node, $i$ – inclination, $a$ – semimajor axis).

| Method | $RA$ [°] | $DEC$ [°] | $V_g$ [km/s] | $q$ [AU] | $e$ | $\omega$ [°] | $\Omega$ [°] | $i$ [°] | $a$ [AU] | $D_{SH}$ |
|---|---|---|---|---|---|---|---|---|---|---|
| IAU MDC | 50.2 | +39.4 | 64.5 | 0.742 | — | 241.9 | 171.3 | 138.9 | 31.1 | — |
| 2001–2012 | 47.2 | +39.5 | 63.8 | 0.709 | 0.931 | 247.3 | 166.9 | 138.7 | 10.3 | 0.03 |
| SD | 2.2 | 0.6 | 0.42 | 0.016 | 0.034 | 2.2 | 1.9 | 0.9 | — | 0.01 |
| 2007–2012 | 47.9 | +39.3 | 63.5 | 0.707 | 0.919 | 247.9 | 166.9 | 139.0 | 8.8 | — |
| SD | 5.5 | 1.7 | 2.52 | 0.090 | 0.134 | 13.5 | 0.1 | 3.9 | — | — |
| SPE 2013 | 47.6 | +39.4 | 64.3 | 0.714 | 0.959 | 246.1 | 167.2 | 139.1 | 17.4 | 0.04 |
| SD | 0.7 | 0.5 | 0.52 | 0.012 | 0.032 | 1.8 | 0.0 | 1.1 | — | 0.02 |


Kornoš L., Koukal J., Piffl R., and Tóth J. (2013). "Database of meteoroid orbits from several European video networks". In Gyssens M. and Roggemans P., editors, *Proceedings of the IMC 2012*. IMO, pages 21–25.

Kornoš L., Koukal J., Piffl R., and Tóth J. (2014). "EDMOND meteor database". In Gyssens M., Roggemans P., and Żołądek P., editors, *Proceedings of the International Meteor Conference, Poznań, Poland, Aug. 22-25, 2013*. International Meteor Organization. (submitted).

Porubčan V. and Gavajdová M. (1994). "A search for fireball streams among photographic meteors". *Planet. Space Sci.*, **42**, 151–155.

Rendtel J. (1993). "Delta Aurigids and September Perseids". In Štohl J. and Williams I., editors, *Meteoroids and their parent bodies*. Astronomical Inst., Slovak Acad. Sci., Bratislava, pages 185–188.

Rendtel J. and Arlt R., editors (2008). *Handbook for meteor observers*. IMO, Potsdam.

Rendtel J. and Molau S. (2010). "Meteor activity from the Perseus-Auriga region in September and October". *WGN, Journal of the IMO*, **38:5**, 161–166.

SonotaCo (2009). "A meteor shower catalog based on video observations in 2007-2008". *WGN, Journal of the IMO*, **37:2**, 55–62.

Southworth R. and Hawkins G. (1963). "Statistics of meteor streams". *Smithson. Contr. Astrophys.*, **7**, 261–285.

Terentjeva A. K. (1989). "Fireball streams". *WGN, Journal of the IMO*, **17**, 242–245.

Welch P. G. (2001). "A new search for streams in meteor data bases and its appplication". *MNRAS*, **328**, 101–111.

Zigo P., Tóth J., and Kalmančok D. (2013). "All-sky Meteor Orbit System (AMOS)". In Gyssens M. and Roggemans P., editors, *Proceedings of the IMC 2012*. IMO, pages 18–20.


*Handling Editor:* Javor Kac
This paper has been typeset from a LaTeX file prepared by the authors.

*Table 5* – Summary of available sources on SPE and incidental meteor showers: solar longitude $\lambda_\odot$ (in degrees), radiant coordinates (right ascension, declination, in degrees) and geocentric velocity $V_g$ in km/s).

| Source | $\lambda_\odot$ | RA | DEC | $V_g$ |
|---|---|---|---|---|
| W. F. Denning (1882) | — | 61.5 | +36.2 | — |
| C. Hoffmeister (1948) | — | 53 | +41 | — |
| I. S. Astapovič & A. K. Terentjeva (1968) | — | 54.8 | +36.2 | — |
| J. D. Drummond (1982, Delta Aurigids) | — | 83.5 | +50.4 | 64.9 |
| A. K. Terentjeva (1989) | — | 54.8 | +36.2 | 67.1 |
| J. Rendtel (1993) | — | 51.5 | +39.5 | 65.6 |
| V. Porubčan & M. Gavajdová (1994) | — | 47.2 | +38.9 | 65.4 |
| M. Gavajdová (1994, $\leq -9^{\mathrm{m}}$) | — | 47.2 | +39.5 | 64.9 |
| P. G. Welch (2001) | 165.6 | 48.3 | +39.1 | — |
| Š. Gajdoš & V. Porubčan (2005) | — | 47.4 | +39.0 | 65.6 |
| Š. Gajdoš (2005) | — | 51.0 | +38.8 | 65.7 |
| P. Jenniskens (2006) | 170.0 | 50.2 | +39.4 | 64.5 |
| SonotaCo (2009) | 167.1 | 47.3 | +39.3 | 63.9 |
| J. Rendtel & R. Arlt (2008), IMO Handbook | 166.7 | 60 | +47 | 64 |
| B. Cooke (2008) | 166.9 | 49.5 | +43.0 | — |
| C. Hergenrother (2008) | 166.9 | 49 | +39 | — |
| Š. Gajdoš, J. Tóth, L. Kornoš (2008) | 166.6 | 47.4 | +39.7 | — |
| Š. Gajdoš & J. Tóth (2013), for AGO | 167.2 | 47.5 | +39.4 | — |
| Š. Gajdoš & J. Tóth (2013), for ARBO | 167.2 | 47.3 | +39.6 | — |
| This work | 167.2 | 47.6 | +39.4 | 64.3 |

# New showers from parent body search across several video meteor databases

*Damir Šegon*[1], *Peter Gural*[2], *Željko Andreić*[3], *Ivica Skokić*[4,5], *Korado Korlević*[6], *Denis Vida*[4,7], *and Filip Novoselnik*[4,8]

This work was initiated by utilizing the latest complete set of both comets and NEOs downloaded from the JPL small-body database search engine. Rather than search for clustering within a single given database of meteor orbits, the method employed herein is to use all the known parent bodies with their individual orbital elements as the starting point, and find statistically significant associations across a variety of meteor databases (SonotaCo, 2013; CMN, 2013). Fifteen new showers possibly related to a comet or a NEO were found.

Received 2013 September 25

## 1 Introduction

The Croatian Meteor Network (CMN) is in operation since 2007 and is described in Andreić & Šegon (2010) and Andreić et al. (2010). The catalogues of orbits for 2007 to 2009 are already published (Šegon et al., 2012; Korlević et al., 2013) and the catalogue for 2010, together with all previous ones, is available on the CMN download page (CMN, 2013). Simultaneously, the skies over Japan were monitored by the SonotaCo Meteor Network (SonotaCo, 2009; 2013). These database catalogues contain over one hundred thousand meteoroid orbits (114 280 SonotaCo from 2007 to 2011; 19 372 CMN from 2007 to 2010) that were obtained through multi-station trajectory and orbital parameter estimation. In addition, the IMO video meteor database (IMO, 2012) contains nearly one and a half million single station records (1993–2012) that were used to provide further statistical relevance to a given shower's existence. Combined, these datasets cover radiants down to declination −30°.

The processing approach employed an extensive search for meteor orbit relationships to potential parent bodies (comets and NEOs) by applying several D-criteria restrictions with appropriate thresholds on shower membership. These are $D_{SH}$, $D_D$ and $D_H$ and were developed by Southworth & Hawkins (1963), Drummond (1981) and Jopek (1993) respectively. Each independent potential parent body was compared against every meteor orbit available, selecting orbits satisfying $D_{SH} \leq 0.15$, $D_H \leq 0.15$ and $D_D \leq 0.075$. The latest complete set of both comets and NEOs (Near-Earth Objects) was downloaded from the JPL small-body database search engine (JPL, 2013) for this purpose.

From that processing, a short list of parent bodies was obtained and the individual meteor orbits were analyzed in greater depth to evaluate the significance of each result. Thus in cases where the comet's or NEO's orbital parameters led us to the shower (using these quite strict threshold values for the D-criteria), we then searched for additional shower members by allowing a slightly larger threshold in $D_{SH}$. The final set of orbits for a particular shower candidate was then analyzed in more detail, including radiant plots, plots of orbital data as functions of solar longitude, mean value of D-criteria, etc. Last, single station observation data from IMO were analyzed in order to find out if the new showers could be detected in that dataset, too.

## 2 New showers

The file with all individual orbits of the new showers described in this article can be downloaded from the CMN download page mentioned before. The 15 showers were reported to the IAU, following the standard procedure (Jenniskens et al., 2009), and temporary shower numbers were obtained for them. The search method automatically produced the best possible parent body candidate. The orbital elements of showers discussed in this article are summarized in Table 15. Members of 13 showers discussed here were detected through analysis of the IMO single station observation database. The only 2 showers that were not found are 535 THC and 536 FSO.

### 2.1 $\gamma$ Aquilids (531 GAQ) and C/1853 G1 (Schweizer)

A possible new meteor shower consisting of 27 meteors with mean orbit similar to C/1853 G1 (Schweizer). Shower mean orbit and comet orbit (see Table 1) are quite similar with $D_{SH} = 0.11$. This shower is active from April 27 to May 11, with peak activity around May 4. The mean daily motion of the radiant is about dRA = 0.66°, dDEC = 0.25°.

[1]Astronomical Society Istra Pula, Park Monte Zaro 2, 52100 Pula, Croatia; and Višnjan Science and Education Center, Istarska 5, 51463 Višnjan, Croatia. Email: damir.segon@pu.htnet.hr

[2]351 Samantha Drive, Sterling, VA 20164-5539, USA. Email: peter.s.gural@saic.com

[3]University of Zagreb, Faculty of Mining, Geology and Petroleum Engineering, Pierottijeva 6, 10000 Zagreb, Croatia. Email: zandreic@rgn.hr

[4]Astronomical Society "Anonymus", B. Radića 34, 31550 Valpovo, Croatia and Faculty of Electrical Engineering, University of Osijek, Kneza Trpimira 2B, 31000 Osijek, Croatia.

[5]Email: ivica.skokic@gmail.com

[6]Višnjan Science and Education Center, Istarska 5, 51463 Višnjan, Croatia. Email: korado@astro.hr

[7]Email: denis.vida@gmail.com

[8]Email: novoselnikf@gmail.com

IMO bibcode WGN-422-segon-newshowers
NASA-ADS bibcode 2014JIMO...42...57S

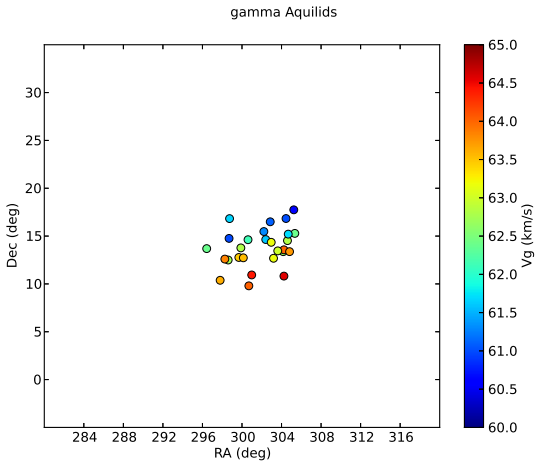


*Figure 1* – Radiant plot of $\gamma$ Aquilids.

*Table 1* – Comparison of orbital elements of $\gamma$ Aquilids (mean orbit) and the orbit of comet C/1853 G1 (Schweizer). The quantity n. dist. is nodal distance of the comet orbit from the Earth, at the node associated with the shower.

| parameter | 531 GAQ | C/1853 G1 |
|---|---|---|
| $q$ | 0.988 | 0.909 |
| $e$ | 0.957 | 0.989 |
| $\omega$ | 196.2 | 199.2 |
| $\Omega$ | 44.5 | 43.0 |
| $i$ | 123.4 | 122.2 |
| $D_{SH}$ | 0.11 | |
| n. dist. | 0.07 | |

## 2.2 May $\lambda$ Draconids (532 MLD) and 209P/LINEAR

A possible new meteor shower consisting of 23 meteors with mean orbit similar to 209P/LINEAR. Shower mean orbit and comet orbit (see Table 2) differ by only $D_{SH} = 0.12$. This shower is active from April 24 to June 4, with peak activity around May 12. The mean daily motion of the radiant is about dRA $= -1.87°$, dDEC $= -0.08°$.

When we did this search, some meteor showers listed in IAU MDC database had no orbital parameters listed, not even geocentric (or any other) velocity data, but just information on mean solar longitude activity and RA, Dec. One of those showers was the 8-member shower 451 CAM, Camelopardalids, for which only $\lambda_\odot = 39.1°$, RA $= 172.6°$ and DEC $= 83.7°$ were listed. During the matching phase (between existing and possible new showers) of our search, this shower seemed to be distant from 532 MLD since the difference in solar longitude found was 13° (corresponding to almost two weeks), and radiant distances were separated by well over 10°. However, the data on this shower were updated lately and we found out that the connection with comet 209P has been claimed as well. When orbital parameters of 451 CAM and 532 MLD are compared, we may see that those two showers most probably are the same, with $D_{SH} = 0.13$ between their mean orbits.

*Table 2* – Comparison of orbital elements of May $\lambda$ Draconids (mean orbit) and the orbit of comet 209P/LINEAR.

| parameter | 532 MLD | 209P |
|---|---|---|
| $q$ | 0.987 | 0.912 |
| $e$ | 0.651 | 0.689 |
| $\omega$ | 164.8 | 149.7 |
| $\Omega$ | 51.9 | 66.5 |
| $i$ | 18.7 | 19.2 |
| $D_{SH}$ | 0.12 | |
| n. dist. | 0.03 | |

More observational data should help in finding better orbital parameters for this shower. Moreover, calculations made by Vaubaillon (2013a) suggest that meteors from comet 209P are about to produce an outburst on 2014 May 24 at $\lambda_\odot = 62.9°$, having radiant positions around RA $= 120°$, DEC $= 79°$.

## 2.3 July $\xi$ Arietids (533 JXA) and C/1964 N1 (Ikeya)

A possible new meteor shower consisting of 61 meteors with mean orbit similar to C/1964 N1 (Ikeya). Shower mean orbit and comet orbit (see Table 3) are quite similar with $D_{SH} = 0.10$. This shower is active from July 4 to August 12, with peak activity around July 21. Due to the sufficient number of known orbits it is possible to accurately determine the mean daily motion of the radiant dRA $= 0.66°$, dDEC $= 0.25°$.

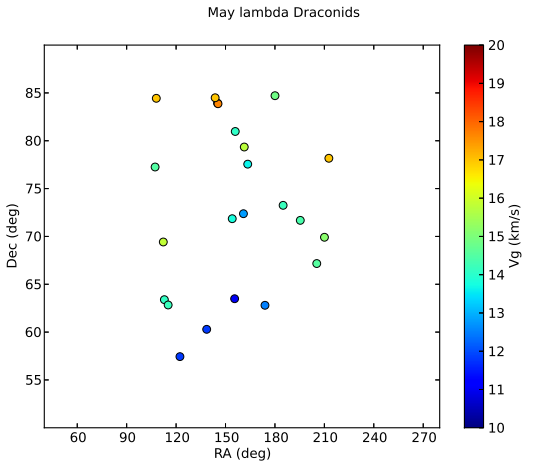


*Figure 2* – Radiant plot of May $\lambda$ Draconids.

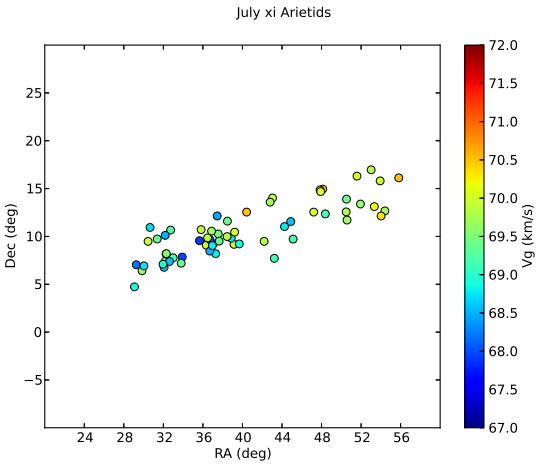


*Figure 3* – Radiant plot of July $\xi$ Arietids.

*Table 3* – Comparison of orbital elements of July $\xi$ Arietids (mean orbit) and the orbit of comet C/1964 N1 (Ikeya).

| parameter | 533 JXA | C/1964 N1 |
|---|---|---|
| $q$ | 0.838 | 0.822 |
| $e$ | 0.975 | 0.985 |
| $\omega$ | 310.3 | 290.8 |
| $\Omega$ | 288.9 | 269.9 |
| $i$ | 171.5 | 171.9 |
| $D_{SH}$ | 0.10 | |
| n. dist. | 0.21 | |

## 2.4 51 Andromedids (534 FOA) and C/1870 K1 (Winnecke)

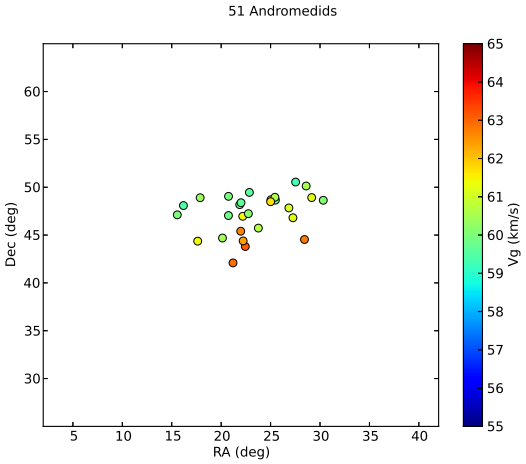


*Figure 4* – Radiant plot of 51 Andromedids.

A possible new meteor shower consisting of 28 meteors with mean orbit similar to C/1870 K1 (Winnecke). Shower mean orbit and comet orbit (see Table 4) differ by $D_{SH} = 0.17$. This shower is active from August 1 to August 15, with peak activity around August 8. The mean daily motion of the radiant is about dRA = 0.90°, dDEC = 0.27°.

The comet C/1870 K1 (Winnecke) has a parabolic orbit, but this is just a best-fit orbit to the positional data, so the possibility that it is actually a long period comet on a highly eccentric elliptical orbit is quite real.

*Table 4* – Comparison of orbital elements of 51 Andromedids (mean orbit) and the orbit of comet C/1870 K1 (Winnecke).

| parameter | 534 FOA | C/1870 K1 |
|---|---|---|
| $q$ | 0.997 | 1.009 |
| $e$ | 0.876 | 1.000 |
| $\omega$ | 194.7 | 198.2 |
| $\Omega$ | 136.0 | 143.6 |
| $i$ | 120.7 | 121.8 |
| $D_{SH}$ | 0.17 | |
| n. dist. | 0.03 | |

## 2.5 $\theta$ Cetids (535 THC) and C/1939 H1 (Jurlof-Achmarof-Hassel)

A possible new meteor shower consisting of 15 meteors with mean orbit similar to C/1939 H1 (Jurlof-Achmarof-Hassel). Shower mean orbit and comet orbit (see Table 5) are very similar, with $D_{SH} = 0.07$ only. This shower is active from July 31 to August 19, with peak activity around August 9. The mean daily motion of the radiant is roughly: dRA = 0.82°, dDEC = 0.37°.

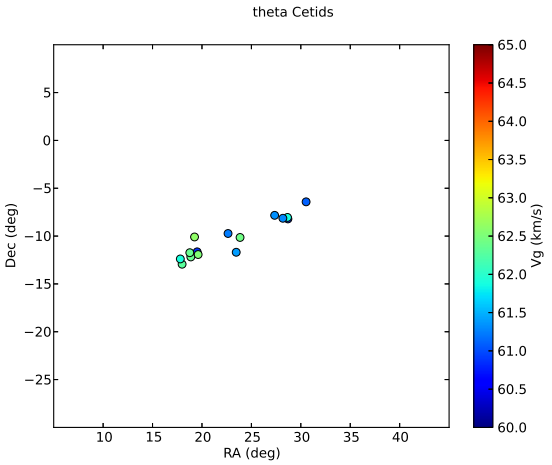


*Figure 5* – Radiant plot of $\theta$ Cetids.

*Table 5* – Comparison of orbital elements of $\theta$ Cetids (mean orbit) and the orbit of comet C/1939 H1 (Jurlof-Achmarof-Hassel). This comet comes near Earth's orbit at both nodes.

| parameter | 535 THC | 536 FSO | C/1939 H1 |
|---|---|---|---|
| $q$ | 0.499 | 0506 | 0.528 |
| $e$ | 0.969 | 0.979 | 0.998 |
| $\omega$ | 91.8 | 90.9 | 89.2 |
| $\Omega$ | 316.8 | 319.7 | 312.3 |
| $i$ | 138.0 | 137.6 | 138.1 |
| $D_{SH}$ | 0.07 | 0.11 | |
| n. dist. | 0.04 | 0.07 | |

The search also found 3 meteors that may be the second shower associated with this parent body, the 47 Ophiuchids (536 FSO, also shown in Table 5). Very roughly this second shower is active from January 31 to February 13, with a very rough estimation of daily motion of dRA = 0.8°, dDEC = 0.0°.

## 2.6 $\kappa$ Aurigids (537 KAU) and C/1957 U1 (Latyshev-Wild-Burnham)

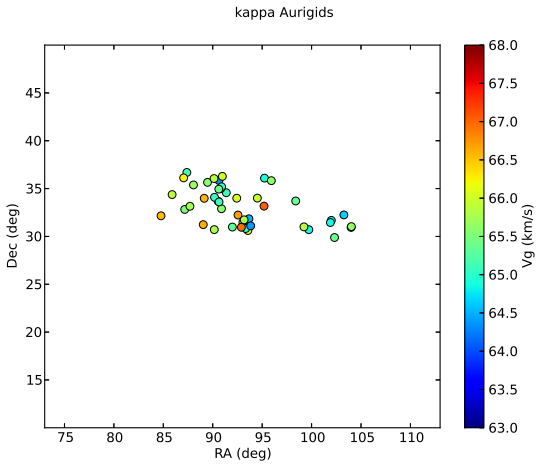


*Figure 6* – Radiant plot of $\kappa$ Aurigids.

A possible new meteor shower consisting of 45 meteors with mean orbit similar to C/1957 U1 (Latyshev-Wild-Burnham). Shower mean orbit and comet orbit (see Table 6) are very similar, with $D_{SH} = 0.07$ only. This shower is active from October 11 to October 31, with peak activity around October 20. Due to the sufficient number of known orbits it is possible to determine the mean daily motion of the radiant accurately: dRA = 1.03°, dDEC = −0.19°.

Again, the nominal orbit of comet C/1957 U1 (Latyshev-Wild-Burnham) is parabolic, but the possibility that it actually is a long period comet on a highly eccentric elliptical orbit is quite real.

*Table 6* – Comparison of orbital elements of $\kappa$ Aurigids (mean orbit) and the orbit of comet C/1957 U1 (Latyshev-Wild-Burnham).

| parameter | 537 KAU | C/1957 U1 |
|---|---|---|
| $q$ | 0.543 | 0.539 |
| $e$ | 0.958 | 1.000 |
| $\omega$ | 266.0 | 277.6 |
| $\Omega$ | 207.5 | 210.9 |
| $i$ | 158.8 | 156.7 |
| $D_{SH}$ | 0.07 | |
| n. dist. | 0.05 | |

## 2.7 55 Arietids (538 FFA) and C/1948 L1 (Honda-Bernasconi)

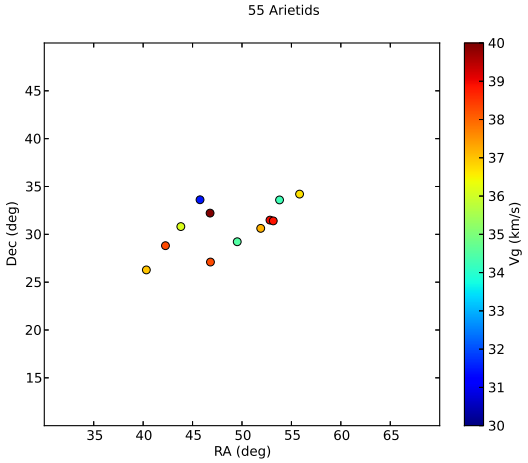


*Figure 7* – Radiant plot of 55 Arietids.

A possible new meteor shower consisting of 12 meteors with mean orbit similar to the orbit of C/1948 L1 (Honda-Bernasconi). Shower mean orbit and comet orbit (see Table 7) are similar, with $D_{SH} = 0.10$. This shower is active from October 19 to November 3, with peak activity around October 27. An estimation of the mean daily motion of the radiant is about: dRA = 0.98°, dDEC = 0.22°.

This is another case of a long period comet with eccentricity very close to 1. The nodal distance is at the moment very large, but it is quite possible that the meteors observed recently are ejected a sufficiently long time ago so that orbital evolution eventually brought them into collision with Earth.

*Table 7* – Comparison of orbital elements of 55 Arietids (mean orbit) and the orbit of comet C/1948 L1 (Honda-Bernasconi).

| parameter | 538 FFA | C/1948 L1 |
|---|---|---|
| $q$ | 0.213 | 0.208 |
| $e$ | 0.942 | 0.99987 |
| $\omega$ | 308.5 | 317.1 |
| $\Omega$ | 214.0 | 203.8 |
| $i$ | 24.2 | 23.1 |
| $D_{SH}$ | 0.10 | |
| n. dist. | 0.55 | |

## 2.8 $\alpha$ Cepheids (539 ACP) and 255P/Levy

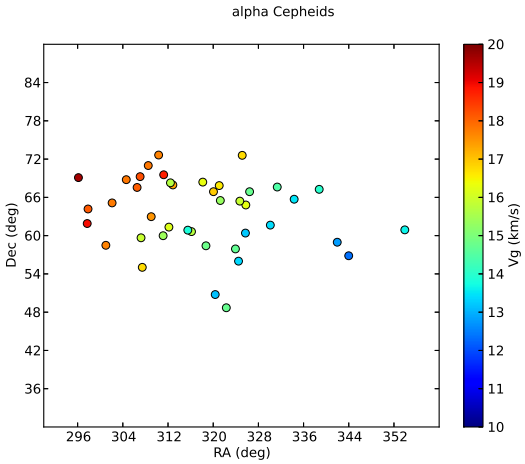


*Figure 8* – Radiant plot of $\alpha$ Cepheids.

A possible new meteor shower consisting of 41 meteors with mean orbit similar to the orbit of 255P/Levy. Shower mean orbit and comet orbit (see Table 8) are similar, with $D_{SH} = 0.10$. This shower is active from December 16 to January 17, with peak activity around January 2. Due to the sufficient number of known orbits it is possible to determine the mean daily motion of the radiant: dRA = −0.45°, dDEC = −0.32°.

The connection of a meteor shower to the comet 255P/Levy was predicted by Vaubaillon (2013b). He linked this comet's theoretical shower to the December

*Table 8* – Comparison of orbital elements of $\alpha$ Cepheids (mean orbit), the orbit of comet 255P/Levy and radiant data.

| parameter | 539 ACP | 255P/Levy | Vaubaillon |
|---|---|---|---|
| max. | Jan. 2 | | Dec. 31 |
| RA | 318 | | 332.8 |
| DEC | 64 | | 55.8 |
| $v_g$ | 15.9 | | 13.5 |
| $q$ | 0.979 | 1.008 | |
| $e$ | 0.635 | 0.668 | |
| $\omega$ | 181.7 | 179.7 | |
| $\Omega$ | 281.0 | 279.7 | |
| $i$ | 22.9 | 18.3 | |
| $D_{SH}$ | 0.10 | | |
| n. dist. | 0.01 | | |

$\phi$ Cassiopeiids (446 DPC) from the IAU MDC database. However, the two showers (539 ACP and 446 DPC) are clearly unrelated, as the radiants are separated by about 60° in RA and moreover, the maximum activity of 446 DPC falls almost a month earlier, at December 5. The radiant of 539 ACP is much closer to the theoretical comet radiant, but still about 15° from Vaubaillon's prediction. However, the spread of the 539 ACP radiant is quite large and the radiant of the shower predicted by Vaubaillon falls inside the radiants of individual meteors of 539 ACP. Also, the maximum activities of the two differ by less than 3 days.

## 2.9 $\theta$ Craterids (540 TCR) and C/2012 C2 (Bruenjes)

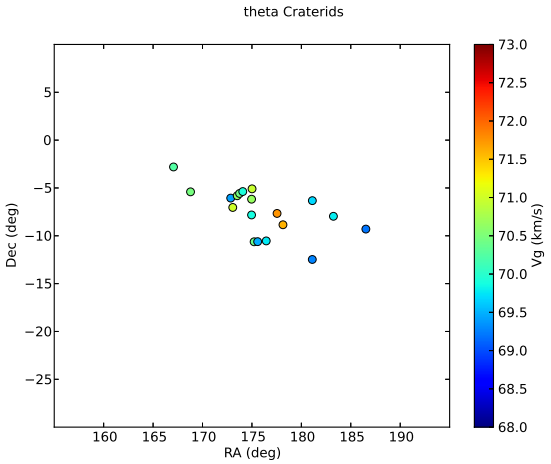


*Figure 9* – Radiant plot of $\theta$ Craterids.

A possible new meteor shower consisting of 19 meteors with mean orbit similar to C/2012 C2 (Bruenjes). Shower mean orbit and comet orbit (see Table 9) are very similar, with $D_{SH} = 0.07$ only. This shower is active from December 20 to January 17, with peak activity around January 4. The mean daily motion of the radiant is about dRA = 0.70°, dDEC = −0.28°.

*Table 9* – Comparison of orbital elements of $\theta$ Craterids (mean orbit) and the orbit of comet C/2012 C2 (Bruenjes).

| parameter | 540 TCR | C/2012 C2 |
|---|---|---|
| $q$ | 0.821 | 0.802 |
| $e$ | 0.971 | 1.003 |
| $\omega$ | 48.1 | 62.7 |
| $\Omega$ | 103.3 | 118.0 |
| $i$ | 164.5 | 162.8 |
| $D_{SH}$ | 0.07 | |
| n. dist. | 0.10 | |

## 2.10 66 Draconids (541 SSD) and 2001 XQ

A possible new meteor shower consisting of 43 meteors with mean orbit similar to 2001 XQ. Shower mean orbit and asteroid orbit (see Table 10) are quite similar with $D_{SH} = 0.09$. This shower is active from November 23 to December 21, with peak activity around December 7.

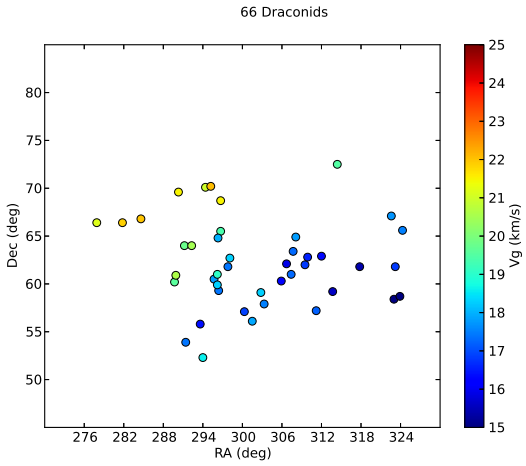


*Figure 10* – Radiant plot of 66 Draconids.

*Table 10* – Comparison of orbital elements of 66 Draconids (mean orbit) and the orbit of asteroid 2001 XQ.

| parameter | 541 SSD | 2001 XQ |
|---|---|---|
| $q$ | 0.981 | 1.035 |
| $e$ | 0.657 | 0.716 |
| $\omega$ | 184.8 | 190.1 |
| $\Omega$ | 255.2 | 251.4 |
| $i$ | 27.2 | 29.0 |
| $D_{SH}$ | 0.094 | |
| n. dist. | 0.04 | |

The mean daily motion of the radiant is dRA = −0.54°, dDEC = −0.30°, but the fit to actual data is poor.

2001 XQ is classified as an asteroid, but the body is on an orbit typical of the Jupiter family of comets opening the possibility that it is actually a dormant or extinct comet, which was active in the recent past, rather than an asteroidal body.

## 2.11 $\delta$ Sextantids (542 DES) and C/1943 R1 (Daimaca)

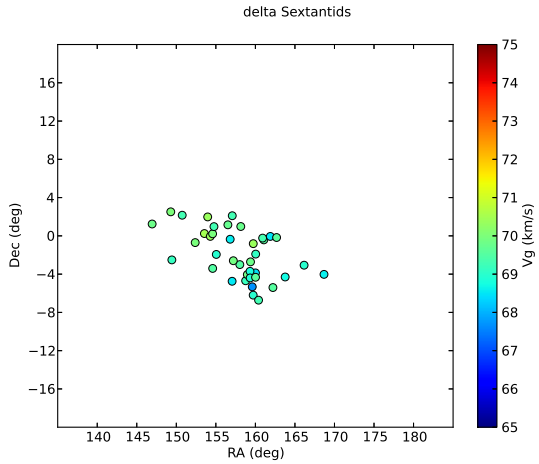


*Figure 11* – Radiant plot of $\delta$ Sextantids.

39 meteors with mean orbit similar to C/1943 R1 (Daimaca) were found by our search. Shower mean orbit and comet orbit (see Table 11) are similar with $D_{SH} = 0.21$. Although this value is a little above the

maximum we allowed when identifying parent-stream associations (the limit is set to $D_{SH} = 0.20$), we included this comet as small inaccuracies in the mean orbit of the shower (or the orbit of the comet itself) could shift the $D_{SH}$ under, or above, the preset limit. For sure, this case should be studied in more detail before further conclusions can be drawn.

This shower is active from November 29 to December 29, with peak activity around December 15. The mean daily motion of the radiant is dRA = 0.72°, dDEC = −0.29°.

This is another case of a comet on a nominally parabolic orbit, but using the same line of argument as before, we cannot exclude the possibility that it is in reality a long period comet.

*Table 11* – Comparison of orbital elements of δ Sextantids (mean orbit) and the orbit of C/1943 R1 (Daimaca).

| parameter | 542 DES | C/1943 R1 |
|---|---|---|
| $q$ | 0.835 | 0.758 |
| $e$ | 0.920 | 1.000 |
| $\omega$ | 46.7 | 36.4 |
| $\Omega$ | 83.3 | 83.4 |
| $i$ | 161.0 | 161.3 |
| $D_{SH}$ | 0.21 | |
| n. dist. | 0.16 | |

## 2.12 22 Bootids (543 TTB) and C/1793 A1 (Gregory)

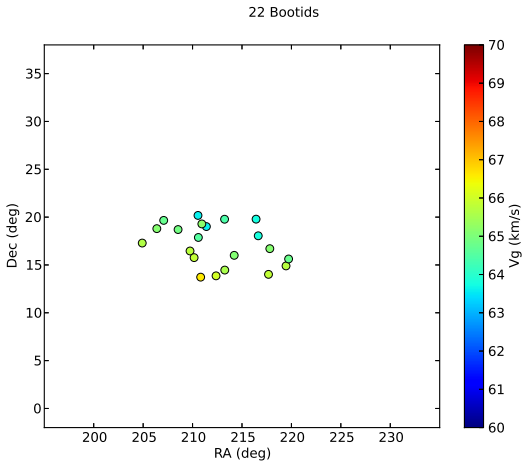


*Figure 12* – Radiant plot of 22 Bootids.

21 meteors with mean orbit similar to C/1793 A1 (Gregory) were found. Shower mean orbit and comet orbit (see Table 12) are quite similar with $D_{SH} = 0.14$. This shower is active from December 25 to January, 14, with peak activity around January 5. The mean daily motion of the radiant is dRA = 0.75°, dDEC = −0.21°.

This is another case of a comet on a parabolic orbit, but using the same line of argument as before, it may well be a long period comet.

*Table 12* – Comparison of orbital elements of 22 Bootids (mean orbit) and the orbit of C/1793 A1 (Gregory).

| parameter | 543 TTB | C/1793 A1 |
|---|---|---|
| $q$ | 0.928 | 0.966 |
| $e$ | 0.922 | 1.000 |
| $\omega$ | 152.3 | 147.2 |
| $\Omega$ | 284.1 | 286.2 |
| $i$ | 130.3 | 131.0 |
| $D_{SH}$ | 0.14 | |
| n. dist. | 0.05 | |

## 2.13 January ν Hydrids (544 JNH) and C/1787 G1 (Mechain)

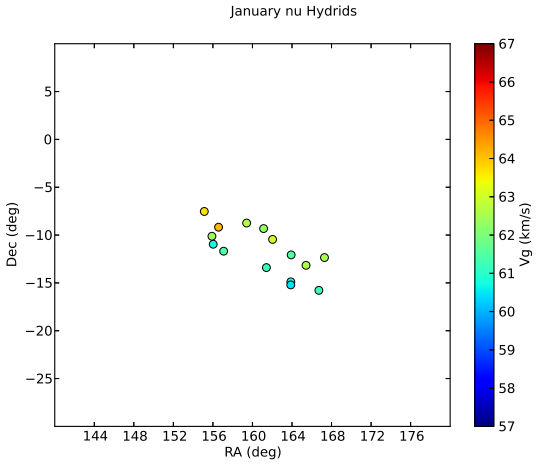


*Figure 13* – Radiant plot of January ν Hydrids.

A possible new meteor shower consisting of 15 meteors with mean orbit similar to C/1787 G1 (Mechain). Shower mean orbit and comet orbit (see Table 13) are quite similar with $D_{SH} = 0.09$. This shower is active from January 2 to January 17, with peak activity around January 10. The mean daily motion of the radiant is dRA = 0.69°, dDEC = −0.36°.

Yet another case of a comet with a parabolic orbital elements, that may actually be a long period comet.

*Table 13* – Comparison of orbital elements of January ν Hydrids (mean orbit) and the orbit of C/1787 G1 (Mechain).

| parameter | 544 JNH | C/1787 G1 |
|---|---|---|
| $q$ | 0.417 | 0.349 |
| $e$ | 0.976 | 1.000 |
| $\omega$ | 99.6 | 99.2 |
| $\Omega$ | 109.6 | 109.9 |
| $i$ | 135.1 | 131.7 |
| $D_{SH}$ | 0.094 | |
| n. dist. | 0.17 | |

## 2.14 ξ Cassiopeiids (545 XCA) and C/1871 V1 (Tempel)

A possible new meteor shower consisting of 13 meteors with mean orbit similar to C/1871 V1 (Tempel). Shower mean orbit and comet orbit (see Table 14) are quite similar with $D_{SH} = 0.12$. This shower is active from August 20 to August 30, with peak activity around

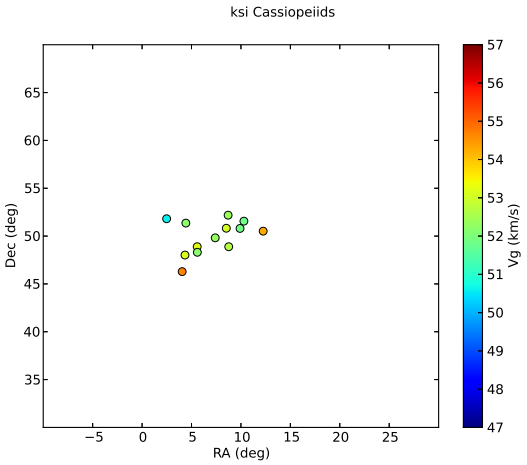


*Figure 14* – Radiant plot of ξ Cassiopeiids.

*Table 14* – Comparison of orbital elements of ξ Cassiopeiids (mean orbit) and the orbit of C/1871 V1 (Tempel).

| parameter | 545 XCA | C/1871 V1 |
|---|---|---|
| $q$ | 0.727 | 0.691 |
| $e$ | 0.990 | 0.996 |
| $\omega$ | 244.2 | 242.9 |
| $\Omega$ | 154.3 | 148.9 |
| $i$ | 94.9 | 98.3 |
| $D_{SH}$ | 0.12 | |
| n. dist. | 0.05 | |

August 27. The mean daily motion of the radiant is dRA = 0.72°, dDEC = 0.51°.

## 3 Discussion and conclusions

Using the latest complete set of both comets and NEOs downloaded from the JPL small-body database search engine as a starting point, we searched across a variety of meteor databases for orbits similar to the orbit of a particular comet/NEO. Statistically significant associations were found in 15 cases, which may represent hitherto unknown minor meteor streams. Additionally, the method automatically provides the best possible parent body candidate for the stream in question.

Also, in most cases the number of stream orbits was sufficient to determine the daily motion of the radiant with good accuracy. It is interesting to note that in the case of three showers (532 MLD, 539 ACP and 541 SSD) the daily motion dRA turned out to be negative. It seems that this is the combined effect of high declination of the radiant (all three radiants lie at declinations between 62° and 73° and show a large dispersion of radiants of individual meteors, so the obtained values of the daily motion are rather uncertain), small geocentric (and thus also entry) velocities, and possible short-term perturbations of parent bodies by Jupiter. The individual meteor radiants have been calculated without accounting for meteor deceleration, so the initial velocity could be a little different and consequently the orbital parameters also. The small difference in entry velocity at such small velocities may cause quite significant differences in true radiant positions due to zenith attraction. Last, but not least, the possible parent bodies are short-period comets and an asteroid on Jupiter family comets orbit, so they are constantly being perturbed, mainly by Jupiter, but possibly also by Earth and Mars. Thus the resulting coordinates of the radiant for observed meteors may differ a lot depending on the exact moment of the ejection of the particular meteoroid and the following perturbations by major planets.

In the case of one shower (535 THC) three meteors were found that may represent its twin shower, i.e. shower with a very similar orbit but different radiant and activity period, suggesting that the particular stream orbit intersects Earth's orbit in two points. This "three meteor shower" was thus also reported to the IAU MDC and bears the temporary designation 536 FSO.

## Acknowledgements

Our acknowledgements go to all members of the Croatian Meteor Network, in alphabetical order of first name: Alan Pevec, Aleksandar Borojević, Aleksandar Merlak, Alen Žižak, Berislav Bračun, Dalibor Brdarić, Damir Matković, Damir Šegon, Dario Klarić, Dejan Kalebić, Denis Štogl, Denis Vida, Dorian Božićević, Filip Lolić, Filip Novoselnik, Gloryan Grabner, Goran Ljaljić, Ivica Ćiković, Ivica Pletikosa, Janko Mravik, Josip Belas, Korado Korlević, Krunoslav Vardijan, Luka Osokruš, Maja Crnić, Mark Sylvester, Mirjana Malarić, Reiner Stoos, Saša Švagelj, Sonja Janeković, Tomislav Sorić, VSA group 2007, Zvonko Prihoda, Željko Andreić, Željko Arnautović, Željko Krulić.

This work was partially supported by the Ministry of Science, Education and Sports of the Republic of Croatia, Faculty of Mining, Geology and Petroleum Engineering, University of Zagreb, Višnjan Science and Education Center and by private funds of CMN members.

## References

Andreić Ž. and Šegon D. (2010). "The first year of Croatian Meteor Network". In Kaniansky S. and Zimnikoval P., editors, *Proceedings of the International Meteor Conference, Šachtička, Slovakia, 18–21 September 2008*. International Meteor Organization, pages 16–23.

Andreić Ž., Šegon D., and Korlević K. (2010). "The second year of Croatian Meteor Network". In Andreić Ž. and Kac J., editors, *Proceedings of the International Meteor Conference, Poreč, Croatia, 24–27 September 2009*. International Meteor Organization, pages 26–30.

CMN (2007-2013). "CMN catalogues 2007–2010". `http://cmn.rgn.hr/downloads/downloads.html`.

Drummond J. D. (1981). "A test of comet and meteor shower associations". *Icarus*, **45**, 545–553.

IMO (1993-2012). "IMO video meteor database". `http://www.imonet.org/database.html` .

Jenniskens P., Jopek T. J., Rendtel J., Porubčan V., Spurný P., Baggaley J., Abe S., and Hawkes R. (2009). "On how to report new meteor showers". *WGN, Journal of the IMO*, **37:1**, 19–20.

Jopek T. J. (1993). "Remarks on the meteor orbital similarity D-criterion". *Icarus*, **106**, 603–607.

JPL (2013). "JPL small-body database search engine". `http://ssd.jpl.nasa.gov/sbdb_query.cgi` .

Korlević K., Šegon D., Andreić Ž., Novoselnik F., Vida D., and Skokić I. (2013). "Croatian Meteor Network catalogues of orbits for 2008 and 2009". *WGN, Journal of the IMO*, **41:2**, 48–51.

SonotaCo (2005-2013). "SonotaCo Network simultaneously observed meteor data sets (catalogues 2007–2011)". `http://sonotaco.jp/doc/SNM/` .

SonotaCo (2009). "A meteor shower catalog based on video observations in 2007–2008". *WGN, Journal of the IMO*, **37:2**, 55–62.

Southworth R. B. and Hawkins G. S. (1963). "Statistics of meteor streams". *Smithsonian Contr. Astrophys.*, **7**, 261–285.

Šegon D., Andreić Ž., Korlević K., Novoselnik F., and Vida D. (2012). "Croatian Meteor Network catalogue of orbits for 2007". *WGN, Journal of the IMO*, **40:3**, 94–97.

Vaubaillon J. (2013a). "The next big meteor shower". `http://www.imcce.fr/langues/en/ephemerides/phenomenes/meteor/DATABASE/209_LINEAR/2014` .

Vaubaillon J. (2013b). "IMCCE meteor showers – calendar". `http://www.imcce.fr/langues/en/ephemerides/phenomenes/meteor/predictions.php` . (On List of Ephemerids choose DecemberPhiCassiopeiids).

*Handling Editor:* David Asher
This paper has been typeset from a LaTeX file prepared by the authors.

*Table 15* – Mean orbits of the new showers. ID and name are the IAU identification and name of the shower, $\lambda_\odot$ solar longitudes of the activity period, $\overline{\lambda_\odot}$ average solar longitude, RA and DEC are coordinates of the mean radiant, $v_g$ is geocentric velocity, $q$ perihelion distance, $e$ eccentricity, $\omega$ argument of perihelion, $\Omega$ longitude of ascending node, $i$ inclination and $N$ is the number of known orbits. The $\pm$ values are standard deviations. In the case of RA and DEC there is a contribution of the daily motion to the dispersion of the radiants.

| ID | name | $\lambda_\odot$ | $\overline{\lambda_\odot}$ | RA | DEC | $v_g$ | $q$ | $e$ | $\omega$ (peri) | $\Omega$ (node) | $i$ | $N$ |
|---|---|---|---|---|---|---|---|---|---|---|---|---|
| 531 | GAQ $\gamma$ Aquilids | 38–51 | 45 | 301.8±3 | 13.8±2 | 62.7±1.1 | 0.988±0.007 | 0.957±0.048 | 196.2±3.3 | 44.5±4 | 123.4±3 | 27 |
| 532 | MLD May $\lambda$ Draconids | 35–74 | 52 | 155.0±33 | 73±9 | 14.4±1.8 | 0.987±0.024 | 0.651±0.040 | 165±13 | 52±11 | 18.7±4 | 23 |
| 533 | JXA July $\xi$ Arietids | 103–140 | 119 | 40.1±8 | 10.6±2.8 | 69.4±0.7 | 0.883±0.047 | 0.965±0.047 | 318±8 | 299±10 | 171.6±2.6 | 61 |
| 534 | FOA 51 Andromedids | 130–143 | 136 | 23.3±4 | 47.3±2.1 | 60.8±1.1 | 0.997±0.01 | 0.876±0.058 | 195±5 | 136±4 | 120.7±3 | 28 |
| 535 | THC $\theta$ Cetids | 129–147 | 137 | 23.0±5 | −10.2±2.1 | 61.8±0.6 | 0.499±0.032 | 0.969±0.032 | 92±4 | 317±5 | 138.0±1.1 | 15 |
| 536 | FSO 47 Ophiuchids | 311–325 | 320 | 259.0±6 | −4.1±0.3 | 63.3±0.4 | 0.506±0.031 | 0.979±0.006 | 90.9±4 | 320±7 | 137.6±0.5 | 3 |
| 537 | KAU $\kappa$ Aurigids | 198–218 | 208 | 93.1±5 | 33.2±2.0 | 65.5±0.7 | 0.543±0.035 | 0.958±0.041 | 266±4 | 208±5 | 159±4 | 45 |
| 538 | FFA 55 Arietids | 206–221 | 214 | 48.6±5 | 30.8±2.5 | 36.9±2.5 | 0.213±0.014 | 0.942±0.044 | 308.5±3.1 | 214±5 | 24±4 | 12 |
| 539 | ACP $\alpha$ Cepheids | 265–297 | 281 | 318.0±13 | 64±6 | 15.9±1.9 | 0.979±0.004 | 0.635±0.040 | 182±9 | 281±9 | 22.9±3.7 | 41 |
| 540 | TCR $\theta$ Craterids | 269–297 | 283 | 175.9±5 | −7.4±2.4 | 70.2±0.7 | 0.821±0.036 | 0.971±0.062 | 48±6 | 103±6 | 164.5±3.4 | 19 |
| 541 | SSD 66 Draconids | 242–270 | 255.2 | 302±12 | 62±4 | 18.2±2.0 | 0.981±0.006 | 0.657±0.044 | 184.8±7 | 255.2±7 | 27.2±4 | 43 |
| 542 | DES $\delta$ Sextantids | 248–278 | 263.3 | 158±4 | −1.9±2.6 | 69.4±0.6 | 0.835±0.033 | 0.920±0.047 | 46.7±6 | 83.3±6 | 161.0±4 | 39 |
| 543 | TTB 22 Bootids | 274–294 | 284.1 | 212.5±4 | 17.1±2.2 | 65.0±0.9 | 0.928±0.018 | 0.922±0.039 | 152.3±5 | 284.1±5 | 130.3±3 | 21 |
| 544 | JNH January $\nu$ Hydrids | 281–297 | 289.6 | 161±4 | −11.7±2.4 | 62.0±1.1 | 0.417±0.030 | 0.976±0.031 | 99.6±3 | 109.6±6 | 135.1±4 | 15 |
| 545 | XCA $\xi$ Cassiopeiids | 148–157 | 154.3 | 7.1±2.5 | 49.9±1.8 | 52.7±1.1 | 0.727±0.021 | 0.990±0.044 | 244.2±37 | 154.3±3 | 94.9±3 | 13 |

# Bright Perseids 2007–2013 and artificial Earth satellites collision risk assessment

*Andrey Murtazov*[1]

The 2007–2013 bright Perseids observation statistics are presented. The collision risk of these meteoroids with space vehicles is assessed.

Received 2014 January 11

## 1 Introduction

A lot of attention has been paid recently to meteor investigations in the context of the different types of hazards caused by comparatively small meteoroids.

Furthermore, the investigation of risk distribution related to collisions of meteoroids over 1 mm with space vehicles is quite important for the long-term forecast regarding the development of space research and circumterrestrial ecology problems (Beech et al., 1997; Foschini, 1998; Wiegert & Vaubaillon, 2009).

## 2 Bright Perseids wide-angle CCD monitoring statistics

In the Perseids shower hazardous are particles with radius greater than 1 mm and weight greater than 0.01 g (such meteoroid's kinetic energy for a velocity of $\sim$ 60 km/s relative to the Earth exceeds a the energy of a bullet fired from a pistol). According to Babadzhanov (1987) a hazardous Perseids brightness is more intense than zero magnitude.

To monitor meteor showers we used equipment based on the CCD camera Watec-902H with wide-angle Computar T2314FICS lens directed towards the local zenith (Murtazov et al., 2008; Murtazov et al., 2013). The meteor cameras are set on the observation sites of the Ryazan observatory ($\lambda = 2^{\rm h}39^{\rm m}$, $\phi = 54°38'$) and a settlement not far from Ryazan ($\lambda = 2^{\rm h}39^{\rm m}$, $\phi = 54°28'$).

In total during 2007–2013 (excluding 2010) about 300 bright meteors of the Perseids shower were observed.

The comparison of the measured bright Perseids flux average values with the total shower flux based on the 2007–2013 IMO visual data is shown in Figure 1. Taken as the unit value is the average maximum IMO shower spatial density $D = 81 \cdot 10^{-9}$ km$^{-3}$.

In terms of statistics the distribution of bright meteors appeared to be close to all the Perseids meteors distribution.

During the Perseids maximum the hazardous particle flux reached the instantaneous value $F = (3.8 \pm 1.1) \cdot 10^{-7}$ km$^{-2}$s$^{-1}$, which conformed with the hourly rate of meteors in the all-sky camera FOV $HR \approx 15$.

The ratio of the bright Perseids flux maximum to that of the IMO data is 0.076.

The total number of brighter than $0^{\rm m}$ meteors in the Perseids is equal to the ratio of the $\int_\lambda D\, d\lambda$ integrals under the curves, and in 2007–2013 it was $0.051 \pm 0.008$.

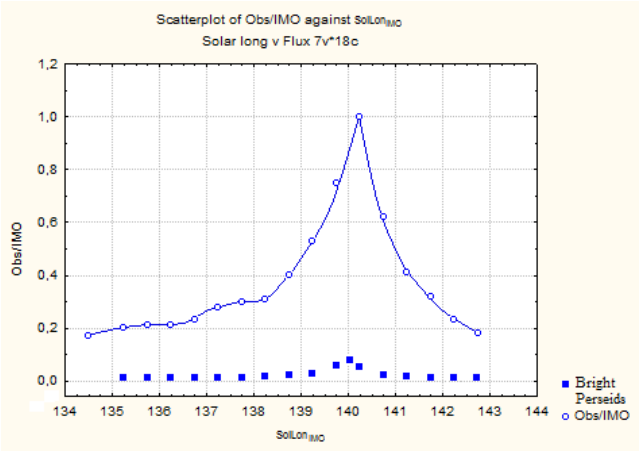


*Figure 1* – Comparison between the results of bright Perseids wide-angle CCD monitoring and IMO data regarding the whole shower.

The normalized results of the 2007–2013 bright Perseids monitoring are shown in Figure 2 versus the IMO data and (Koseki, 2012).

Shown here are the rates describing the shower activity for photo- and TV-observations (SonotaCo), as well as the estimates obtained in work (Koseki, 2012). The same units are used to show our 2007–2013 averaged results (bright Perseids) and the IMO averaged

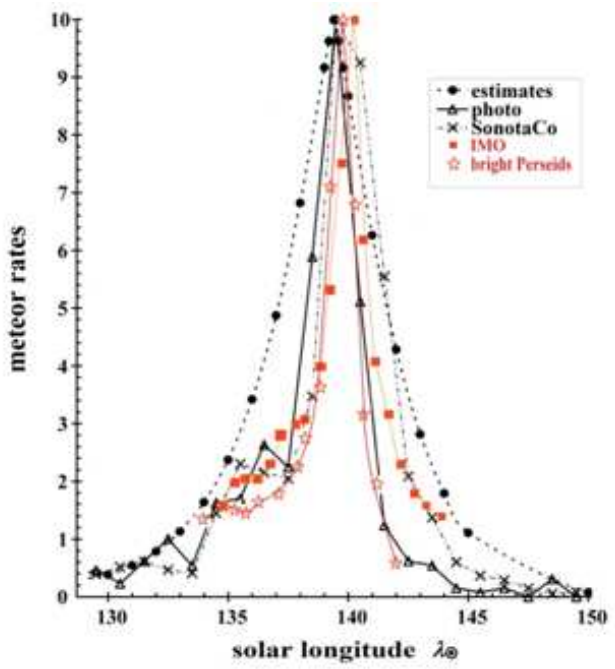


*Figure 2* – Comparison of 2007–2013 bright Perseids monitoring with other observations' data and model estimates.

[1]Ryazan State University named for S. Yesenin, Ryazan, Russia. Email: a.murtazov@rsu.edu.ru

IMO bibcode WGN-422-murtazov-perseids
NASA-ADS bibcode 2014JIMO...42...65M

results of Perseids visual observations during the same period.

Conspicuous is a small discrepancy in the shower maximum longitudes which were determined by different methods.

We observed the shower maximum with the Solar longitudes close to $\lambda_\odot = 140°$, whereas the IMO maximum falls within the range $\lambda_\odot = 140\overset{\circ}{.}0$–$140\overset{\circ}{.}5$, and the photo- and TV-observations Koseki reach maximum near $\lambda_\odot = 139\overset{\circ}{.}5$.

## 3 Assessment of risk related to Perseids hazardous meteoroids' collision with space vehicles

The hazardous meteoroid flux $F$ is defined as a number of particles crossing a unit surface per time: $F(\lambda) = D(\lambda)v$, where: $v$ – the meteor shower velocity, $D(\lambda)$ – the shower spatial density at the corresponding Solar longitude $\lambda_\odot$.

A satellite rotating around the Earth constantly changes its orientation relative to the meteor shower radiant direction and the Sun. From time to time the Earth shades the satellite from the meteors.

In general, the total number of collisions with a satellite during its orbiting time $T$ is calculated as $N = K_1K_2K_3SF(\lambda_\odot)T$ (Murtazov, 2013). Here $K_1$ accounts for the Earth's position in it's orbit relative to the meteor shower radiant and is determined by the difference between ecliptic longitudes of the Sun and the meteor shower radiant; $K_2$ depends on the orientation of a satellite with respect to the Sun and the attitude of its components (e.g. solar panels) relative to the shower radiant; $K_3$ accounts for the satellite orbit orientation relative to Earth's equatorial plane and ecliptic, duration of the satellite's time in the 'shadow' of the Earth, and the shower gravitation gain.

The shower flux is defined by the distribution $F = F_0 \exp\{-B|\lambda_\odot - \lambda_0|^2\}$, where $F_0$ is the maximum flux of the shower near solar longitude $\lambda_0$, $B$ – is the factor empirically estimated from observations of the shower.

The calculations were carried out in the satellite-centric reference system (Figure 3), provided the assumption that a satellite is located in the ecliptic. In this figure $\mathbf{N}$ – the normal to the satellite surface; ♈, ⊙, $\mathbf{E}$ – directions to the vernal equinox point, the Sun, and the Earth; $\lambda_\mathbf{R}$, $\lambda_\odot$ – meteor radiant and the Sun ecliptic longitudes; $\lambda_\mathbf{E}$ – the Earth ecliptic longitude; $\mathbf{b_R}$ and $\mathbf{b_E}$ – consequent ecliptic latitudes of the meteor radiant and the Earth relative to the satellite.

The collision number is determined only by the shower flux density $F(\lambda_\odot)$, the area of the satellite hemisphere facing the radiant, the time spent in the shade of the Earth screened from the shower, and the time $T$.

For a spherical satellite rotating around the Earth along a circular orbit, $K_1 = K_2 = 1$.

$K_3$ determines the part of the satellite orbital period during which the satellite is screened off by the Earth (Cour-Palais, 1969).

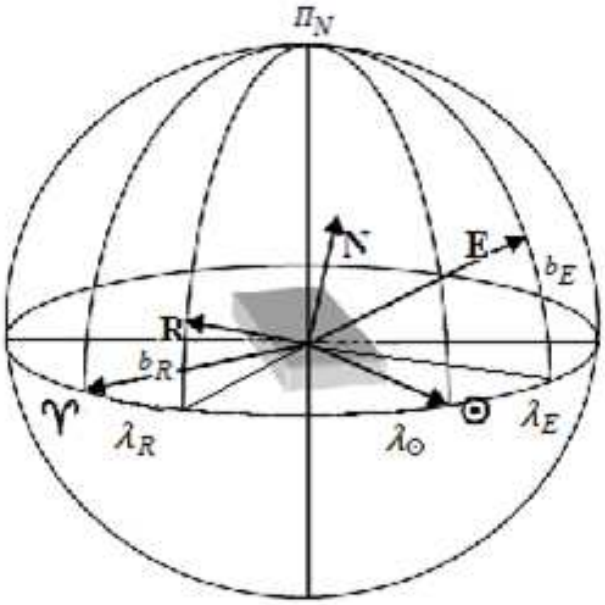


*Figure 3* – Reference system for circumterrestrial collision risk calculation.

The condition of entering the shade: the angular distance between the visible Earth disk center and the shower radiant must not exceed the visible Earth disk radius $\rho_E$.

In the ecliptic coordinates $|b_R - b_E| \le \rho_E$, the Earth ecliptic latitude is calculated as $b_E = i + \varepsilon$. Here $i$ – the satellite orbit inclination against the Earth equator plane, $\varepsilon = 23°27'$ – the ecliptic inclination against the equator.

In the satellite celestial sphere of the satellite-centric reference system the Earth disk moves along the satellite orbit equator, while the meteor radiant makes a small circle in a plane parallel to the equatorial plane (Figure 4).

Since the latitude of the Earth disk center shown here is equal to 0, in satellite-centric coordinate system (Figure 4):

$$\begin{cases} \Phi_R = b_R - i - \varepsilon, \\ \Phi_E = 0 \end{cases}$$

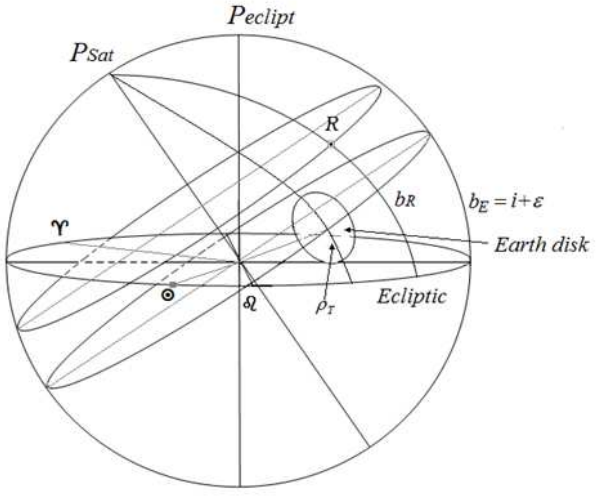


*Figure 4* – Celestial sphere in satellite-centric reference system.

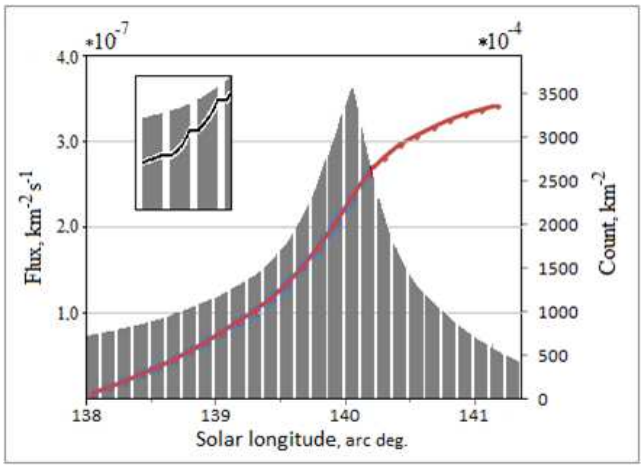


*Figure 5* – Perseids' dangerous meteoroid shower flux in the period of its maximum in 2007–2013 accounting for spherical satellites.

and the condition of entering the shade is $b_R - i - \varepsilon \le \rho_E$, The angular dimensions of the shadow for a satellite are calculated from $\sin\rho = \frac{R_m}{R_E+h}$, where $R_m$ – the Earth's radius with respect to the altitude of the atmosphere layer in which meteors burn up ($\sim$ 100 km), $h$ – the satellite orbital height; $R_E = 6400$ km.

For instance, for a satellite having a circular orbit with the height $h = 4000$ km (radius = 10400 km) and inclination equal to the inclination of the meteor shower plane relative to the Earth's equator plane, the period $T = 3$ h. $\sin\rho = 0.625$, $\rho = 38.7°$, $2\rho = 77.4°$, i.e. the duration in the shade $t_T = 0.215T$ or $38^{\rm m}7$ per three hours.

Figure 5 shows the results of Perseids 2007–2013 dangerous meteoroid flux calculations for a spherical satellite in the case where a shower radiant lies in its orbit plane $\phi_R = \phi_E = 0$ during 3 days near the shower maximum.

The gravitational effect for this satellite's orbit and Perseids' velocity is rather mild and its correction factor is close to 1.

The dates close to the Perseids maximum activity are August 10–13. The solar longitude difference approximately corresponds to the days' difference $\Delta\lambda_\odot = 0.9863°\text{day}^{-1}$.

The shaded portions are the areas during which satellites are subject to meteoroid bombardment. During the intervals between them a satellite is shaded from meteoroids by the Earth.

The smooth curve results from the calculation of the total number of collisions between meteoroids and satellites over a given period of time. More accurately this curve is represented as graduated – during the satellite's stay behind the Earth there are no collisions and no summation
$N = N_0 \sum_{i=1}^{n} \left[\lambda_{i+1} e^{-B(\lambda_{i+1}-\lambda_0)^2} - \lambda_i e^{-B(\lambda_i-\lambda_0)^2}\right]$.
The total collision number $N$ over the calculation period (3.2 days) appeared to be close to 0.35 km$^{-2}$.

The collision risk is defined here as the value reciprocal of the collision number, i.e. approximately 0.1 collision per day in the interval $\Delta\lambda_\odot = 3.2°$.

The risk of collision between a satellite and the Perseids dangerous meteoroids (over 1 mm) near their maximum in 2007–2013 was $R \approx 0.1$ km$^{-2}$day$^{-1}$.

It should be noted that the sporadic meteor flux with magnitude brighter than $0^{\rm m}$ is close to the values we obtained for the Perseids meteoroids, which means that their risk must be taken into consideration, too.

## 4 Conclusions

The calculated risk value shows that it is not large. However, as the probability of collision between bright Perseids and satellites is not equal to zero, this risk should be taken into account while projecting long-term space missions.

Therefore, fairly simple meteor observations make it possible to assess the risk of collisions between dangerous meteoroids within meteor showers and circumterrestrial space vehicles.

## References

Babadzhanov P. B. (1987). *Meteors and their observation.* Nauka, Moscow.

Beech M., Brown P., Jones J., and Webster A. R. (1997). "The danger to satellites from meteor storm". *Adv. Space Res*, **20**, 1509–1512.

Cour-Palais B. (1969). *Meteoroid Environment Model – 1969 [Near Earth to Lunar surface].* NASA, Washington, DC, United States. (NASA SP-8013).

Foschini L. (1998). "The meteoroid hazard for space navigation". In *Proceedings of Second National Meeting of Planetary Sciences*, Italy.

Koseki M. (2012). "A simple model of spatial structure of meteoroid streams". *WGN, Journal of the IMO*, **40:5**, 162–165.

Murtazov A. K. (2013). "Bright Perseids 2007-2013 statistics. estimation of collision risk in circumterrestrial space". In *European Planetary Science Congress 2013. London, UK, EPSC Abstracts, 8, EPSC2013-346-1.*

Murtazov A. K., Efimov A., and Kolosov D. (2008). "Bright Perseids in 2007". *WGN, Journal of the IMO*, **36:4**, 77–78.

Murtazov A. K., Efimov A., and Titov P. (2013). "Double-station meteor observations in Ryazan, Russia". In *Proceedings of the International Meteor Conference, 31st IMC, La Palma, Canary Islands, Spain, 2012.* pages 192–195.

Wiegert P. and Vaubaillon J. (2009). "The sporadic meteoroid complex and spacecraft risk". In Kleiman J. I., editor, *Proceedings of the 9th International Conference "Protection of Materials and Structured from Space Environment"*. American Institute of Physics, pages 567–571.

*Handling Editor:* Javor Kac

# Meteor showers of the southern hemisphere

*Sirko Molau*[1] *and Steve Kerr*[2]

We present the results of an exhaustive meteor shower search in the southern hemisphere. The underlying data set is a subset of the IMO Video Meteor Database comprising 50,000 single station meteors obtained by three Australian cameras between 2001 and 2012. The detection technique was similar to previous single station analysis. In the data set we find 4 major and 6 minor northern hemisphere meteor showers, and 12 segments of the Antihelion source (including the Northern and Southern Taurids and six streams from the MDC working list). We present details for 14 southern hemisphere showers plus the Centaurid and Puppid-Velid complex, with the $\eta$ Aquariids and the Southern $\delta$ Aquariids being the strongest southern showers. Two of the showers ($\theta^2$ Sagittariids and $\tau$ Cetids) were previously unknown and have received preliminary designations by the MDC. Overall we find that the fraction of southern meteor showers south of $-30°$ declination (roughly 25%) is clearly smaller than the fraction of northern meteor showers north of $+30°$ declination (more than 50%) obtained in our previous analysis.

Received 2013 December 17

## 1 Introduction

The search for meteor showers in the optical domain has reached a new quality in the first decade of the 21st century. Thanks to the efficiency of large video meteor networks, plenty of single- and multi-station data has become available. Major and minor showers in the working list of the IAUs Meteor Data Center (MDC) (IAU MDC, 2013) have been confirmed on a regular basis by investigations based on IMO Network, SonotaCo Network and CAMS data, to name just the biggest contributors. To date, the majority of all cameras are located in the northern hemisphere (central Europe, Japan, US). They are efficient in detecting meteor showers down to declination $-20°$, but they cannot detect far southern meteor showers.

Over the years, the IMO Video Meteor Network (Molau & Barentsen, 2014) has had three observers in Australia that contributed single station observations for a number of years. Their data are an integral part of the IMO Network database and thus were used in all previous analysis, but they were by far outnumbered by northern hemisphere observations and were effectively lost in the data set.

In this paper, we selected only the data from these three Australian cameras located between $-23°$ and $-32°$ latitude. We applied the same procedure as for the recent overall IMO Network survey (Molau, 2014) and searched specifically for southern hemisphere meteor showers.

## 2 Data-set

Rob McNaught started to contribute observations with his intensified camera Sso1 in February 2001. He observed for three month and provided a total of more than 5 000 meteors that were submitted to the IMO Network.

[1]Abenstalstr. 13b, 84072 Seysdorf, Germany.
Email: sirko@molau.de
[2]22 Green Avenue, Glenlee 4711, Queensland, Australia.
Email: srkak@optusnet.com.au

IMO bibcode WGN-422-molau-southern
NASA-ADS bibcode 2014JIMO...42...68M

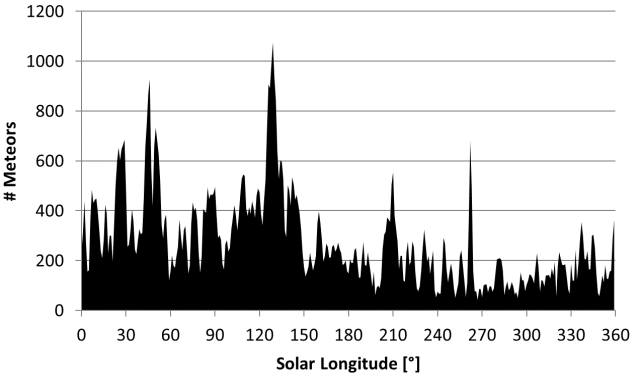


*Figure 1* – Distribution of meteors over solar longitude.

In April 2002, Steve Quirk jumped in with the non-intensified camera Sso-wat1. Until November 2003, he submitted a total of over 10 000 meteors to the IMO Network.

Finally, Steve Kerr joined the IMO network in January 2010. He contributed to this analysis almost 34 000 meteors recorded until December 2012, which is the latest IMO Network data set currently available.

All three data sets together make up a total of almost 50 000 meteors obtained over more than 8 000 hours of effective observing time. The details are given in Table 1.

The same single station analysis procedure was applied as in a previous analysis (Molau, 2014). The interval length was 2° solar longitude with a shift of 1°. That is, each meteor contributed to two consecutive bins. Figure 1 depicts the distribution of meteors over solar longitude. Obviously, the data set is much smaller than in the previous analysis, but still there were only two solar longitude intervals without meteors (267° and 271°). In these two, and 14 further bins with less than 50 meteors, we doubled the bin size to four degrees to ensure a minimum number of 50 meteors per bin. The median was 230 meteors per bin.

After the detection of the radiants, we searched for showers with noticeable activity in at least four consecutive solar longitude intervals. That resulted in a list of 83 meteor shower candidates, which were manually quality-checked and corrected.

*Table 1* – Data set from three Australian cameras used for this analysis.

| Observer | Time | Site | Camera | Nights | Eff. obs. time (h) | Meteors |
|---|---|---|---|---|---|---|
| R. McNaught | 02/01–04/01 | Coonabarabran | SSO1 | 52 | 383 | 5 278 |
| S. Quirk | 04/02–11/03 | Mudgee | SSO1-WAT1 | 344 | 3 042 | 10 116 |
| S. Kerr | 01/10–12/12 | Glenlee | GOCAM1 | 647 | 4 667 | 33 971 |
| | | | Total | 1 043 | 8 092 | 49 365 |

## 3 Northern hemisphere showers

Two of the most prominent meteor showers of the northern hemisphere, the Perseids (7 PER) and Quadrantids (10 QUA), were not found in the Australian data set (the Perseids were only detected in three solar longitude intervals), but all other major showers like the Lyrids (6 LYR), Orionids (8 ORI), Taurids (2 STA, 17 NTA), Leonids (13 LEO) and Geminids (4 GEM) were present in the list. Also five smaller northern showers were clearly detected: $\phi$ Piscids (372 PPS), July Pegasids (175 JPE), September $\pi$ Orionids (430 POR), November Orionids (250 NOO) and December Monocerotids (19 MON). Most of the northern hemisphere showers were detected in the second half of the year, where they sometimes even outnumbered their southern counterparts. In the first half of the year, on the other hand, the Lyrids were the only shower with positive declination.

### 3.1 Antihelion source

The Antihelion source (ANT) is active all year long, and in the southern hemisphere it is often the strongest source in the sky. The MDC does not list the Antihelion source as one shower, but there are numerous "streamlets" with slightly different characteristics. So we also find individual showers in our data set belonging to the Antihelion source. These are:

- an unnamed ANT segment at the boundary of March/April with almost 80 meteors
- the $\lambda$ Virginids (49 LVI) with 80 meteors
- the April $\chi$ Librids (140 XLI) with almost 100 meteors
- the Northern May Ophiuchids (149 NOP) with almost 150 meteors
- the Southern May Ophiuchids (150 SOP) with over 200 meteors
- the Southern $\mu$ Sagittariids (69 SSG) with over 120 meteors
- the Southern $\sigma$ Sagittariids (168 SSS) with almost 220 meteors
- an unnamed ANT segment at the boundary of August/September with over 60 meteors
- an unnamed ANT segment in mid-September with almost 50 meteors
- the Southern Taurids (2 STA) with over 670 meteors
- twice the Northern Taurids (17 NTA) with over 110 meteors

In most cases, there is significant scatter in the day-to-day radiant data of these showers which is typical for diffuse sporadic sources. Details for the "streamlets" are given in Table 2.

Data from northern hemisphere showers and the Antihelion source were obtained more accurately in the last full analysis of the IMO network database (Molau, 2014). In the following we are focusing on southern hemisphere showers (with one exception). For each shower, we give a short overview of the dataset and quality. We will present the meteor shower parameters obtained by us and compare them with the MDC

*Table 2* – Parameters of the Antihelion shower where detected as an independent source. UNK refers to "streamlets" which are not listed as individual showers by the MDC.

| Source | Solar longitude | | Right Ascension | | Declination | | $v_g$ | |
|---|---|---|---|---|---|---|---|---|
| | Mean | Interval | Mean | Drift | Mean | Drift | Mean | Drift |
| | [°] | [°] | [°] | [°] | [°] | [°] | [km/s] | [km/s] |
| UNK | 10 | 8–12 | 200 | +1.7 | −16 | +0.6 | 27 | — |
| 49 LVI | 20 | 15–22 | 197 | +0.5 | −12 | −0.6 | 25 | — |
| 140 XLI | 41 | 38–44 | 244 | +1.2 | −22 | +1.0 | 37 | — |
| 149 NOP | 50 | 46–52 | 243 | −1.2 | −22 | −1.1 | 31 | — |
| 150 SOP | 63 | 50–66 | 260 | +0.9 | −17 | −0.0 | 32 | — |
| 69 SSG | 77 | 74–80 | 266 | +1.3 | −26 | −1.6 | 24 | — |
| 168 SSS | 86 | 79–94 | 271 | +1.9 | −29 | −0.1 | 24 | — |
| UNK | 158 | 156–161 | 355 | −0.3 | −1 | +1.2 | 30 | — |
| UNK | 174 | 171–176 | 9 | +0.7 | +6 | −1.2 | 31 | — |
| 2 STA | 212 | 182–241 | 44.4 | +0.79 | +11.0 | +0.16 | 27.5 | −0.04 |
| 17 NTA | 186 | 184–188 | 18 | 0 | +12 | +0.2 | 27 | — |
| 17 NTA | 234 | 230–238 | 63 | +0.8 | +23 | +0.5 | 28 | — |

*Table 3* – Parameters of the $\alpha$ Hydrids.

| Source | Solar longitude | | Right Ascension | | Declination | | $v_g$ | |
|---|---|---|---|---|---|---|---|---|
| | Mean | Interval | Mean | Drift | Mean | Drift | Mean | Drift |
| | [°] | [°] | [°] | [°] | [°] | [°] | [km/s] | [km/s] |
| MDC | 285.5 | — | 127.6 | +0.65 | −7.9 | −0.17 | 43.6 | — |
| IMO 2013 | 280 | 270–288 | 125.0 | +0.7 | −7.4 | −0.2 | 43 | — |
| Here | 282 | 280–285 | 127 | +0.3 | −7 | +1 | 46 | — |

*Table 4* – Parameters of different streamlets in February in Centaurus.

| Source | Solar longitude | | Right Ascension | | Declination | | $v_g$ | |
|---|---|---|---|---|---|---|---|---|
| | Mean | Interval | Mean | Drift | Mean | Drift | Mean | Drift |
| | [°] | [°] | [°] | [°] | [°] | [°] | [km/s] | [km/s] |
| MDC OCA | 322.7 | — | 177 | — | −56 | — | 51 | — |
| MDC TCN | 322.7 | — | 210 | — | −40 | — | 59 | — |
| MDC ACE | 319.4 | — | 212.1 | +1.9 | −59.4 | — | 58.2 | — |
| Here | 325 | 323–326 | 199 | — | −55 | — | 48 | — |
| | 325 | 323–327 | 209 | — | −29 | — | 65 | — |
| | 325 | 323–326 | 215 | — | −56 | — | 68 | — |

*Table 5* – Parameters of the $\gamma$ Normids.

| Source | Solar longitude | | Right Ascension | | Declination | | $v_g$ | |
|---|---|---|---|---|---|---|---|---|
| | Mean | Interval | Mean | Drift | Mean | Drift | Mean | Drift |
| | [°] | [°] | [°] | [°] | [°] | [°] | [km/s] | [km/s] |
| MDC | 353 | — | 251.6 | — | −51.3 | — | 64 | — |
| Here | 4 | 2–7 | 246 | +1.3 | −51 | +0.8 | 68 | — |

list value and with the results of our own full analysis (where available). Beside established working list meteor showers, we will introduce two newly detected showers, which have received preliminary shower codes from the Meteor Data Center. The showers are sorted by the time of their maximum.

## 4 Southern hemisphere showers

### 4.1 $\alpha$ Hydrids

The $\alpha$ Hydrids (331 AHY) are detected right at the begin of year. 40 meteors of that shower were recorded between January 1 to 6, and in that time interval it is the strongest source in the southern skies. Given the small data set, the data quality is acceptable. There is no clear peak in activity, which is why we list the radiant position for the center of the activity interval in Table 3. Our results agree well with the values in the MDC working list obtained by Brown et al. (2008) from Canadian radar data, and with our own analysis from the full IMO Network database.

### 4.2 February streamlets in Centaurus

Between February 12 and 16, three streamlets can be detected in the constellation of Centaurus. Each of them contains less than 30 meteors, and there is large scatter in the meteor shower parameters. Hence we cannot confirm any of these with certainty. However, at the same time the MDC lists three shower in that region of the sky, namely the $\alpha$ Centaurids (102 ACE), $\theta$ Centaurids (317 TCN) and $\omega$ Centaurids (315 OCA). From this we would conclude, that at least some of these structures are real (Table 4).

### 4.3 $\gamma$ Normids

The $\gamma$ Normids (118 GNO) cannot be unequivocally detected in our data set, but we find a stream with 40 meteors between March 23 and 28, that has at least some similarity. The radiant position and meteor shower velocity match approximately, but the reference solar longitude of MDC (based on Australian radar data; see Gartrell and Elford, 1975) is 11° off. So depending on the radiant drift, the gap may in fact be larger. Also in this case the activity profile shows no clear peak, and the data quality is acceptable given the small data set (Table 5).

### 4.4 $\eta$ Aquariids

The $\eta$ Aquariids (31 ETA) are one of the two strongest southern hemisphere meteor showers. The three Australian cameras recorded over 1 600 shower members between April 24 and May 18, which is about as much data as was collected from all the northern hemisphere cameras of the IMO Network. Consequently, the radiant position and velocity matches perfectly to our previous results, and it is also in fine agreement with the MDC data. The shower can even be detected 4 days earlier than reported by Molau (2014b) before (Table 6).

### 4.5 $\theta^2$ Sagittariids

Between May 10 and 15, we recorded over 60 meteors belonging to a fast shower that has some remote similarity with the May $\beta$ Capricornids (520 MBC) and the $\chi$ Capricornids (420 CCA). The shower is located south of −30° declination (Table 7) which explains why it was not found in earlier IMO Network analysis. The scatter in the meteor shower parameters is relatively small

*Table 6* – Parameters of the $\eta$ Aquariids.

| Source | Solar longitude | | Right Ascension | | Declination | | $v_g$ | |
|---|---|---|---|---|---|---|---|---|
| | Mean | Interval | Mean | Drift | Mean | Drift | Mean | Drift |
| | [°] | [°] | [°] | [°] | [°] | [°] | [km/s] | [km/s] |
| MDC | 46.9 | — | 339.0 | +0.73 | −1.4 | +0.31 | 65.0 | — |
| IMO 2013 | 47 | 38–59 | 339.1 | +0.64 | −0.5 | +0.33 | 66.5 | +0.1 |
| Here | 47 | 34–57 | 338.9 | +0.62 | −0.6 | +0.31 | 65.4 | +0.04 |

*Table 7* – Parameters of the $\theta^2$ Sagittariids.

| Source | Solar longitude | | Right Ascension | | Declination | | $v_g$ | |
|---|---|---|---|---|---|---|---|---|
| | Mean | Interval | Mean | Drift | Mean | Drift | Mean | Drift |
| | [°] | [°] | [°] | [°] | [°] | [°] | [km/s] | [km/s] |
| Here | 53 | 49–54 | 301 | +1.2 | −33 | +0.2 | 67 | — |

*Table 8* – Parameters of the Northern June Aquilids.

| Source | Solar longitude | | Right Ascension | | Declination | | $v_g$ | |
|---|---|---|---|---|---|---|---|---|
| | Mean | Interval | Mean | Drift | Mean | Drift | Mean | Drift |
| | [°] | [°] | [°] | [°] | [°] | [°] | [km/s] | [km/s] |
| MDC | 86 | — | 298.3 | — | −7.1 | — | 36.3 | — |
| IMO 2013 | 82 | 79–84 | 293 | +1.0 | −12 | −0.4 | 42 | — |
| Here | 92 | 89–95 | 303 | +0.6 | −8 | +0.2 | 41 | — |

*Table 9* – Parameters of the Microscopiids.

| Source | Solar longitude | | Right Ascension | | Declination | | $v_g$ | |
|---|---|---|---|---|---|---|---|---|
| | Mean | Interval | Mean | Drift | Mean | Drift | Mean | Drift |
| | [°] | [°] | [°] | [°] | [°] | [°] | [km/s] | [km/s] |
| MDC | 104 | — | 320.3 | +0.89 | −28.3 | +0.29 | 38 | — |
| IMO 2013 | 105 | 98–111 | 320 | +1.1 | −27 | +0.15 | 39 | — |
| Here | 105 | 100–111 | 320 | +1.0 | −26 | +0.2 | 40 | — |

and there is a weak activity peak on May 13. A closer comparison with the two MDC showers above shows a deviation of about 20° in the radiant position, which is why we assume this to be an unknown shower and reported it to the MDC, where it got the preliminary designation $\theta^2$ Sagittariids (597 TTS).

## 4.6 Northern June Aquilids

The Northern June Aquilids (164 NZC) are close to the celestial equator, which is why they were already picked up by the previous analysis (earlier in time, though). The Australian data set contains almost 100 shower meteors which is about half of the overall data set. The scatter is relatively small and there is a clear activity peak on June 24. The parameters we find here (Table 8) fit slightly better to the MDC list values obtained by Sekanina (1976) from American radar data than our previously reported data (Molau, 2014).

## 4.7 Microscopiids

The Microscopiids (370 MIC) were one of the southernmost showers detected in our previous analysis (Molau, 2014). About 160 meteors were provided from the Australian cameras. The full data set has about three times that size, but the results are virtually identical (Table 9). The shower parameters show only a little scatter and the activity profile has a weak maximum at about 105° solar longitude. The agreement with the MDC data, which were provided by Brown et al. (2010) from Canadian radar data, is excellent.

## 4.8 $\sigma$ Capricornids

The $\sigma$ Capricornids (179 SCA) are the strongest southern hemisphere meteor source of early July and they are close to the celestial equator, which is why they were also easily picked up by our overall analysis (Molau, 2014). Only 110 of the over 2 400 meteors in the overall analysis were provided by the Australian cameras. The activity interval found here is much shorter and there is more scatter in the day-to-day radiant data (in particular the velocity), but otherwise the parameters of both data sets agree remarkably well (Table 10). There is significant disagreement with the MDC data which were based on radar data analysis by Sekanina in the 1970s, so it is subject of discussion whether this indeed the same shower or whether we found a new source close to but independent of the Antihelion source. We should postpone this decision until the shower is confirmed by independent observations of other teams.

## 4.9 $\tau$ Cetids

In mid-July, we find a short but well-defined and relatively strong shower with almost 60 members, that has no counterpart in the MDC list and that was also not detected in our overall analysis. The source is not too far from the southern Apex source, but at a distance

*Table 10* – Parameters of a meteor shower maybe related to the $\sigma$ Capricornids.

| Source | Solar longitude | | Right Ascension | | Declination | | $v_g$ | |
|---|---|---|---|---|---|---|---|---|
| | Mean | Interval | Mean | Drift | Mean | Drift | Mean | Drift |
| | [°] | [°] | [°] | [°] | [°] | [°] | [km/s] | [km/s] |
| MDC | 110 | — | 311.1 | — | −14.5 | — | 26.9 | — |
| IMO 2013 | 105 | 88–121 | 313.2 | +0.81 | −4.5 | +0.23 | 40.1 | −0.12 |
| Here | 106 | 102–110 | 313 | +0.9 | −5 | +0.5 | 41 | — |

*Table 11* – Parameters of the $\tau$ Cetids.

| Source | Solar longitude | | Right Ascension | | Declination | | $v_g$ | |
|---|---|---|---|---|---|---|---|---|
| | Mean | Interval | Mean | Drift | Mean | Drift | Mean | Drift |
| | [°] | [°] | [°] | [°] | [°] | [°] | [km/s] | [km/s] |
| Here | 119 | 118–121 | 28 | +0.3 | −18 | +0.5 | 65 | — |

*Table 12* – Parameters of the $\alpha$ Capricornids.

| Source | Solar longitude | | Right Ascension | | Declination | | $v_g$ | |
|---|---|---|---|---|---|---|---|---|
| | Mean | Interval | Mean | Drift | Mean | Drift | Mean | Drift |
| | [°] | [°] | [°] | [°] | [°] | [°] | [km/s] | [km/s] |
| MDC | 127 | — | 306.6 | +0.54 | −8.2 | +0.26 | 22.2 | — |
| IMO 2013 | 125 | 113–137 | 305.3 | +0.52 | −10.0 | +0.24 | 21.3 | −0.19 |
| Here | 122 | 106–137 | 303.9 | +0.55 | −11.4 | +0.25 | 22.2 | −0.22 |

*Table 13* – Parameters of the Southern $\delta$ Aquariids.

| Source | Solar longitude | | Right Ascension | | Declination | | $v_g$ | |
|---|---|---|---|---|---|---|---|---|
| | Mean | Interval | Mean | Drift | Mean | Drift | Mean | Drift |
| | [°] | [°] | [°] | [°] | [°] | [°] | [km/s] | [km/s] |
| MDC | 125.6 | — | 340.4 | +0.73 | −16.3 | +0.26 | 40.2 | — |
| IMO 2013 | 126 | 117–138 | 339.7 | +0.80 | −16.4 | +0.21 | 42.7 | −0.34 |
| | 152 | 139–165 | 1.3 | +0.82 | −7.7 | +0.41 | 39.4 | −0.04 |
| Here | 127 | 120–140 | 340.6 | +0.84 | −16.0 | +0.16 | 40.5 | −0.22 |
| | 150 | 141–160 | 359.6 | +0.90 | −8.3 | +0.52 | 37.8 | — |

of almost 20 degree we consider it to be an independent meteor shower. The parameters are given in Table 11. It has received the preliminary designation $\tau$ Cetids (598 TCT) from MDC.

## 4.10 $\alpha$ Capricornids

The $\alpha$ Capricornids (1 CAP) are a well-known meteor shower of July, which is not too far away from the celestial equator. It was easily picked up by the overall analysis as well. Still, the $\alpha$ Capricornids perform particularly well in the southern hemisphere, where they are the strongest source in most of July, before the Southern $\delta$ Aquariids take over towards the end of the month. We can detect the shower in the Australian data for over a month between July 6 and August 10 with almost 800 meteors. Due to the large data set, there is only very little scatter in the shower data if we omit bins at the edges of the activity interval. The activity profile is well formed with a clear peak on July 25. The overall IMO database contains almost 6 000 shower meteors, but the $\alpha$ Capricornids are detected earlier in the Australian subset (Table 12). That is, the radiant can be tracked to earlier solar longitudes in the full database as well, but we omitted these early intervals because of stronger deviation from the average shower parameters. The agreement between the two data sets and the list values of MDC (provided by Jenniskens, 2006) could not be any better. The only interesting point is the deviation in the peak time. Our Australian data set show a clear peak on July 25. The overall IMO database yields slightly higher activity on July 27/28, and the MDC data provided by different authors report a maximum at July 30, where the activity in the Australian data has dropped already by 50%.

## 4.11 Southern $\delta$ Aquariids

Clearly the strongest annual meteor shower of the southern hemisphere are the Southern $\delta$ Aquariids (5 SDA). Almost 2 100 meteors or 4% of the Australian data set belong to this shower, which is comparable to the contribution of the Orionids and Geminids to the full IMO database. We can detect the shower from July 23 till September 3, which is slightly less than the activity interval of the full analysis based on 13 000 shower members. In (Molau, 2014), we split the shower into two parts, because in particular the drift in declination and velocity changes at about 139° solar longitude. The same effect can be observed in the Australian data subset (Table 13). Here we put the break at 141° solar longitude. The agreement between both data sets is as

*Table 14* – Parameters of the southern $\eta$ Eridanids.

| Source | Solar longitude | | Right Ascension | | Declination | | $v_g$ | |
|---|---|---|---|---|---|---|---|---|
| | Mean | Interval | Mean | Drift | Mean | Drift | Mean | Drift |
| | [°] | [°] | [°] | [°] | [°] | [°] | [km/s] | [km/s] |
| MDC | 137.5 | — | 45 | — | −12.9 | — | 64 | — |
| IMO 2013 | 133 | 123–142 | 40.1 | +0.82 | −12.3 | +0.41 | 65.7 | +0.03 |
| Here | 136 | 128–146 | 42.6 | +0.84 | −12.3 | +0.17 | 63.7 | — |

*Table 15* – Parameters of the August $\beta$ Piscids (MDC) / $\theta$ Piscids (IMO).

| Source | Solar longitude | | Right Ascension | | Declination | | $v_g$ | |
|---|---|---|---|---|---|---|---|---|
| | Mean | Interval | Mean | Drift | Mean | Drift | Mean | Drift |
| | [°] | [°] | [°] | [°] | [°] | [°] | [km/s] | [km/s] |
| MDC | 140 | 129–151 | 346.2 | +0.74 | +1.4 | +0.22 | 38.3 | — |
| IMO 2013 | 147 | 135–158 | 352 | +0.78 | +4.1 | +0.36 | 39.0 | −0.16 |
| Here | 142 | 137–146 | 348 | +0.8 | +2 | +0.3 | 38.4 | — |

*Table 16* – Parameters of the $\kappa$ Aquariids.

| Source | Solar longitude | | Right Ascension | | Declination | | $v_g$ | |
|---|---|---|---|---|---|---|---|---|
| | Mean | Interval | Mean | Drift | Mean | Drift | Mean | Drift |
| | [°] | [°] | [°] | [°] | [°] | [°] | [km/s] | [km/s] |
| MDC | 179 | — | 338 | — | −8 | — | 14 | — |
| Here | 168 | 166–171 | 340 | +0.4 | −13 | −0.4 | 16 | — |

expected very good. The Australian radar data results presented by Galligan and Baggaley (2002) in the MDC list fit perfectly into this picture.

## 4.12 $\eta$ Eridanids

The $\eta$ Eridanids (191 ERI) are also picked up easily in the Australian data. They are the second strongest source of August represented by 380 shower meteors. We can trace them between July 31 and August 19. They are moving uniformly in right ascension, but show some scatter in declination and velocity. The activity profile is well-defined with a flat peak on August 9. The IMO Network database is dominated by the Perseids in August, which are noticeable only between 138° and 140° solar longitude in Australia. The database contains five times as many $\eta$ Eridanids as the Australian subset, but the data quality is comparable (Table 14) and the agreement with the MDC list values is fine.

## 4.13 August $\beta$ Piscids

The next shower is located slightly north of the celestial equator, but still we want to report it here as there seem to be some confusion about its name and identity. In our analysis it was recognized as the August $\beta$ Piscids (342 BPI). We found the same shower in our IMO database analysis in August 2012 as well (Molau et al., 2012), but there we recognized it as a new shower and reported it to the MDC where it received the preliminary designation $\theta$ Piscids (508 TPI). Now if you check the current MDC list, you will not find the $\beta$ Piscids (originally reported by SonotaCo, 2009), anymore. According to a more recent analysis by Holman and Jenniskens (2012), they are supposed to be identical to the Northern $\delta$ Aquariids (26 NDA). Given our data set, the unification of BPI and NDA may be subject to discussion, as there is significant deviation between the three old reference values for NDA and both BPI and TPI. It becomes clear, however, that BPI and TPI are the same shower, as there is good agreement in their parameters (Table 15).

## 4.14 $\kappa$ Aquariids

The next shower has some similarity with the $\kappa$ Aquariids (76 KAQ). 40 meteors between September 9 and September 14 are assigned to a shower, which is at the limit of detectability but was reported anyway as it should be clearly noticeable due to the extremely low velocity. The MDC gives two parameter sets for this shower – one obtained from three, the other from just fours photographic orbits. Both differ significantly from each other, so we give simply the average of both as reference in Table 16.

## 4.15 $\omega$ Piscids

The $\omega$ Piscids (217 OPC) are a shower that was not found in the overall IMO database analysis. However, 60 meteors of the Australian subset can be assigned to that shower between September 13 and 19. There detection is debatable, as there is significant day-to-day scatter in all parameters, but the shower is among the strongest sources in mid-September. A comparison with the MDC values shows a good agreement with the data provided by Jenniskens (2006) (Table 17).

## 4.16 Puppid-Velid complex

The MDC working list contains a number of similar shower entries in the Puppid-Velid region: Puppid-Velid I Complex (255 PUV), $\zeta$ Puppids (300 ZPU), $\gamma$ Puppids (301 PUP), and b Puppids (302 PVE). We detect this complex with 170 meteors between November 27 and December 18, when it is the strongest or second

*Table 17* – Parameters of the $\omega$ Piscids.

| Source | Solar longitude | | Right Ascension | | Declination | | $v_g$ | |
|---|---|---|---|---|---|---|---|---|
| | Mean [°] | Interval [°] | Mean [°] | Drift [°] | Mean [°] | Drift [°] | Mean [km/s] | Drift [km/s] |
| MDC | 174 | — | 0.5 | — | −8.8 | — | 21.4 | — |
| Here | 173 | 170–176 | 355 | +0.4 | −8 | +1 | 22 | — |

*Table 18* – Parameters of different shower from the Puppid-Velid complex.

| Source | Solar longitude | | Right Ascension | | Declination | | $v_g$ | |
|---|---|---|---|---|---|---|---|---|
| | Mean [°] | Interval [°] | Mean [°] | Drift [°] | Mean [°] | Drift [°] | Mean [km/s] | Drift [km/s] |
| MDC PUV | 254 | — | 128 | — | −45 | — | 36.8 | — |
| MDC ZPU | 254.7 | — | 123 | — | −43 | — | 39 | — |
| MDC PUP | 255 | — | 123 | — | −45 | — | 38 | — |
| MDC PVE | 256.3 | — | 128 | — | −45 | — | 39 | — |
| Here | 255 | 245–259 | 134 | +0.8 | −48 | −0.2 | 42 | — |

*Table 19* – Parameters of the c Velids.

| Source | Solar longitude | | Right Ascension | | Declination | | $v_g$ | |
|---|---|---|---|---|---|---|---|---|
| | Mean [°] | Interval [°] | Mean [°] | Drift [°] | Mean [°] | Drift [°] | Mean [km/s] | Drift [km/s] |
| MDC CVE | 273 | — | 135 | — | −46 | — | 36 | — |
| Here | 277 | 275–280 | 140 | +2 | −54 | 0 | 39 | — |

strongest source in the southern sky. There is significant day-to-day scatter in all parameters, but there is a good overall agreement with the different MDC list entries (Table 18).

Around New Year's Eve, the complex is detected again with over 40 meteors. Between December 27 and January 1, it is once more the strongest source in the southern sky, and this time the day-to-day scatter is a little smaller.

From the different MDC shower entries for this later part of the Puppid-Velid complex, the c Velids (304 CVE) fit best to our data (Table 19).

## 5 Conclusions and summary

Since previous meteor shower searches in the IMO Video Meteor Database were biased towards the northern sky and did not yield any meteor shower below −30° declination, we did an investigation exclusively based on Australian observations. Our analysis confirms the visibility of all major northern hemisphere showers but the Perseids (only visible between 138° and 140° solar longitude) and the Quadrantids (not detected at all).

The first half of the year is dominated by the Antihelion source, which can be traced multiple times in the Australian data. Later in the year, the Southern Taurids are visible for two months. Beside those related to the Antihelion source, we can detect 16 meteor showers in the southern hemisphere, among which the $\eta$ Aquariids in April/May and Southern $\delta$ Aquariids in July/August are most prominent. However, only four of these 16 showers (the Centaurid complex in February, the $\gamma$ Normids in March, the newly detected $\theta^2$ Sagittariids in May and the Pupid-Velid complex in November/December) are located south of −30° declination. There is an obvious asymmetry, because on the other hand well over 50% of all northern meteor showers we found in the analysis of the full IMO database (Molau, 2014) were located north of +30° declination, and two of them were even detected in Australia.

So there are just a few meteor showers which cannot be observed from mid-northern latitudes where the majority of the IMO Network cameras are located.

## References

Brown P., Weryk R. J., Wong D. K., and Jones J. (2008). "A meteoroid stream survey using the Canadian Meteor Orbit Radar. I. Methodology and radiant catalogue". *Icarus*, **195**, 317–339.

Brown P., Wong D. K., Weryk R. J., and Wiegert P. (2010). "A meteoroid stream survey using the Canadian Meteor Orbit Radar. II: Identification of minor showers using a 3D wavelet transform". *Icarus*, **207**, 66–81.

Galligan D. P. and Baggaley W. J. (2002). "Wavelet enhancement for detecting shower structure in radar meteoroid data II. Application to the AMOR data". In Green S. F., Williams I. P., McDonnell J. A. M., and McBride N., editors, *IAU Colloq. 181: Dust in the Solar System and Other Planetary Systems*. page 48.

Gartrell G. and Elford W. G. (1975). "Southern Hemisphere meteor stream determinations". *Australian Journal of Physics*, **28**, 591–620.

Holman D. and Jenniskens P. (2012). "Confirmation of the Northern Delta Aquariids (NDA, IAU #26) and the Northern June Aquilids (NZC, IAU #164)". *WGN, Journal of the IMO*, **40**, 166–170.

IAU MDC (2013). "List of all meteor showers". http://www.astro.amu.edu.pl/~jopek/MDC2007/Roje/roje_lista.php?corobic_roje=0&sort_roje=0 .

Jenniskens P. (2006). *Meteor Showers and their Parent Comets*. Cambridge University Press, Cambridge, UK.

Molau S. (2014). "Meteor showers identified from a million video meteors". In Gyssens M. and Roggemans P., editors, *Proceedings of the International Meteor Conference, Poznań, Poland, Aug. 22–25, 2013*. International Meteor Organization. (submitted).

Molau S. and Barentsen G. (2014). "Status and history of the IMO Video Meteor Network". In Jopek T. J., Rietmeijer F. J. M., Watanabe J., and Williams I. P., editors, *Proceedings of the Meteoroids 2013 Conference, Aug. 26–30, 2013, A. M. University, Poznań, Poland*. A. M. University Press. (submitted).

Molau S., Kac J., Berko E., Crivello S., Stomeo E., Igaz A., and Barentsen G. (2012). "Results of the IMO Video Meteor Network – August 2012". *WGN, Journal of the IMO*, **40**, 201–206.

Sekanina Z. (1976). "Statistical model of meteor streams. IV - A study of radio streams from the synoptic year". *Icarus*, **27**, 265–321.

SonotaCo (2009). "A meteor shower catalog based on video observations in 2007–2008". *WGN, Journal of the IMO*, **37**, 55–62.

*Handling Editor:* Željko Andreić

# Preliminary results

## Results of the IMO Video Meteor Network — December 2013

*Sirko Molau*[1], *Javor Kac*[2], *Stefano Crivello*[3], *Enrico Stomeo*[4], *Geert Barentsen*[5], *Rui Goncalves*[6], *and Antal Igaz*[7]

A summary of the 2013 December results of the IMO Video Meteor Network is presented, based on almost 48 000 meteors collected in about 9 800 hours of observing time. Flux density profiles of the Geminids and Ursids are shown and compared to 2012. An annual review of the 2013 IMO Video Meteor Network observations is presented. More than 350 000 meteors were recorded in over 86 000 hours of observing time.

Received 2014 March 7

### 1 Introduction

December 2013 completed an eventful year. The first third of the month started promising and yielded good observing conditions for most observers. An amazing 63 video cameras were active during the nights of December 2/3 and 3/4. Around December 10, however, the picture changed rapidly. We see large gaps in the observing statistics for the Geminids in Northern and Eastern Europe. The situation worsened further in the second half of the month. Whereas observers in Germany experienced unusually good observing conditions and missed nearly no nights, we had a complete loss of observations from Slovenia, Hungary and Italy for several days.

Overall 80 video cameras were in operation, 33 of which were active in twenty and more nights. The effective observing time increased from 6 800 in 2012 to almost 9 800 hours in 2013. The increase of the meteor count was less prominent, though, because we recorded fewer Geminids than in 2012 (Molau et al., 2013). The number of meteors increased from 40 000 in 2012 to almost 48 000 (Table 4 and Figure 1). At the end of the year, the race to catch up with the 2012 result had become thrilling again. Whether it was sufficient to surpass the outcome of that year before will be shown later.

In December, we saw a number of changes in the IMO Network again. Whereas the camera Acr of Wolfgang Hinz died and forced him to take a long break, we welcomed back Carl Hergenrother with Salsa3 after a break of almost two years. Rainer Arlt obtained a new Mintron camera, which is now dubbed Ludwig2 and which is much more powerful that its predecessor Ludwig2. Rui Goncalves introduced Templar5, another Mintron camera with 6 mm $f/0.75$ Panasonic lens, and Zoltan Zelko extended his equipment with Huvcse04, which consists (similar to Huvcse03) of a KPC-350BH video camera and a $f/1.0$ Tamron zoom lens (fixed at roughly 4 mm focal length). Meanwhile, every observer of the IMO Network operates on average two video cameras.

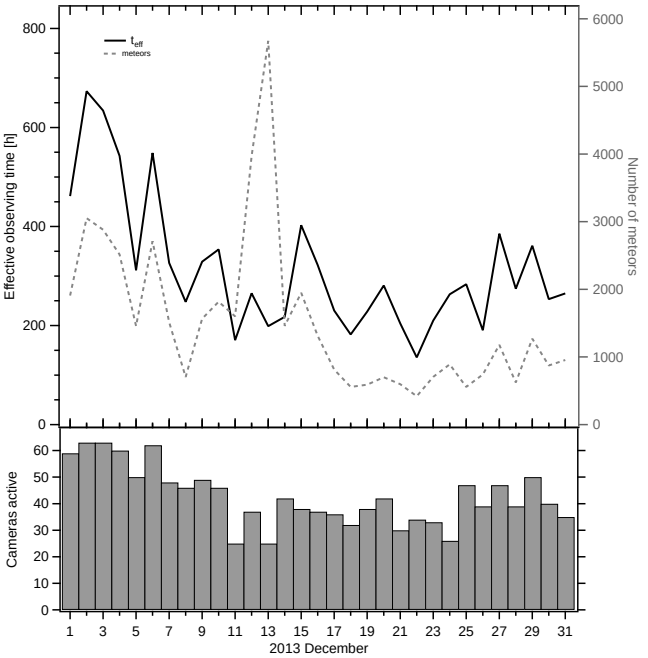


*Figure 1* – Monthly summary for the effective observing time (solid black line), number of meteors (dashed gray line) and number of cameras active (bars) in 2013 December.

### 2 Geminids

The highlight of December were the Geminids. Whereas we recorded over 15 000 meteors in three nights of 2012 December 12–15 (Molau et al., 2013), it was "only" about 11 000 meteors in the same three nights of 2013. The main reasons were the full Moon, which illuminated the night sky, and the weather. Those few observers who enjoyed clear skies recorded 600 meteors and more in a single night, whereas others missed the Geminids completely.

[1]Abenstalstr. 13b, 84072 Seysdorf, Germany. Email: sirko@molau.de
[2]Na Ajdov hrib 24, 2310 Slovenska Bistrica, Slovenia. Email: javor.kac@orion-drustvo.si
[3]Via Bobbio 9a/18, 16137 Genova, Italy. Email: stefano.crivello@libero.it
[4]via Umbria 21/d, 30037 Scorze (VE), Italy. Email: stom@iol.it
[5]University of Hertfordshire, Hatfield AL10 9AB, United Kingdom. Email: geert@barentsen.be
[6]Urbanizacao da Boavista, Lote 46, Linhaceira, 2305-114 Asseiceira, Tomar, Portugal. Email: rui.goncalves@ipt.pt
[7]Húr u. 9/D, H-1223 Budapest, Hungary. Email: antaligaz@yahoo.com

IMO bibcode WGN-422-molau-viddec
NASA-ADS bibcode 2014JIMO...42...76M

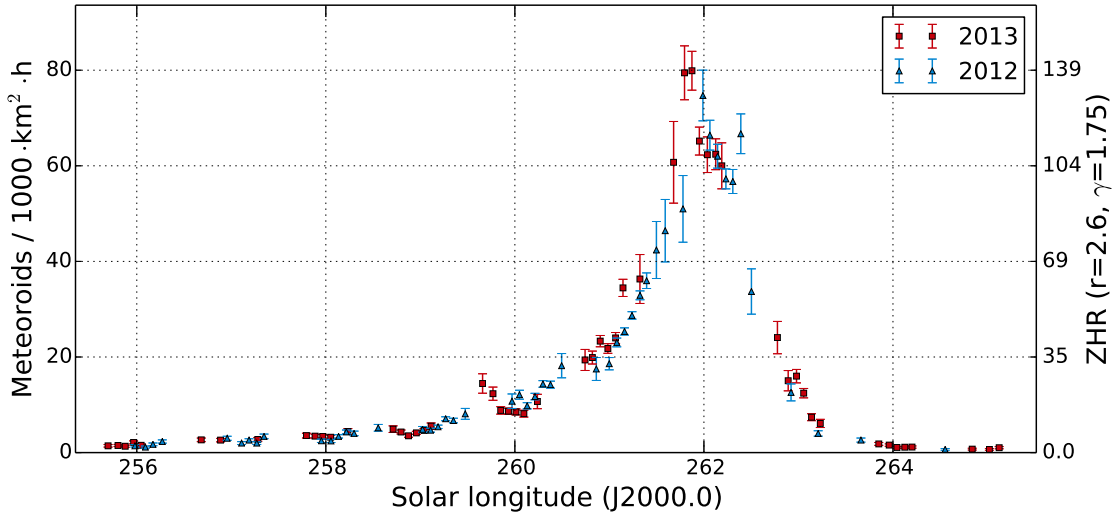


*Figure 2* – Flux density profile of the Geminids, obtained from data of the IMO Video Meteor Network in 2012 and 2013.

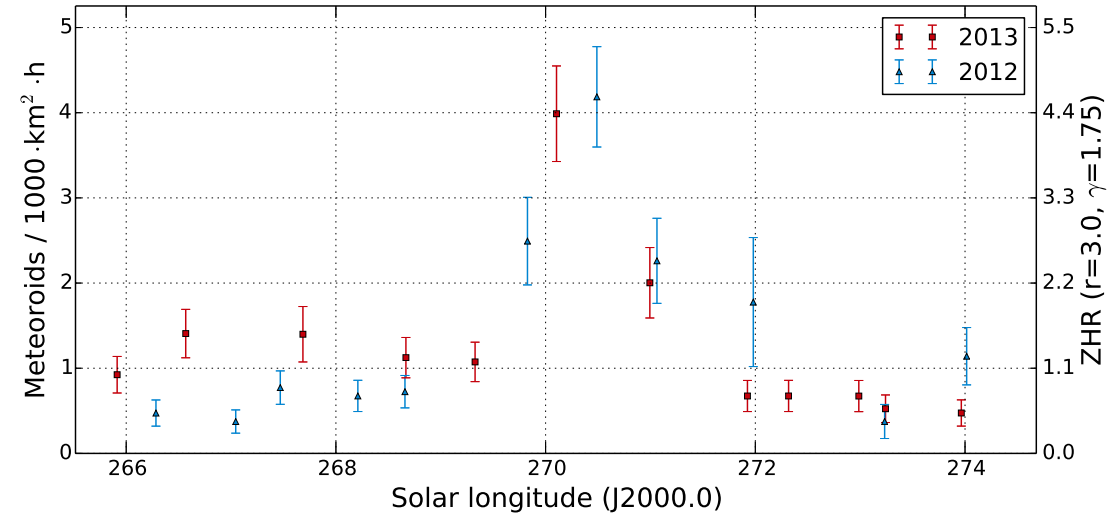


*Figure 3* – Flux density profile of the Ursids, obtained from the IMO Network data 2012 and 2013.

If the flux density profiles of the previous years are compared, we find a good agreement between 2012 and 2013 (Figure 2), but significant deviation from the 2011 profile. Also the zenith exponent was "less cooperative" than for other showers. On the one hand we have observing interval in the evening hours of December 11/12 and 12/13 with higher rates than the following intervals, which hints at a zenith exponent below 1.5. On the other hand, the profile of the previous two years fit best to one another if the zenith exponent is around 1.7 to 1.8. Maybe this is linked to a "sub-optimal" default population index of $r = 2.6$.

Apropos population index: Of course, we determined this figure for the Geminids as well. In the night of December 13/14, the $r$-value was about 0.3 smaller than in the night before, which reflects the well-known fact that after the peak the Geminids are on average brighter than before. Still, with values below 2.0, the population index was again smaller than the $r$-values typically obtained from visual data. For this reason, we are currently undertaking a rigorous check of the full procedure. The results are still pending and will be presented in one of the upcoming monthly reports.

## 3 Ursids

Also the Ursids show a nice agreement of the flux density profiles from the last two years. (Figure 3).

## 4 2013 summary

Let us finally come to the traditional end-of-year review. In the first few months of 2013 the weather was so poor that at some times we did not even obtain half of the 2012 output. With the exception of April, the monthly totals of every single month in the first half of 2013

*Table 1* – Monthly distribution of video observations in the IMO Network 2013.

| Month | Observing Nights | Eff. Observing Time | Meteors | Meteors / Hour |
|---|---|---|---|---|
| January | 31 | 4 922.1 | 13 474 | 2.7 |
| February | 28 | 5 012.8 | 10 492 | 2.1 |
| March | 31 | 6 002.3 | 12 134 | 2.0 |
| April | 30 | 7 137.1 | 14 311 | 2.0 |
| May | 31 | 5 124.0 | 12 654 | 2.5 |
| June | 30 | 5 686.9 | 16 250 | 2.9 |
| July | 31 | 8 061.9 | 35 829 | 4.4 |
| August | 31 | 9 878.2 | 75 405 | 7.6 |
| September | 30 | 8 490.8 | 37 458 | 4.4 |
| October | 31 | 9 462.6 | 44 010 | 4.7 |
| November | 30 | 7 100.3 | 30 419 | 4.3 |
| December | 31 | 9 753.3 | 47 566 | 4.9 |
| Overall | 365 | 86 632.3 | 350 002 | 4.0 |

decreased compared to 2012, so that we had amassed a deficit of almost 40 000 meteors by the end of June. In the second half of 2013, the situation improved. In this period we could record at least as many meteors as in 2012, and in most months even a few thousand more. Still, it was not sufficient to reach the results of 2012 (Molau et al., 2013). Some of the best meteors are shown in Figure 4.

49 observers (2012: 46) from 16 countries (2012: 15) operated a total of 88 video cameras (2012: 80) in the IMO Network. There were no changes in the global ranking: Germany is still leading with 18 cameras, closely followed by Hungary (17), and followed by Italy (12) and Slovenia (11). 8 cameras were operated in Portugal, and 3 cameras in Poland, Spain, Belgium and the Czech Republic. Two cameras were active in the USA, and single cameras in Australia, the Netherlands, Greece, Finland, France and Russia.

In 365 observing nights (2012: 366) and 86 632 hours of effective observing time (2012: 93 563), we recorded a total of 350 002 meteors (2012: 353 627). The hourly average increased slightly from 3.8 to 4.0 meteors per hours. Even though the network further expanded, we saw a small reduction in observing time (−7%), whereas the meteor counts remained almost the same (−1%). Overall, the output of 2013 has been by far the second best in the history of the IMO Network.

Table 1 presents the distribution of observations over the months.

In 2012 there were four observers that managed to obtain more than 300 observing nights; in 2013 the number increased to five. Thanks to perfect observing conditions, Detlef Koschny took over the lead with his two image-intensified cameras on Tenerife and La Palma. Together with a third camera in the Netherlands he obtained 339 observing nights. Antal Igaz ranked second with 318 nights, followed by Sirko Molau with 317, Rui Goncalves with 313 and Stefano Crivello with 308 nights. There were 18 observers with over 200 nights, and another 11 with more than 100 nights.

With respect to the effective observing time, Rui Goncalves could clearly increase his yield from 2012 and defend the pole position with over 8 100 hours. He was followed by Sirko Molau with nearly 7 000 and Carlos Saraiva with almost 5 600 observing hours.

The ranking with respect to the number of meteors changed in 2013. Enrico Stomeo, who had dominated this table for the last three years, ranked in 2013 "only" third with 27 000 meteors, closely followed by Rui Goncalves. The undisputed leader of 2013 was Detlef Koschny with well above 41 000 meteors, followed by Sirko Molau with almost 36 000 meteors. So for every image intensified cameras on the Canaries you have to come up with two or three powerful Mintron cameras at a good central European location. Let us see whether someone can catch up with Detlef in 2014.

In the long-term statistics of the IMO Network, three more observers got "supersonic" by collecting more than 1 000 observing nights: Mitja Govedič, Hans Schremmer and Maurizio Eltri. Stefano Crivello and Javor Kac are observers number three and four who contributed overall more than 100 000 meteors to the IMO Video Meteore Database.

Table 2 lists all active observers of the IMO Network in 2013, whereby the number of cameras and stations refers to the majority of the year.

In the statistics of the most successful video cameras (Table 3) we have once more a photo finish between Templar3 and Sco38. They are followed by the image-intensified camera Icc7 at Teneriffe. Her twin-camera Icc9 at La Palma started operation in February, which is why it did not made it into the top 10, even thought it was the camera that recorded most meteors in 2013 (19 411).

The complete data set of 2013 is ready for download at the IMO Video Meteor Network Homepage, `http://www.imonet.org`.

As always, we would like to thank the many observers, whose passion is a guarantor for the success of the IMO Network. Special thanks to Stefano Crivello, Enrico Stomeo, Rui Goncalves and Antal Igaz, who check together with Sirko Molau every month the consistency of the data set and ensure the high quality of the database.

*Table 2* – Distribution of video observations over the observers in 2013.

| Observer | Country | Observing Nights | Eff. Observing Time [h] | Meteors | Meteors / h | Cameras (Stations) |
|---|---|---|---|---|---|---|
| Detlef Koschny | Netherlands | 339 | 4 949.9 | 41 536 | 8.4 | 3 (3) |
| Antal Igaz | Hungary | 318 | 4 543.7 | 10 660 | 2.3 | 4 (3) |
| Sirko Molau | Germany | 317 | 6 950.8 | 35 596 | 5.1 | 5 (2) |
| Rui Goncalves | Portugal | 313 | 8 129.3 | 27 003 | 3.3 | 3 (1) |
| Stefano Crivello | Italy | 308 | 5 304.1 | 24 126 | 4.5 | 3 (1) |
| Enrico Stomeo | Italy | 284 | 4 382.8 | 27 179 | 6.2 | 3 (1) |
| Carlos Saraiva | Portugal | 271 | 5 596.3 | 13 279 | 2.4 | 3 (1) |
| József Morvai | Hungary | 260 | 1 532.0 | 3 387 | 2.2 | 1 (1) |
| Bernd Brinkmann | Germany | 260 | 2 059.3 | 6 286 | 3.1 | 2 (2) |
| Hans Schremmer | Germany | 255 | 1 226.7 | 4 291 | 3.5 | 1 (1) |
| Jörg Strunk | Germany | 245 | 3 499.4 | 13 116 | 3.7 | 4 (1) |
| Mike Otte | USA | 245 | 1 317.4 | 5 173 | 3.9 | 1 (1) |
| Mitja Govedič | Slovenia | 244 | 3 150.0 | 10 069 | 3.2 | 3 (1) |
| Maciej Maciejewski | Poland | 241 | 3 530.2 | 9 765 | 2.8 | 3 (1) |
| Istvan Tepliczky | Hungary | 238 | 1 768.0 | 7 130 | 4.0 | 1 (1) |
| Szabolcs Kiss | Hungary | 230 | 1 187.6 | 1 269 | 1.1 | 1 (1) |
| Karoly Jonas | Hungary | 228 | 1 391.1 | 2 959 | 2.1 | 1 (1) |
| Grigoris Maravelias | Greece | 226 | 1 392.4 | 4 309 | 3.1 | 1 (1) |
| Zsolt Perkó | Hungary | 225 | 1 285.1 | 7 220 | 5.6 | 1 (1) |
| Flavio Castellani | Italy | 223 | 2 120.0 | 7 613 | 3.6 | 2 (1) |
| Mario Bombardini | Italy | 221 | 1 102.3 | 7 886 | 7.2 | 1 (1) |
| Martin Breukers | Netherlands | 212 | 1 807.7 | 4 123 | 2.4 | 2 (1) |
| Rok Pucer | Slovenia | 205 | 1 161.1 | 4 822 | 4.2 | 1 (1) |
| Javor Kac | Slovenia | 192 | 3 406.3 | 16 371 | 4.8 | 5 (3) |
| Erno Berkó | Hungary | 188 | 3 322.5 | 13 350 | 4.0 | 3 (1) |
| Mihaela Triglav | Slovenia | 184 | 591.0 | 2 983 | 5.0 | 1 (1) |
| Maurizio Eltri | Italy | 171 | 1 009.9 | 4 996 | 4.9 | 1 (1) |
| Leo Scarpa | Italy | 154 | 782.5 | 2 838 | 3.6 | 1 (1) |
| Péter Bánfalvi | Hungary | 154 | 766.2 | 1 905 | 2.5 | 1 (1) |
| Ilkka Yrjölä | Finland | 152 | 815.1 | 3 207 | 3.9 | 1 (1) |
| Szofia Biro | Hungary | 150 | 806.9 | 1 952 | 2.4 | 1 (1) |
| Eckehard Rothenberg | Germany | 145 | 772.2 | 1 749 | 2.3 | 1 (1) |
| Stane Slavec | Slovenia | 136 | 639.7 | 1 406 | 2.2 | 1 (1) |
| Jenni Donati | Italy | 111 | 809.1 | 6 304 | 7.8 | 1 (1) |
| Mikhail Maslov | Russia | 93 | 374.2 | 2 713 | 7.3 | 1 (1) |
| Paolo Ochner | Italy | 89 | 263.5 | 1 211 | 4.6 | 1 (1) |
| Steve Kerr | Australia | 81 | 343.3 | 1 740 | 5.1 | 1 (1) |
| Francisco Ocaña González | Spain | 77 | 558.2 | 473 | 0.8 | 1 (1) |
| Wolfgang Hinz | Germany | 72 | 380.6 | 2 478 | 6.5 | 1 (1) |
| Rainer Arlt | Germany | 66 | 468.4 | 790 | 1.5 | 1 (1) |
| Zoltán Zelko | Hungary | 51 | 287.4 | 726 | 2.6 | 1 (1) |
| Arnaud Leroy | France | 48 | 201.3 | 143 | 0.7 | 1 (1) |
| Karl-Heinz Gansel | Germany | 40 | 178.7 | 197 | 1.1 | 1 (1) |
| Luc Bastiaens | Belgium | 39 | 186.3 | 159 | 0.9 | 1 (1) |
| Szilárd Csizmadia | Hungary | 19 | 35.6 | 100 | 2.8 | 1 (1) |
| Tomasz Łojek | Poland | 14 | 71.4 | 179 | 2.5 | 1 (1) |
| Rosta Štork | Czech Rep. | 13 | 101.4 | 3 070 | 30.3 | 2 (2) |
| Carl Hergenrother | USA | 7 | 70.4 | 151 | 2.1 | 1 (1) |
| Jakub Koukal | Czech Rep. | 1 | 3.0 | 14 | 4.7 | 1 (1) |

## References

Molau S., Kac J., Crivello E. B. S., Stomeo E., Igaz A., Barentsen G., and Goncalves R. (2013). "Results of the IMO Video Meteor Network – December 2012". *WGN, Journal of the IMO*, **41:2**, 52–60.

*Handling Editor:* Javor Kac

*Table 3* – The ten most successful video systems in 2013.

| Camera | Location | Observer | Observing Nights | Eff. Observing Time [h] | Meteors | Meteors / h |
|---|---|---|---|---|---|---|
| Templar3 | Tomar (PT) | Rui Goncalves | 292 | 2 135.4 | 5 830 | 2.7 |
| Stg38 | Valbrevenna (IT) | Stefano Crivello | 292 | 1 860.2 | 9 751 | 5.2 |
| Icc7 | Tenerife (ES) | Detlef Koschny | 290 | 2 350.6 | 18 837 | 8.0 |
| Bilbo | Valbrevenna (IT) | Stefano Crivello | 288 | 1 766.5 | 8 267 | 4.7 |
| C3p8 | Scorze (IT) | Enrico Stomeo | 283 | 1 677.4 | 6 108 | 3.6 |
| Min38 | Scorze (IT) | Enrico Stomeo | 272 | 1 455.4 | 9 517 | 6.5 |
| Remo2 | Ketzür (DE) | Sirko Molau | 268 | 1 488.3 | 7 249 | 4.8 |
| Remo1 | Ketzür (DE) | Sirko Molau | 267 | 1 474.1 | 10 121 | 6.9 |
| Sco38 | Scorze (IT) | Enrico Stomeo | 266 | 1 508.8 | 9 994 | 6.6 |
| Templar2 | Tomar (PT) | Rui Goncalves | 261 | 2 047.9 | 6 912 | 3.4 |

Sporadic meteor on 2013 January 31 at $00^h00^m53^s$ UT, by Carlos Saraiva with Ro2.

Sporadic meteor on 2013 May 21 at $20^h45^m53^s$ UT, by Leo Scarpa with Leo.

Sporadic meteor on 2013 July 23 at $21^h08^m36^s$ UT, by Jörg Strunk with Mincam3.


Capricornid on 2013 July 26 at $00^h20^m29^s$ UT, by Bernd Brinkmann with Klemoi.


Sporadic meteor on 2013 July 31 at $02^h11^m21^s$ UT, by Rui Goncalves with Templar4.

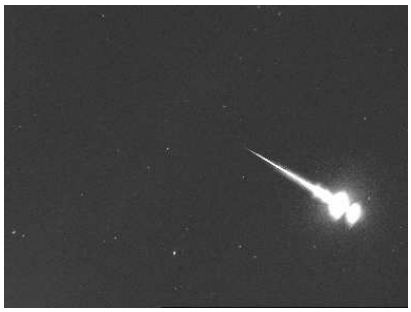

Antihelion meteor on 2013 August 16 at $01^h55^m16^s$ UT, by Javor Kac with Stefka.

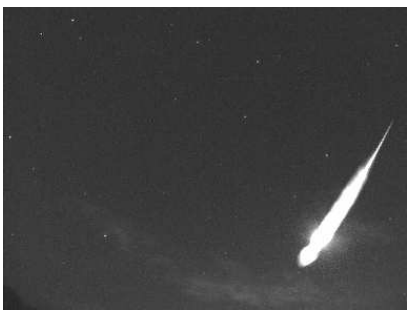

Sporadic meteor on 2013 August 30 at $00^h10^m42^s$ UT, by Stefano Crivello with Bilbo.

Sporadic meteor on 2013 September 1 at $03^h08^m11^s$ UT, by Stefano Crivello with C3p8.

Southern Taurid meteor exactly inside the airplane contrail on 2013 September 28 at $02^h37^m48^s$ UT, by Sirko Molau with Remo1.

*Figure 4* – Collection of best meteor captures by the cameras of the IMO Video Meteor Network in 2013.

*Table 4* – Observers contributing to 2013 December data of the IMO Video Meteor Network. Eff.CA designates the effective collection area.

| Code | Name | Place | Camera | FOV [°²] | Stellar LM [mag] | Eff.CA [km²] | Nights | Time [h] | Meteors |
|---|---|---|---|---|---|---|---|---|---|
| ARLRA | Arlt | Ludwigsfelde/DE | Ludwig1 (0.8/8) | 1488 | 4.8 | 726 | 1 | 8.3 | 8 |
| | | | Ludwig2 (0.8/8) | 1534 | 5.8 | 2467 | 14 | 96.2 | 354 |
| BANPE | Bánfalvi | Zalaegerszeg/HU | Huvcse01 (0.95/5) | 2423 | 3.4 | 361 | 10 | 61.2 | 187 |
| BERER | Berkó | Ludányhalászi/HU | Hulud1 (0.8/3.8) | 5542 | 4.8 | 3847 | 15 | 110.0 | 779 |
| | | | Hulud3 (0.95/4) | 4357 | 3.8 | 876 | 12 | 107.6 | 179 |
| BOMMA | Bombardini | Faenza/IT | Mario (1.2/4.0) | 5794 | 3.3 | 739 | 23 | 186.7 | 1647 |
| BREMA | Breukers | Hengelo/NL | Mbb3 (0.75/6) | 2399 | 4.2 | 699 | 7 | 40.0 | 73 |
| | | | Mbb4 (0.8/8) | 1470 | 5.1 | 1208 | 13 | 79.1 | 158 |
| BRIBE | Klemt | Herne/DE | Hermine (0.8/6) | 2374 | 4.2 | 678 | 13 | 62.7 | 127 |
| | | Bergisch Gladbach/DE | Klemoi (0.8/6) | 2286 | 4.6 | 1080 | 21 | 113.2 | 425 |
| CASFL | Castellani | Monte Baldo/IT | Bmh1 (0.8/6) | 2350 | 5.0 | 1611 | 21 | 135.9 | 1315 |
| | | | Bmh2 (1.5/4.5)* | 4243 | 3.0 | 371 | 4 | 45.5 | 148 |
| CRIST | Crivello | Valbrevenna/IT | Bilbo (0.8/3.8) | 5458 | 4.2 | 1772 | 19 | 174.3 | 1500 |
| | | | C3P8 (0.8/3.8) | 5455 | 4.2 | 1586 | 21 | 201.0 | 1042 |
| | | | Stg38 (0.8/3.8) | 5614 | 4.4 | 2007 | 21 | 178.2 | 1598 |
| DONJE | Donani | Faenza/IT | Jenni (1.2/4) | 5886 | 3.9 | 1222 | 23 | 229.3 | 1895 |
| ELTMA | Eltri | Venezia/IT | Met38 (0.8/3.8) | 5631 | 4.3 | 2151 | 20 | 188.6 | 783 |
| GANKA | Gansel | Dingden/DE | Daro01 (1.4/3.6) | 7141 | 3.1 | 652 | 8 | 33.1 | 62 |
| GONRU | Goncalves | Tomar/PT | Templar1 (0.8/6) | 2179 | 5.3 | 1842 | 15 | 172.1 | 825 |
| | | | Templar2 (0.8/6) | 2080 | 5.0 | 1508 | 16 | 175.6 | 762 |
| | | | Templar3 (0.8/8) | 1438 | 4.3 | 571 | 22 | 227.0 | 853 |
| | | | Templar4 (0.8/3.8) | 4475 | 3.0 | 442 | 16 | 166.1 | 655 |
| | | | Templar5 (0.75/6) | 2312 | 5.0 | 2259 | 10 | 91.9 | 292 |
| GOVMI | Govedič | Središče ob Dravi/SI | Orion2 (0.8/8) | 1447 | 5.5 | 1841 | 19 | 124.8 | 475 |
| | | | Orion3 (0.95/5) | 2665 | 4.9 | 2069 | 15 | 100.3 | 208 |
| | | | Orion4 (0.95/5) | 2662 | 4.3 | 1043 | 17 | 121.0 | 282 |
| HERCA | Hergenrother | Tucson/US | Salsa3 (1.2/4)* | 2198 | 4.6 | 894 | 7 | 70.4 | 151 |
| HINWO | Hinz | Schwarzenberg/DE | Acr (2.0/35)* | 557 | 7.3 | 5002 | 5 | 46.3 | 432 |
| IGAAN | Igaz | Baja/HU | Hubaj (0.8/3.8) | 5552 | 2.8 | 403 | 16 | 86.5 | 388 |
| | | Debrecen/HU | Hudeb (0.8/3.8) | 5522 | 3.2 | 620 | 17 | 142.3 | 412 |
| | | Hódmezővásárhely/HU | Huhod (0.8/3.8) | 5502 | 3.4 | 764 | 18 | 104.1 | 363 |
| | | Budapest/HU | Hupol (1.2/4) | 3790 | 3.3 | 475 | 13 | 86.6 | 103 |
| JONKA | Jonas | Budapest/HU | Husor (0.95/4) | 2286 | 3.9 | 445 | 17 | 127.3 | 282 |
| KACJA | Kac | Ljubljana/SI | Orion1 (0.8/8) | 1402 | 3.8 | 331 | 13 | 55.6 | 84 |
| | | Kamnik/SI | Cvetka (0.8/3.8)* | 4914 | 4.3 | 1842 | 10 | 66.7 | 336 |
| | | | Rezika (0.8/6) | 2270 | 4.4 | 840 | 6 | 31.1 | 130 |
| | | | Stefka (0.8/3.8) | 5471 | 2.8 | 379 | 10 | 79.8 | 330 |
| | | Kostanjevec/SI | Metka (0.8/12)* | 715 | 6.4 | 640 | 7 | 59.5 | 273 |
| KISSZ | Kiss | Sülysáp/HU | Husul (0.95/5)* | 4295 | 3.0 | 355 | 13 | 85.7 | 104 |
| KOSDE | Koschny | Izana Obs./ES | Icc7 (0.85/25)* | 714 | 5.9 | 1464 | 24 | 187.2 | 1642 |
| | | La Palma/ES | Icc9 (0.85/25)* | 683 | 6.7 | 2951 | 25 | 138.0 | 1270 |
| | | Noordwijkerhout/NL | Lic4 (1.4/50)* | 2027 | 6.0 | 4509 | 15 | 85.6 | 251 |

*Table 4* – Observers contributing to 2013 December data of the IMO Video Meteor Network – continued from previous page.

| Code | Name | Place | Camera | FOV [°²] | Stellar LM [mag] | Eff.CA [km²] | Nights | Time [h] | Meteors |
|---|---|---|---|---|---|---|---|---|---|
| LOJTO | Łojek | Grabniak/PL | Pav57 (1.0/5) | 1631 | 3.5 | 269 | 6 | 33.5 | 96 |
| MACMA | Maciejewski | Chełm/PL | Pav35 (0.8/3.8) | 5495 | 4.0 | 1584 | 22 | 160.4 | 739 |
| | | | Pav36 (0.8/3.8)* | 5668 | 4.0 | 1573 | 23 | 182.5 | 831 |
| | | | Pav43 (0.75/4.5)* | 3132 | 3.1 | 319 | 17 | 135.2 | 246 |
| | | | Pav60 (0.75/4.5) | 2250 | 3.1 | 281 | 21 | 118.5 | 347 |
| MARGR | Maravelias | Lofoupoli-Crete/GR | Loomecon (0.8/12) | 738 | 6.3 | 2698 | 17 | 102.7 | 269 |
| MASMI | Maslov | Novosibirsk/RU | Nowatec (0.8/3.8) | 5574 | 3.6 | 773 | 17 | 88.8 | 705 |
| MOLSI | Molau | Seysdorf/DE | Avis2 (1.4/50)* | 1230 | 6.9 | 6152 | 26 | 151.0 | 996 |
| | | | Mincam1 (0.8/8) | 1477 | 4.9 | 1084 | 23 | 140.4 | 424 |
| | | Ketzür/DE | Remo1 (0.8/8) | 1467 | 6.5 | 5491 | 22 | 173.7 | 1072 |
| | | | Remo2 (0.8/8) | 1478 | 6.4 | 4778 | 22 | 160.8 | 731 |
| | | | Remo3 (0.8/8) | 1420 | 5.6 | 1967 | 22 | 156.0 | 244 |
| | | | Remo4 (0.8/8) | 1478 | 6.5 | 5358 | 21 | 164.6 | 906 |
| MORJO | Morvai | Fülöpszállás/HU | Huful (1.4/5) | 2522 | 3.5 | 532 | 22 | 145.3 | 305 |
| OCHPA | Ochner | Albiano/IT | Albiano (1.2/4.5) | 2944 | 3.5 | 358 | 15 | 98.8 | 483 |
| OTTMI | Otte | Pearl City/US | Orie1 (1.4/5.7) | 3837 | 3.8 | 460 | 16 | 97.3 | 440 |
| PERZS | Perkó | Becsehely/HU | Hubec (0.8/3.8)* | 5498 | 2.9 | 460 | 20 | 161.8 | 1052 |
| PUCRC | Pucer | Nova vas nad Dragonjo/SI | Mobcam1 (0.75/6) | 2398 | 5.3 | 2976 | 16 | 118.7 | 736 |
| ROTEC | Rothenberg | Berlin/DE | Armefa (0.8/6) | 2366 | 4.5 | 911 | 12 | 79.1 | 145 |
| SARAN | Saraiva | Carnaxide/PT | Ro1 (0.75/6) | 2362 | 3.7 | 381 | 20 | 210.1 | 679 |
| | | | Ro2 (0.75/6) | 2381 | 3.8 | 459 | 22 | 221.3 | 828 |
| | | | Sofia (0.8/12) | 738 | 5.3 | 907 | 21 | 223.1 | 610 |
| SCALE | Scarpa | Alberoni/IT | Leo (1.2/4.5)* | 4152 | 4.5 | 2052 | 21 | 171.6 | 485 |
| SCHHA | Schremmer | Niederkrüchten/DE | Doraemon (0.8/3.8) | 4900 | 3.0 | 409 | 24 | 133.6 | 783 |
| SLAST | Slavec | Ljubljana/SI | Kayak1 (1.8/28) | 563 | 6.2 | 1294 | 14 | 104.6 | 207 |
| STOEN | Stomeo | Scorze/IT | Min38 (0.8/3.8) | 5566 | 4.8 | 3270 | 23 | 204.6 | 1494 |
| | | | Noa38 (0.8/3.8) | 5609 | 4.2 | 1911 | 22 | 198.7 | 1191 |
| | | | Sco38 (0.8/3.8) | 5598 | 4.8 | 3306 | 23 | 216.4 | 1625 |
| STRJO | Strunk | Herford/DE | Mincam2 (0.8/6) | 2354 | 5.4 | 2751 | 23 | 118.3 | 1029 |
| | | | Mincam3 (0.8/6) | 2338 | 5.5 | 3590 | 22 | 121.0 | 891 |
| | | | Mincam4 (1.0/2.6) | 9791 | 2.7 | 552 | 21 | 100.3 | 662 |
| | | | Mincam5 (0.8/6) | 2349 | 5.0 | 1896 | 22 | 118.9 | 957 |
| TEPIS | Tepliczky | Agostyán/HU | Huago (0.75/4.5) | 2427 | 4.4 | 1036 | 18 | 112.6 | 268 |
| | | Budapest/HU | Humob (0.8/6) | 2388 | 4.8 | 1607 | 12 | 99.0 | 344 |
| TRIMI | Triglav | Velenje/SI | Sraka (0.8/6)* | 2222 | 4.0 | 546 | 19 | 124.4 | 733 |
| YRJIL | Yrjölä | Kuusankoski/FI | Finexcam (0.8/6) | 2337 | 5.5 | 3574 | 8 | 50.9 | 563 |
| ZELZO | Zelko | Budapest/HU | Huvcse03 (1.0/4.5) | 2224 | 4.4 | 933 | 6 | 36.2 | 140 |
| | | | Huvcse04 (1.0/4.5) | 1484 | 4.4 | 573 | 5 | 36.2 | 127 |
| | | | | | | Overall | 31 | 9 753.3 | 47 566 |

* active field of view smaller than video frame

# Results of the IMO Video Meteor Network — January 2014

*Sirko Molau*[1], *Javor Kac*[2], *Stefano Crivello*[3], *Enrico Stomeo*[4], *Geert Barentsen*[5], *Rui Goncalves*[6], *and Antal Igaz*[7]

The 2014 January results of the IMO Video Meteor Network are presented, based on more than 18 000 meteors collected in almost 6 000 hours of observing time. Flux density profile of the Quadrantids around the maximum (January 3/4) is presented and a population index of $r = 1.8$ is obtained for the night of maximum.

Received 2014 April 9

## 1 Introduction

There was nothing spectacular about the start of the new year. With 6 000 observing hours and 18 000 meteors (Table 1 and Figure 1) we have been more successful than in the previous year, but we could not reach the perfect result of January 2012 despite the fact that the boundary conditions were not so bad. The Quadrantids fell into a moon-free period (two days after new moon) and could be covered by many observers. However, in the end it is the exact time of the maximum and the weather in the rest of January that govern the output. The first half of the month was quite good, but in the second half we have large gaps in the observing statistics. Only 12 out of the 82 active cameras managed to obtain twenty and more observing nights, eight of which were located in Germany. Our southern European observers were less successful and in particular the Hungarians suffered from poor conditions. Many of their cameras reported less than ten observing nights.

The larger number of active camera hints on further growth of the network. In Italy, Fabio Moschini joined the network with Rover, a Mintron camera with 4.5 mm $f/1.4$ lens. From Portugal we can report the first light for Ro3, the fourth camera of Carlos Saraiva. That is a Mintron camera as well, operated with a 12 mm lens to minimize the overlap with the other cameras operated at the same site.

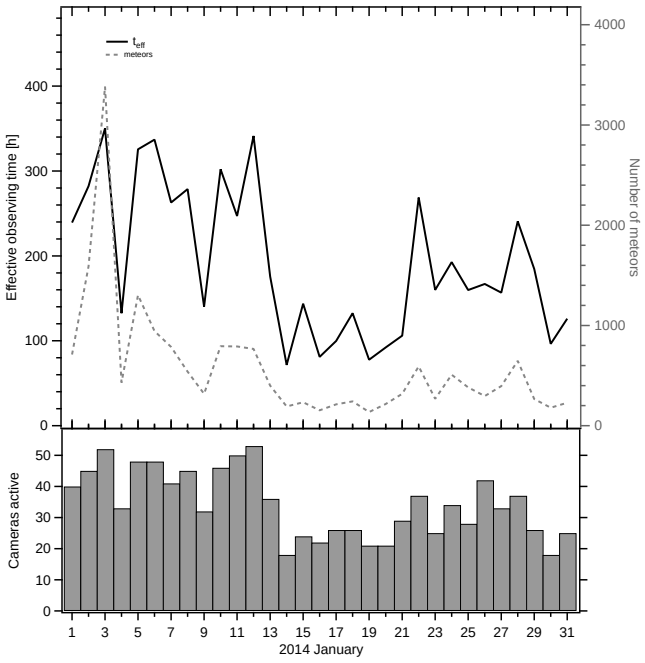


*Figure 1* – Monthly summary for the effective observing time (solid black line), number of meteors (dashed gray line) and number of cameras active (bars) in 2014 January.

## 2 Quadrantids

Let us have a closer look at the Quadrantids. Their peak was predicted for the evening hours of January 3 ($19^h30^m$ UT) (McBeath, 2013). Unfortunately the Quadrantid peak is very short – the long-term visual observations revealed a full-width-at-half-maximum (FWHM) of just 14 hours – and the radiant was at lower culmination in Europe at the predicted peak time. Only at local midnight it reached sufficient heights. However, the case was not hopeless, since the radiant of the Quadrantids is circumpolar at mid-northern latitudes, so even in the evening hours of January 3 it was a few degrees above the horizon. That is reflected in the activity profile (Figure 2), which was obtained from video footage of over 1500 Quadrantids. Flux density was the highest in the first intervals on January 3/4, and then declined continuously. At around midnight UT it had fallen to half of the peak value, and in the morning hours of January 4 it had almost reached the background level again.

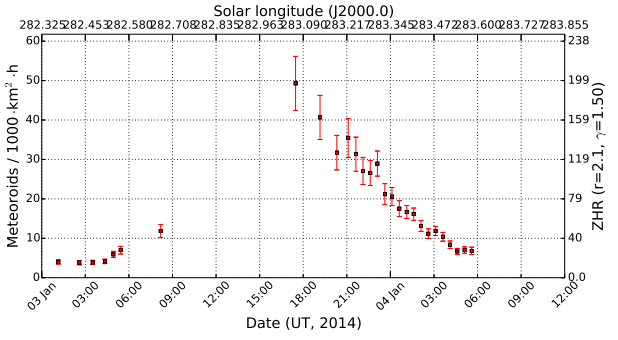


*Figure 2* – Flux density profile of the Quadrantids, derived from observations of the IMO Video Meteor Network.

[1]Abenstalstr. 13b, 84072 Seysdorf, Germany.
Email: sirko@molau.de
[2]Na Ajdov hrib 24, 2310 Slovenska Bistrica, Slovenia.
Email: javor.kac@orion-drustvo.si
[3]Via Bobbio 9a/18, 16137 Genova, Italy.
Email: stefano.crivello@libero.it
[4]via Umbria 21/d, 30037 Scorze (VE), Italy.
Email: stom@iol.it
[5]University of Hertfordshire, Hatfield AL10 9AB, United Kingdom. Email: geert@barentsen.be
[6]Urbanizacao da Boavista, Lote 46, Linhaceira, 2305-114 Asseiceira, Tomar, Portugal. Email: rui.goncalves@ipt.pt
[7]Húr u. 9/D, H-1223 Budapest, Hungary.
Email: antaligaz@yahoo.com

IMO bibcode WGN-422-molau-vidjan
NASA-ADS bibcode 2014JIMO...42...83M

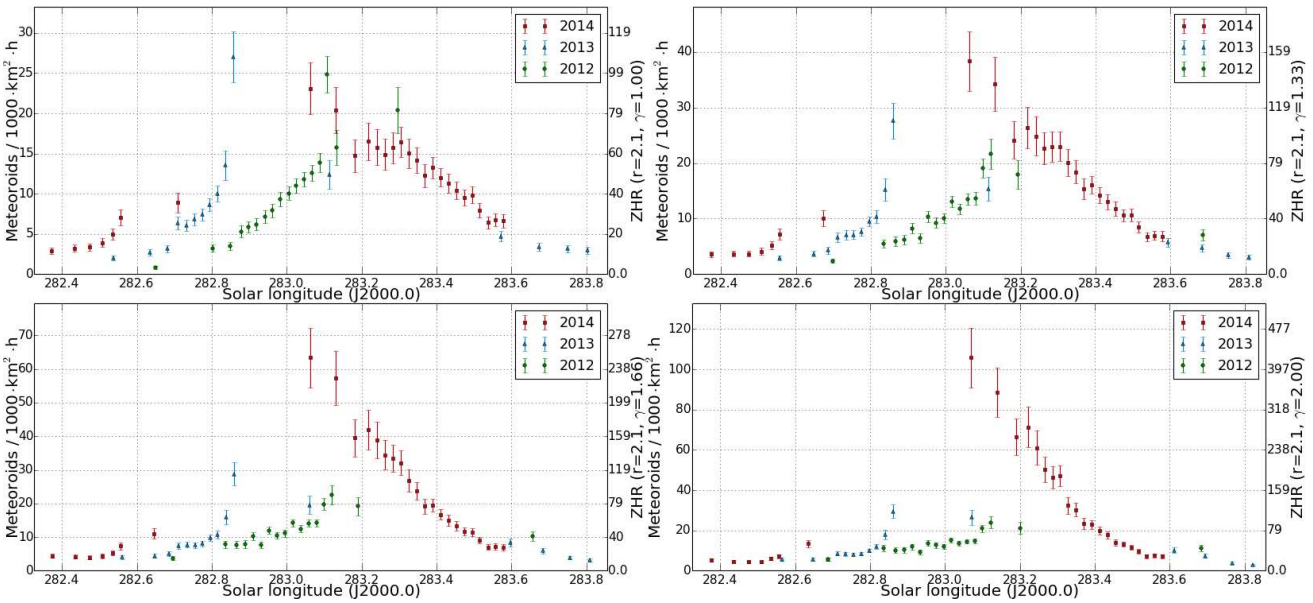


*Figure 3* – Combined flux density profiles of the Quadrantids 2012 till 2014, calculated with a zenith exponent between 1.0 (upper left) and 2.0 (lower right).

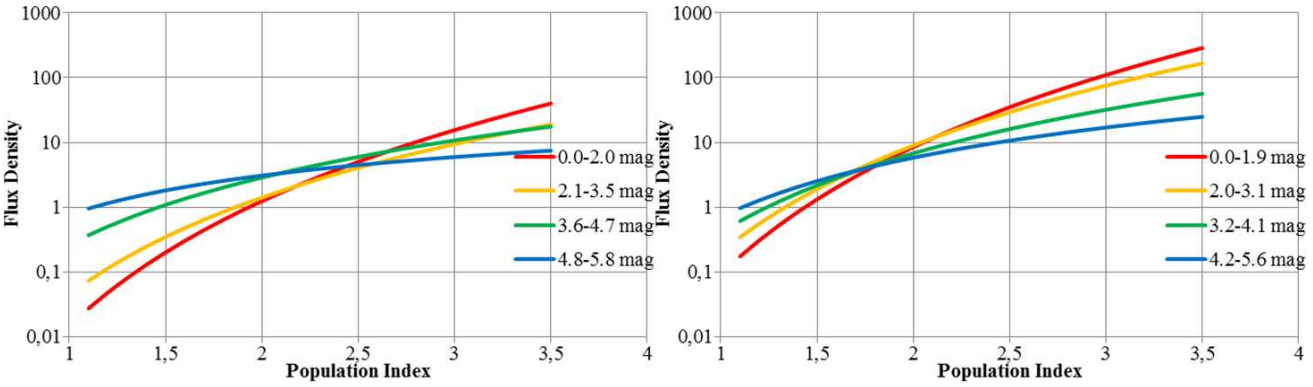


*Figure 4* – Population index vs. flux density for different limiting Quadrantid magnitudes on 2014 January 2/3 (left) and 3/4 (right).

The peak value of the flux density is difficult to estimate, since it strongly depends from the zenith exponent at such low radiant altitudes. At a moderate level of $\gamma = 1.5$ we obtain a flux density of up to 50 meteoroids per 1 000 km$^2$ per hour, which is comparable to the Perseids. At $\gamma = 2.0$, the flux density is already twice as high.

We might get a little better impression if we look at the flux data of the previous two years as well. Since the peak then occurred at a different time and radiant altitude, we might in the best case estimate the zenith exponent from the combination of all graphs. The reality is different, though (Figure 3). At no zenith exponent value we get a somewhat consistent overall picture.

Two possible explanations are that either the time or the strength of the peak varies. Indeed it can be read in the IMO Handbook for Visual Observers that the peak time of the Quadrantids varies from one year to the next (Rendtel & Arlt, 2008). The long-term activity profile shows high activity between 283.°0 and 283.°5 solar longitude, even though the individual peaks are much shorter as described.

For the determination of the population index we did not use fixed limiting magnitude intervals in one-magnitude steps, but adapted the intervals dynamically to the data set. For the pre-maximum night we obtain a value of $r = 2.5$ and in the peak night a population index of $r = 1.8$ (Figure 4). Visual observations in the past yielded a population index of 2.1 at the peak (Rendtel et al., 1993).

## References

McBeath A. (2013). "2014 Meteor Shower Calendar". International Meteor Organization. IMO INFO(2-13).

Rendtel J. and Arlt R., editors (2008). *Handbook for meteor observers*. International Meteor Organization, Potsdam.

Rendtel J., Koschack R., and Arlt R. (1993). "The 1992 Quadrantid meteor shower". *WGN, Journal of the IMO*, **21:3**, 97–109.

*Handling Editor:* Javor Kac

*Table 1* – Observers contributing to 2014 January data of the IMO Video Meteor Network. Eff.CA designates the effective collection area.

| Code | Name | Place | Camera | FOV [°²] | Stellar LM [mag] | Eff.CA [km²] | Nights | Time [h] | Meteors |
|---|---|---|---|---|---|---|---|---|---|
| ARLRA | Arlt | Ludwigsfelde/DE | Ludwig2 (0.8/8) | 1534 | 5.8 | 2467 | 19 | 115.7 | 442 |
| BERER | Berkó | Ludányhalászi/HU | Hulud1 (0.8/3.8) | 5542 | 4.8 | 3847 | 6 | 37.3 | 216 |
| | | | Hulud3 (0.95/4) | 4357 | 3.8 | 876 | 5 | 42.2 | 42 |
| BOMMA | Bombardini | Faenza/IT | Mario (1.2/4.0) | 5794 | 3.3 | 739 | 10 | 64.0 | 232 |
| BREMA | Breukers | Hengelo/NL | Mbb3 (0.75/6) | 2399 | 4.2 | 699 | 19 | 137.0 | 225 |
| | | | Mbb4 (0.8/8) | 1470 | 5.1 | 1208 | 18 | 106.4 | 178 |
| BRIBE | Klemt | Herne/DE | Hermine (0.8/6) | 2374 | 4.2 | 678 | 23 | 160.2 | 340 |
| | | Bergisch Gladbach/DE | Klemoi (0.8/6) | 2286 | 4.6 | 1080 | 23 | 109.4 | 292 |
| CASFL | Castellani | Monte Baldo/IT | Bmh1 (0.8/6) | 2350 | 5.0 | 1611 | 20 | 68.6 | 377 |
| | | | Bmh2 (1.5/4.5)* | 4243 | 3.0 | 371 | 16 | 104.1 | 207 |
| CRIST | Crivello | Valbrevenna/IT | Bilbo (0.8/3.8) | 5458 | 4.2 | 1772 | 16 | 86.0 | 216 |
| | | | C3P8 (0.8/3.8) | 5455 | 4.2 | 1586 | 16 | 103.1 | 186 |
| | | | Stg38 (0.8/3.8) | 5614 | 4.4 | 2007 | 14 | 75.8 | 194 |
| DONJE | Donani | Faenza/IT | Jenni (1.2/4) | 5886 | 3.9 | 1222 | 12 | 84.8 | 264 |
| ELTMA | Eltri | Venezia/IT | Met38 (0.8/3.8) | 5631 | 4.3 | 2151 | 8 | 55.8 | 109 |
| GANKA | Gansel | Dingden/DE | Daro01 (1.4/3.6) | 7141 | 3.1 | 652 | 13 | 97.9 | 257 |
| GONRU | Goncalves | Tomar/PT | Templar1 (0.8/6) | 2179 | 5.3 | 1842 | 10 | 73.4 | 175 |
| | | | Templar2 (0.8/6) | 2080 | 5.0 | 1508 | 16 | 96.3 | 151 |
| | | | Templar3 (0.8/8) | 1438 | 4.3 | 571 | 19 | 59.5 | 84 |
| | | | Templar4 (0.8/3.8) | 4475 | 3.0 | 442 | 15 | 75.1 | 157 |
| | | | Templar5 (0.75/6) | 2312 | 5.0 | 2259 | 22 | 93.6 | 158 |
| GOVMI | Govedič | Središče ob Dravi/SI | Orion2 (0.8/8) | 1447 | 5.5 | 1841 | 18 | 58.4 | 238 |
| | | | Orion3 (0.95/5) | 2665 | 4.9 | 2069 | 9 | 26.6 | 41 |
| | | | Orion4 (0.95/5) | 2662 | 4.3 | 1043 | 14 | 56.9 | 125 |
| HERCA | Hergenrother | Tucson/US | Salsa3 (1.2/4)* | 2198 | 4.6 | 894 | 29 | 307.1 | 635 |
| IGAAN | Igaz | Baja/HU | Hubaj (0.8/3.8) | 5552 | 2.8 | 403 | 9 | 28.5 | 71 |
| | | Debrecen/HU | Hudeb (0.8/3.8) | 5522 | 3.2 | 620 | 8 | 44.5 | 68 |
| | | Hódmezővásárhely/HU | Huhod (0.8/3.8) | 5502 | 3.4 | 764 | 13 | 44.3 | 71 |
| | | Budapest/HU | Hupol (1.2/4) | 3790 | 3.3 | 475 | 8 | 21.1 | 19 |
| JONKA | Jonas | Budapest/HU | Husor (0.95/4) | 2286 | 3.9 | 445 | 9 | 57.5 | 62 |
| KACJA | Kac | Ljubljana/SI | Orion1 (0.8/8) | 1402 | 3.8 | 331 | 8 | 17.6 | 35 |
| | | Kamnik/SI | Cvetka (0.8/3.8)* | 4914 | 4.3 | 1842 | 4 | 18.7 | 91 |
| | | | Rezika (0.8/6) | 2270 | 4.4 | 840 | 5 | 29.4 | 193 |
| | | | Stefka (0.8/3.8) | 5471 | 2.8 | 379 | 5 | 16.9 | 58 |
| | | Kostanjevec/SI | Metka (0.8/12)* | 715 | 6.4 | 640 | 2 | 5.3 | 9 |
| KERST | Kerr | Glenlee/AU | Gocam1 (0.8/3.8) | 5189 | 4.6 | 2550 | 7 | 11.3 | 83 |
| KISSZ | Kiss | Sülysáp/HU | Husul (0.95/5)* | 4295 | 3.0 | 355 | 8 | 27.8 | 27 |
| KOSDE | Koschny | Izana Obs./ES | Icc7 (0.85/25)* | 714 | 5.9 | 1464 | 16 | 148.6 | 903 |
| | | La Palma/ES | Icc9 (0.85/25)* | 683 | 6.7 | 2951 | 18 | 143.5 | 1361 |
| | | Noordwijkerhout/NL | Lic4 (1.4/50)* | 2027 | 6.0 | 4509 | 15 | 75.4 | 102 |
| LOJTO | Łojek | Grabniak/PL | Pav57 (1.0/5) | 1631 | 3.5 | 269 | 9 | 41.8 | 94 |

*Table 1* – Observers contributing to 2014 January data of the IMO Video Meteor Network – continued from previous page.

| Code | Name | Place | Camera | FOV [°²] | Stellar LM [mag] | Eff.CA [km²] | Nights | Time [h] | Meteors |
|---|---|---|---|---|---|---|---|---|---|
| MACMA | Maciejewski | Chełm/PL | Pav35 (0.8/3.8) | 5495 | 4.0 | 1584 | 16 | 71.4 | 324 |
| | | | Pav36 (0.8/3.8)* | 5668 | 4.0 | 1573 | 16 | 73.5 | 382 |
| | | | Pav43 (0.75/4.5)* | 3132 | 3.1 | 319 | 10 | 57.3 | 122 |
| | | | Pav60 (0.75/4.5) | 2250 | 3.1 | 281 | 11 | 54.1 | 157 |
| MARGR | Maravelias | Lofoupoli-Crete/GR | Loomecon (0.8/12) | 738 | 6.3 | 2698 | 14 | 96.5 | 165 |
| MASMI | Maslov | Novosibirsk/RU | Nowatec (0.8/3.8) | 5574 | 3.6 | 773 | 16 | 72.2 | 238 |
| MOLSI | Molau | Seysdorf/DE | Avis2 (1.4/50)* | 1230 | 6.9 | 6152 | 11 | 93.0 | 663 |
| | | | Mincam1 (0.8/8) | 1477 | 4.9 | 1084 | 14 | 101.9 | 202 |
| | | Ketzür/DE | Remo1 (0.8/8) | 1467 | 6.5 | 5491 | 19 | 117.9 | 678 |
| | | | Remo2 (0.8/8) | 1478 | 6.4 | 4778 | 20 | 125.7 | 581 |
| | | | Remo3 (0.8/8) | 1420 | 5.6 | 1967 | 5 | 33.8 | 40 |
| | | | Remo4 (0.8/8) | 1478 | 6.5 | 5358 | 22 | 122.6 | 657 |
| MORJO | Morvai | Fülöpszállás/HU | Huful (1.4/5) | 2522 | 3.5 | 532 | 13 | 81.2 | 101 |
| MOSFA | Moschner | Rovereto/IT | Rover (1.4/4.5) | 3896 | 4.2 | 1292 | 3 | 11.8 | 33 |
| OCHPA | Ochner | Albiano/IT | Albiano (1.2/4.5) | 2944 | 3.5 | 358 | 13 | 56.2 | 101 |
| OTTMI | Otte | Pearl City/US | Orie1 (1.4/5.7) | 3837 | 3.8 | 460 | 23 | 159.1 | 381 |
| PERZS | Perkó | Becsehely/HU | Hubec (0.8/3.8)* | 5498 | 2.9 | 460 | 13 | 60.9 | 302 |
| PUCRC | Pucer | Nova vas nad Dragonjo/SI | Mobcam1 (0.75/6) | 2398 | 5.3 | 2976 | 7 | 16.8 | 30 |
| ROTEC | Rothenberg | Berlin/DE | Armefa (0.8/6) | 2366 | 4.5 | 911 | 9 | 56.4 | 143 |
| SARAN | Saraiva | Carnaxide/PT | Ro1 (0.75/6) | 2362 | 3.7 | 381 | 16 | 77.3 | 83 |
| | | | Ro2 (0.75/6) | 2381 | 3.8 | 459 | 13 | 63.3 | 113 |
| | | | Ro3 (0.8/12) | 710 | 5.2 | 619 | 5 | 24.4 | 27 |
| | | | Sofia (0.8/12) | 738 | 5.3 | 907 | 15 | 84.9 | 92 |
| SCALE | Scarpa | Alberoni/IT | Leo (1.2/4.5)* | 4152 | 4.5 | 2052 | 8 | 39.2 | 55 |
| SCHHA | Schremmer | Niederkrüchten/DE | Doraemon (0.8/3.8) | 4900 | 3.0 | 409 | 25 | 147.1 | 540 |
| SLAST | Slavec | Ljubljana/SI | Kayak1 (1.8/28) | 563 | 6.2 | 1294 | 3 | 8.5 | 24 |
| STOEN | Stomeo | Scorze/IT | Min38 (0.8/3.8) | 5566 | 4.8 | 3270 | 11 | 50.2 | 195 |
| | | | Noa38 (0.8/3.8) | 5609 | 4.2 | 1911 | 13 | 64.3 | 202 |
| | | | Sco38 (0.8/3.8) | 5598 | 4.8 | 3306 | 15 | 70.7 | 291 |
| STORO | Štork | Kunžak/CZ | Kun1 (1.4/50)* | 1913 | 5.4 | 2778 | 1 | 2.0 | 15 |
| | | Ondřejov/CZ | Ond1 (1.4/50)* | 2195 | 5.8 | 4595 | 2 | 6.0 | 191 |
| STRJO | Strunk | Herford/DE | Mincam2 (0.8/6) | 2354 | 5.4 | 2751 | 20 | 79.4 | 473 |
| | | | Mincam3 (0.8/6) | 2338 | 5.5 | 3590 | 21 | 105.3 | 394 |
| | | | Mincam4 (1.0/2.6) | 9791 | 2.7 | 552 | 16 | 88.8 | 208 |
| | | | Mincam5 (0.8/6) | 2349 | 5.0 | 1896 | 21 | 122.4 | 422 |
| TEPIS | Tepliczky | Agostyán/HU | Huago (0.75/4.5) | 2427 | 4.4 | 1036 | 17 | 83.9 | 132 |
| | | Budapest/HU | Humob (0.8/6) | 2388 | 4.8 | 1607 | 15 | 91.4 | 189 |
| TRIMI | Triglav | Velenje/SI | Sraka (0.8/6)* | 2222 | 4.0 | 546 | 13 | 97.7 | 145 |
| YRJIL | Yrjölä | Kuusankoski/FI | Finexcam (0.8/6) | 2337 | 5.5 | 3574 | 14 | 126.2 | 271 |
| ZELZO | Zelko | Budapest/HU | Huvcse03 (1.0/4.5) | 2224 | 4.4 | 933 | 4 | 31.6 | 29 |
| | | | Huvcse04 (1.0/4.5) | 1484 | 4.4 | 573 | 4 | 17.1 | 41 |
| | | | | | | Overall | 31 | 5 971.4 | 18 220 |

* active field of view smaller than video frame

# The International Meteor Organization

web site http://www.imo.net

## Council

*President:* Cis Verbeeck,
Bogaertsheide 5, 2560 Kessel, Belgium.
e-mail: cis.verbeeck@scarlet.be

*Vice-President* Jürgen Rendtel,
Eschenweg 16, D-14476 Marquardt, Germany.
tel. +49 33208 50753
e-mail: jrendtel@aip.de

*Secretary-General:* Robert Lunsford
1828 Cobblecreek Street, Chula Vista,
CA 91913-3917, USA. tel. +1 619 585 9642
e-mail: lunro.imo.usa@cox.net

*Treasurer:* Marc Gyssens, Heerbaan 74,
B-2530 Boechout, Belgium.
e-mail: marc.gyssens@uhasselt.be
BIC: GEBABEBB
IBAN: BE30 0014 7327 5911
Always state BIC and IBAN codes together!
Check international transfer charges with your bank; you are responsible for paying these.

*Other Council members:*

David Asher, Armagh Observatory, College Hill, Armagh, Northern Ireland BT61 9DG, UK.
e-mail: dja@arm.ac.uk

Geert Barentsen, University of Hertfordshire, Hatfield AL10 9AB, UK. e-mail: geert@barentsen.be

Javor Kac (see details under WGN)

Detlef Koschny, Zeestraat 46,
NL-2211 XH Noordwijkerhout, Netherlands.
e-mail: detlef.koschny@esa.int

Sirko Molau, Abenstalstraße 13b, D-84072 Seysdorf, Germany. e-mail: sirko@molau.de

Jean-Louis Rault, Société Astronomique de France, 16, rue de la Vallée, 91360 Epinay sur Orge, France. e-mail: f6agr@orange.fr

Paul Roggemans (see details under IMC Liaison Officer)

## Commission Directors

*FIreball DAta Center:* André Knöfel
Am Observatorium 2,
D-15848 Lindenberg, Germany.
e-mail: fidac@imo.net

*Photographic Commission:* vacant

*Radio Commission:* Jean-Louis Rault

*Telescopic Commission:* Malcolm Currie
660, N'Aohoku Place, Hilo, HI 96720, USA
e-mail: mjc@star.rl.ac.uk

*Video Commission:* Sirko Molau

*Visual Commission:* Rainer Arlt, Bahnstr. 11,
D-14974 Ludwigsfelde, Germany.
e-mail: rarlt@aip.de

## IMC Liaison Officer

Paul Roggemans, Pijnboomstraat 25, 2800 Mechelen, Belgium, e-mail: paul.roggemans@gmail.com

# WGN

*Editor-in-chief:* Javor Kac
Na Ajdov hrib 24, SI-2310 Slovenska Bistrica, Slovenia. e-mail: wgn@imo.net;
include METEOR in the e-mail subject line

*Editorial board:* Ž. Andreić, R. Arlt, D.J. Asher, J. Correira, M. Gyssens, H.V. Hendrix, C. Hergenrother, J. Rendtel, J.-L. Rault, P. Roggemans, C. Trayner, C. Verbeeck.

# IMO Sales

| *Available from the Treasurer or the Electronic Shop on the IMO Website* | € | $ |
|---|---|---|
| **IMO membership, including subscription to WGN Vol. 42 (2014)** | | |
| Surface mail | 26 | 39 |
| Air Mail (outside Europe only) | 49 | 69 |
| Electronic subscription only | 21 | 29 |
| **Back issues of WGN** on paper (price per complete volume) | | |
| Vols. 26 (1998) – 35 (2007) except 30 (2002), 38 (2010) – 41 (2013) | 15 | 23 |
| Vols. 37 (2009) – 41 (2013) – electronic version only | 9 | 13 |
| **Proceedings of the International Meteor Conference** on paper | | |
| 1990, 1991, 1993, 1995, 1996, 1999, 2000, 2002, 2003, per year | 9 | 13 |
| 2007, 2010, 2011, per year | 15 | 23 |
| 2012 | 25 | 37 |
| **Proceedings of the Meteor Orbit Determination Workshop 2006** | 15 | 23 |
| **Radio Meteor School Proceedings 2005** | 15 | 23 |
| **Handbook for Meteor Observers** | 20 | 29 |
| **Electronic media** | | |
| Meteor Beliefs Project CD-ROM | 6 | 9 |
| DVD: WGN Vols. 6–30 & IMC 1991, 1993–96, 2001–04 | 45 | 69 |

# The 2013 September $\varepsilon$-Perseid outburst

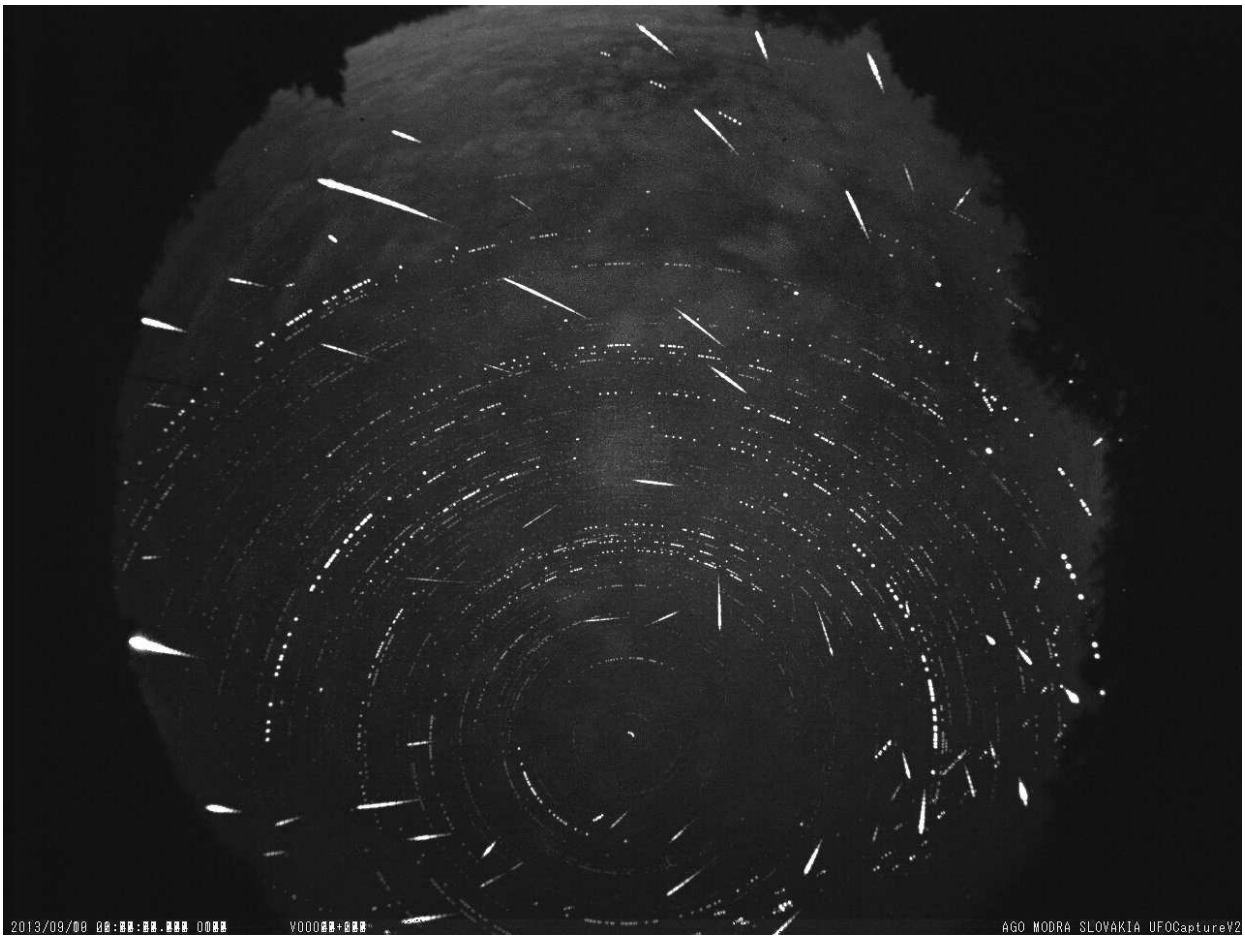



Composite images of meteors captured during the night of the September $\varepsilon$-Perseids (SPE) outburst on 2013 September 9/10. They comprise all SPE meteors recorded by the two all-sky systems AMOS at stations AGO Modra (top image) and ARBO (bottom image), respectively. Observer: Š. Gajdoš. Image processing: J. Tóth. See inside for more details about the outburst.